PROCEEDINGS

of the

San Diego Society of Natural History

Founded 1874

Number 7 1 July 1991

Remipedia
Part 2
Paleontology

Michael J. Emerson* and Frederick R. Schram

Natural History Museum of Los Angeles County, 900 Exposition Blvd., Los Angeles, California 90007

ABSTRACT.—Five recently collected specimens of the Late Mississippian arthropod *Tesnusocaris goldichi* Brooks, 1955, from the Tesnus Formation in Brewster County, Texas, are described, and the holotype is reexamined. Three of the new specimens and the holotype provide details hitherto unknown and allow the first complete reconstruction of the animal to be made. The new specimens are interpreted as juveniles of the species, which otherwise is known only from the adult holotype. The cephalic appendages are shown to resemble those of the living order Nectiopoda (Crustacea: Remipedia). The specialized grappling mouthparts are characteristic of the class and confirm the status of the fossil order Enantiopoda as a sister group of the Nectiopoda. The trunk appendages of the fossil species, though resembling those of the nectiopodans in certain respects, differ fundamentally in structure and probable function from those of any other crustacean. Each trunk segment is shown to bear a homonomous series of two pairs of uniramous, paddle-shaped limbs, a condition we term duplopody (in clear distinction to diplopody seen in uniramians) rather than the single pair of biramous appendages characteristic of the Nectiopoda. We have found it necessary to coin additional terminology to describe *Tesnusocaris*. The ventrolateral series of limbs, or exopedes, apparently functioned as oars in rowing, but the midventral series of appendages, or endopedes, probably functioned as hydrofoils in a unique form of sculling. The duplopodous condition of *Tesnusocaris* is compared to the segmentation patterns of other articulates. The morphology of the trunk segments is not adequately described by the existing concepts of limb homology. Other fossil remipedes are considered, and other possible instances of duplopody in the fossil record are examined.

INTRODUCTION

The problematic arthropod *Tesnusocaris goldichi* Brooks, 1955, was originally collected by S. S. Goldich (pronounced *goal-dick*) in 1939 and was the only identifiable macrofossil specimen found in the Tesnus Formation in the southeastern corner of the Marathon Uplift in western Texas. The calcareous shales from which the fossil came have been assigned to the Mississippian–Pennsylvanian boundary. Brooks (1955) described the specimen in a paper illustrated with a generalized reconstruction and beautifully detailed photographs. Brooks was uncertain of the taxonomic position of this species and consequently used neutral anatomical terms to describe the specimen. He tentatively allied the fossil with the Crustacea and compared it to all major crustacean groups. In the text of the paper, Brooks placed *Tesnusocaris* closest to the Anostraca, but in a footnote added in press he compared the specimen to the then newly described cephalocarids. Birshtein (1960) accepted the latter assignment and proposed for *Tesnusocaris* the order Enantiopoda, which he viewed as related to the order Brachypoda (Birshtein's ordinal name for the living Cephalocarida). Hessler (1969) rightly rejected the suggested cephalocarid affinities of the Texas fossil, and Moore (1969) assigned it an uncertain status within the Malacostraca. Most subsequent authors who dealt with *Tesnusocaris* at all have placed it within the Branchiopoda. Bergström (1979) suggested that the fossil was that of a uniramian, and Schram (1982) voiced uncertainty about the fossil's crustacean affinities.

The situation changed with the discovery of the living representatives of the Class Remipedia (Yager 1981). These creatures are found in anchialine caves in the West Indies, Yucatan, and the Canary Islands (Schram et al. 1986, Yager 1987a,b, Yager 1989). The animals possess a combination of many of the primitive features that arthropod phylogeneticists had predicted would be found in an ancestral crustacean type (e.g., Hessler and Newman 1975, Schram 1982), though the feeding appendages are rather specialized. These plesiomorphic characteristics include a trunk that is not regionalized, a pair of appendages on every body segment, each trunk limb with a biramous form, no carapace extending back from the head, and serial homonomy in internal organ systems. The living remipedes were later sequestered (Schram 1986) into their own order, Nectiopoda, distinct from the fossil Enantiopoda. Certain features present in the nectiopodans, such as the headshield and long unregionalized trunk, were also noted in *Tesnusocaris*. This prompted Schram (1983) to suggest that the living remipedes and

*Deceased, March 22, 1990.

LIST OF ABBREVIATIONS AND KEY

A1 - antennule
A2 - antenna
Aes - aesthetascs
AHS - anterior headshield
AS - anal segment
C - caudal ramus
D - dorsal
Eye - eye
Fp - frontal process
Ics - intercoxal space
IP - incisor process
L - left
Lb - labrum
Lm - lacinia mobilis
MHS - middle headshield
Mp - molar process
MR - marginal rim
Mx1 - maxillule
Mx2 - maxilla
Mxp - maxillipede
N - endopede
Np - endopod
PHS - posterior headshield
Pp - protopod
R - right
S - sternite
Sb - sternal bar
SDSNH - San Diego Society of Natural History
T - tergite
USNMP - United States National Museum (Paleontology)
V - ventral
Vls - ventrolateral sclerite
X - exopede
Xp - exopod
.4 - fourth podite of limb or ramus
? - identification uncertain
( ) - estimated position of insertion of limb

 - microescarpment, hatch marks point to lower level [reversed from couterpart]*

 - rounded microescarpment [hidden or deemphasized; reversed from counterpart]*

 - clearly defined boundary

 - indistinct boundary [hidden or deemphasized boundary]*

 - faint boundary [deemphasized boundary]*

 - high point [reversed from counterpart]*

 - low point [reversed from counterpart]*

 - shaded area keyed to caption

 - stippled area keyed to caption

 - lined area keyed to caption

* - additional attributes of partly reconstructed version in brackets

the Enantiopoda might be related. This possibility was strengthened by a reexamination of the holotype (Schram et al. 1986), then the only known specimen of *Tesnusocaris*. The new study indicated that rather than the setose, filtering mouthparts reconstructed by Brooks (1955), the Texas fossil actually had robust, spinose mouthparts. The recent remipedes appear to be very specialized carnivores (Schram and Lewis 1989), and it seemed possible from study of the *Tesnusocaris* holotype that the Texas form also may have been highly adapted to active predation.

Considering the obvious potential importance of *Tesnusocaris* and the limited value of the single known specimen, we decided to relocate the locality where Goldich collected the type (Brooks 1955). This was done in the fall of 1985, and five new specimens were found (Schram and Emerson 1986). One specimen is exceptionally well preserved throughout nearly its entire length, and two more specimens provide certain details lacking from the others. The two remaining specimens, because of their uniformly poor preservation, can be assigned to this species only by analogy with the other fossils. Along with a restudy of the holotype, the new fossils allow the first complete reconstruction of *T. goldichi*, one that differs significantly from previous interpretations.

A reexamination of the holotype and study of some newly discovered specimens of *Cryptocaris hootchi* Schram, 1974, from the Mazon Creek faunas of Illinois, Middle Pennsylvanian, reveal that this species is not a tanaidacean as originally thought but is related to *Tesnusocaris*.

LOCALITY AND STRATA

Locality.—The holotype specimen of *Tesnusocaris goldichi*, USNMP 124173, was originally collected in 1939 by S. S. Goldich of the University of Minnesota while engaged in a geological field survey of the southeastern Marathon Basin. The specimen was deposited in the U.S. National Museum and eventually was named and described by H. K. Brooks (1955). At that time the type locality (Fig. 1) was recorded merely as "west of Rough Creek, 4,300 ft. S 51 E of Hill 4334 in the northwestern corner of the Dove Mountain quadrangle, Brewster Co. Texas" (Brooks 1955:855).

Our 1985 expedition (Schram and Emerson 1986) precisely located the type locality, SDSNH locality number 3307. Its UTM coordinates are 69478/331915 on the Pine Mountain West, Texas, 7.5' USGS quadrangle (1983 edition); 29°59'23"N, 102°58'52"W

Figure 1. View looking northeast from the entry road to Rough Creek Ranch, Brewster Co., Texas. Arrow points to approximate location of localities for *Tesnusocaris goldichi* on the eastern flanks of Hill 4334.

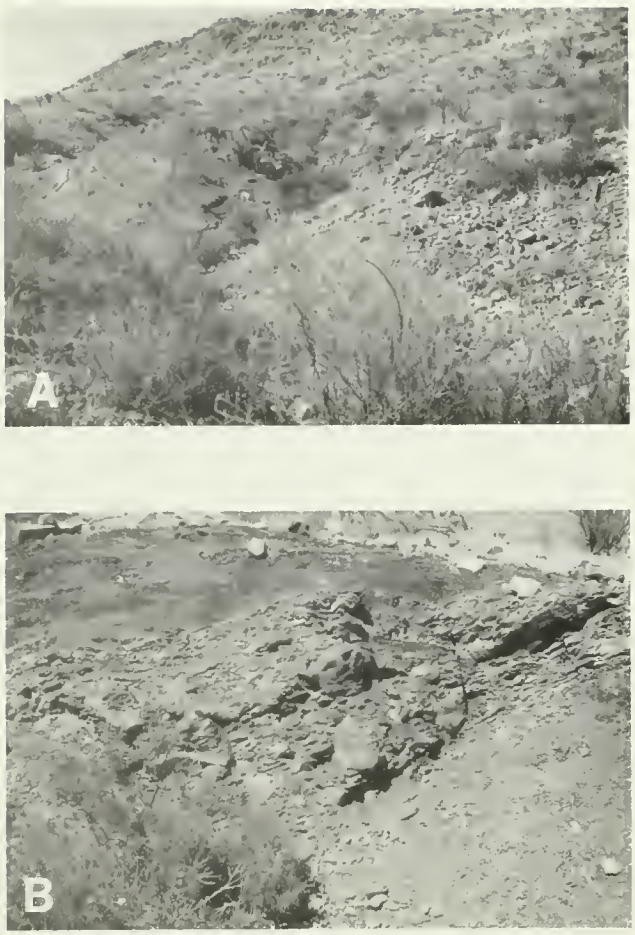

Figure 2. The 1939 type locality of S. S. Goldich for *Tesnusocaris goldichi*, Rough Creek Ranch, Brewster Co., Texas. A, overview of SDSNH locality number 3307; B, closeup view of outcrop.

(Fig. 2). No additional specimens were collected at this site, but a second locality did produce three fossiliferous concretions that contained *Tesnusocaris*. This locality, SDSNH 3308, lies at UTM coordinates 69465/331905 on the Pine Mountain West, Texas, 7.5' quadrangle (1983 edition); 29°59'19"N, 102°58'55"W (Fig. 3). These disjunct outcroppings of the distinctive fossiliferous shale lie on either side of a saddle ridge that links Hill 4334 to Hill 3605 southeast of it.

Our study area is located in the southeast quarter of the Marathon Basin on the Rough Creek Ranch (referred to on some old maps as the Gage Ranch or the western portion of the old San Francisco Ranch). This ranch is situated approximately 25 miles east of Texas Highway 343 south of Marathon, Texas, an hour-and-a-half journey on a private dirt road that extends into an area southeast of Hell's Half Acre.

Regional Geology.—The geology in the area of immediate concern is dominated by the Tesnus Formation, a name derived from an inversion of the word "sunset" applied to Tesnus Station, a siding on the Southern Pacific Railroad east of Marathon. The geologic formation was named by Baker and Bowman (1916), though the most thorough review of the geology of the region is that of King (1937). In the northwestern part of the Marathon Basin, the upper part of the Tesnus is about 300 ft. thick and composed of black shales and some sandstones. In the southeastern part of the basin, including our study area, the lower portion of the Tesnus is approximately 6500 ft. thick and composed of alternating reddish

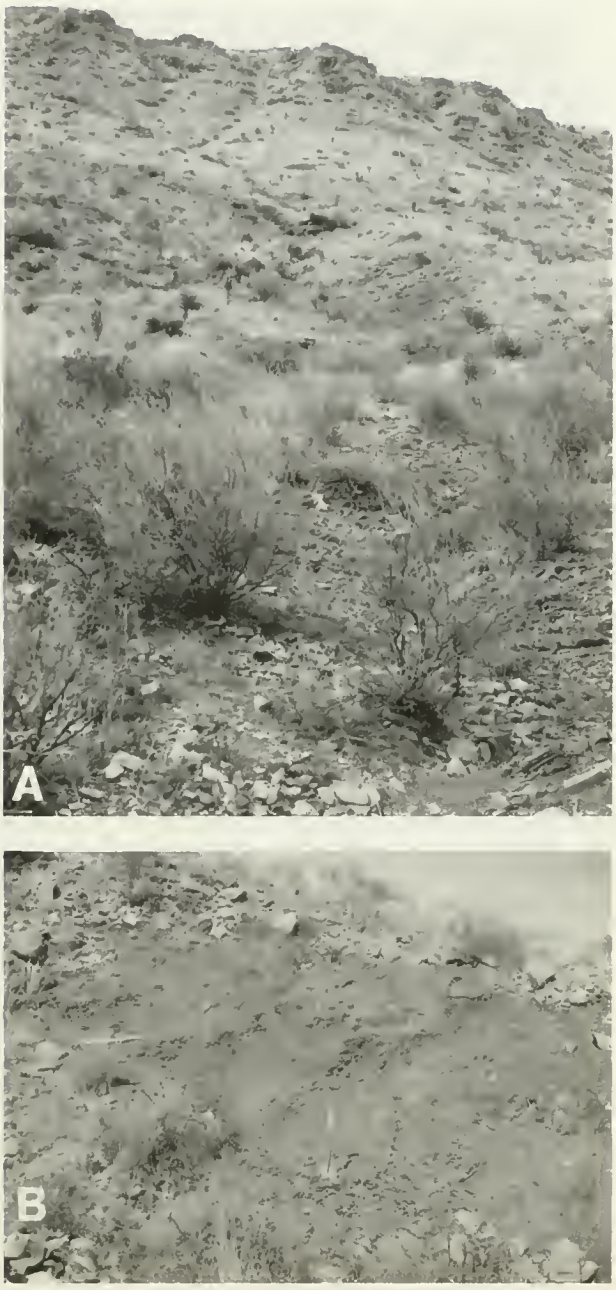

Figure 3. The 1985 locality discovered by M. J. Emerson for *Tesnusocaris goldichi*, Rough Creek Ranch, Brewster Co., Texas. A, overview of SDSNH locality number 3308; B, closeup view of outcrop.

brown sandstone and gray-green shales deformed into nearly vertical layers (King 1930). The more resistant sandstones form cockscomb ridges, and the softer shales erode to form valleys. The Tesnus overlies the Caballos Novaculite, a very resistant cherty Devonian formation.

Along Rough Creek, the Caballos crops out about one mile above the junction with San Francisco Creek (see Schram and Emerson 1986 for details of the geography of the area). At this point, the Caballos is overlain with green shales of the Rough Creek Member that weather to a dark gray. The lower part of these beds is almost entirely shale, with an occasional interbedding of thin sandstone. The sandstones become more abundant and thicker toward the top of this member. Farther west along the road that leads to Rough Creek Ranch, at Indian Creek Ranch, the Caballos is overlain by a rather argillaceous sandstone, and the most basal shale beds that are seen along Rough Creek are missing.

The beds from which *Tesnusocaris goldichi* was collected are sandwiched between two prominent sandstone layers. The Tesnus Formation in that part of the Rough Creek valley is thick but was not measured fully by us since it forms a cliff on the eastern and southeastern flanks of Hill 4334. However, the beds immediately below the cliff in which the fossils were collected were more accessible and measured top to bottom as follows:

Bed 6. Poorly bedded, greenish shale ..... 0.36 m
Bed 5. Finely bedded, blue-gray fissile shale, with scattered concretions ..... 6.1 m
Bed 4. Green-to rust-colored shale with very disturbed and reworked bedding, large calcareous concretions common ..... 5.2 m
Bed 3. Greenish shale, poorly bedded ..... 11.0 m
Bed 2. Greenish gray shale, finely bedded ..... 13.6 m
Bed 1. Sandstone ..... 2.0 m

The concretions with the remipede fossils were collected in situ from Bed 5 (Fig. 2B), which is identified readily by its distinctive blue-gray color. Four medium-sized concretions were collected, only three of which contained fossils. A fifth concretion, very large and badly fragmented, was noted in the field but was not collected since it did not appear to contain any recognizable fossil material.

Stratigraphic Correlation.—The stratigraphic correlation of the Tesnus long has been a problem. Northwest of our localities, the Upper Tesnus crops out in regions called Hell's Half Acre and the Devil's Backbone, though we did not investigate these areas. The Tesnus there is said to resemble closely in appearance the Jackfork Sandstone in the Ouachita Mountains of Oklahoma. Mapel et al. (1979) pointed out that the regional stratigraphy of the Trans-Pecos indicates that the unconformity of the Tesnus and the underlying Devonian Caballos is a gap representing at least a part of the Kinderhookian time of the Mississippian.

In addition to *Tesnusocaris*, most of the fossils collected in the Tesnus itself have been reported in the upper beds of the formation. Baker and Bowman (1916) listed a Pennsylvanian-type fauna collected from sites west and northwest of Marathon that includes a wide array of brachiopods, plants, bryozoans, fusilines, and crinoid stems. The best analysis of floral fossils is King's (1930, 1937). The following plants occur approximately 10 miles southwest of Marathon: *Neuropteris* and *Alethopteris* leaves; parts of *Clamites*, *Stigmaria*, and *Asterophyllites*; and *Lepidodendron*, *Artesia*, *Cordaites*, *Cardiocarpon*, and *Trigonocarpon*. This flora indicates a Pennsylvanian, Middle Pottsville age. A smaller flora collected south of Tesnus Station consists of tips of leaflets of either *N. gigantea* or *N. capitata*, which does not contradict the Pottsville assignment.

Other fossils in the Upper Tesnus are less helpful in determining the age of the strata (King 1937). Fusilinid foraminiferans have been collected approximately 18 miles east of Marathon. These apparently indicate a lowermost Pennsylvanian age for the upper member, since they are equivalent to forams found in the Caney Shale of Oklahoma. Apparent monaxon sponge spicules have been found in the calcareous sandstones on the north slope of West Bourland Mountain south of Marathon, just below the plant horizon. These objects, however, are black and appear to be phosphatic rather than siliceous. We noted similar objects in some of the shale beds along Rough Creek immediately above the novaculite, and we concluded that these were mineral inclusions in the shale.

Although the upper part of the Tesnus Formation has been dated reliably, the age of the more than 6000 feet that are below

the upper member is less certain (Maxwell et al. 1967). King (1937) equated the Tesnus with the Stanley, Jackfork, and Springer formations of Oklahoma and Arkansas, which date from the Upper Mississippian. Crosby and Mapel (1975) stated that the Mississippian–Pennsylvanian boundary probably was located high in the Tesnus. Jones (1953) believed that the Rough Creek member was the approximate equivalent of the early Mississippian Stanley Formation. Hass (1956) felt that the conodonts of the Stanley were early or middle Meremecian Mississippian in age, and Elias (1959) believed that the conodonts in the lower part of the Stanley were early Mississippian. Only Ellison (1962) reported collecting conodonts from the Lower Tesnus itself, and he felt that they indicated a Mississippian age. We collected a single *Hindeodella* (SDSNH 29714) in a concretion from the beds just below those containing the crustaceans, which is consistent with a Carboniferous age but not more explicit than that. More recently, Mapel et al. (1979) equated the Tesnus with the Stanley and concluded that the Lower Tesnus is Mississippian Interval D, i.e., uppermost Meremec, or Chester. It appears that *Tesnusocaris* is most likely Upper Mississippian in age.

Paleoenvironment.—King (1930) equated the Tesnus to the Chester-age Helms group of the Hueco Mountains at the western tip of Texas near El Paso. These latter beds thicken to the southeast, toward the Tesnus Formation, which suggested to King that the Tesnus represents thicker geosynclinal deposits in that region. This opinion was shared by Mapel et al. (1979), who felt that the Stanley and Tesnus formations represent rapidly sinking geosynclinal deposition. King (1937), however, concluded that the Tesnus might represent shallow marine, deltaic, or even continental deposits. The massive shales and interbedded sandstones characteristic of the Tesnus were viewed (Crosbey and Mapel 1975) as deep-water deposits into which clastic sediments were swept off the Carboniferous shelf by turbidity currents (Flawn et al. 1961).

Dutro et al. (1979) indicated that the Mississippian paleogeography of the area included a highland that extended across what is now northern Mexico and southern Texas and was continuous to the northeast with the Appalachian Mountains. The offshore Ouachita Trough, into which the Tesnus sediments were deposited in this interpretation, extended from the Oklahoma region to the Trans-Pecos. Dutro et al. (1979) believed that the continental source of the marine sediments during Tesnus times came from the southeast with the Tesnus Formation apparently the result of deposition in a relatively deep sea. However, turbidity deposits in deep troughs are not noted especially for good fossil preservation. This may stem from the general paucity of life forms in deep-sea environments, coupled with a low rate of fossil preservation in such habitats characterized by coarse clastic sediments. Therefore, the interpretation of Dutro et al. (1979) may explain why the Tesnus Formation, especially the lower member, is so poor in fossils. *Tesnusocaris goldichi* occurs in an unlikely paleontological setting, and the fact that we have good material of this soft-bodied animal is all the more exceptional.

The fossils are enclosed in claystone concretions that are composed largely of phyllite and montmorillinite. Ferromagnesium minerals consist of hornblende altered to sauserite (albite and epidote) with some traces of biotite. There is no calcite as cement, although there are traces of calcium sulfate. Apparently the concretions were cemented by compaction and alteration of the clay minerals (William Estavillo, personal communication).

MATERIALS AND METHODS

The study of *Tesnusocaris* is limited by the small number of available specimens and their generally poor preservation. There is wide variation in size between specimens as well as in their preserved orientations. All these factors contribute to the difficulty of correlating features observed on individual specimens. To derive the maximum information from each specimen, we made detailed camera lucida drawings that incorporated observations made under a variety of conditions of immersion, illumination, and magnification. The drawings were then rigorously cross-checked and combined to produce Figures 4, 10, 12, and 14. Each figure presents unreconstructed views of the most informative specimens (including the counterpart, where applicable) associated with a partly reconstructed, composite view that is labeled.

The precise orientation of each concretion with respect to the depositional interface was not noted in the field. Such knowledge would have proved to be important for interpreting the fossils, since only one-half of the concretion affords a "normal" view of the specimen as it originally lay on the ancient bottom, i.e., dorsal, ventral, or lateral side up. Diagenetic flattening and distortion can be understood accurately only if the original direction of gravitational forces is known. This information is also crucial in determining the spatial relationships of structures preserved on the opposing sides of the split concretion. Our determination of which side of the concretion afforded the normal surface view (henceforth referred to as the "part") and which one needed to be flipped to conform to the normal view (henceforth the "counterpart") was made by an examination of microescarpments on the fossil surfaces that indicate the overlap of structures such as legs (Whittington 1971). Since the part and counterpart were drawn separately under the camera lucida and composite views then generated, minor differences in the depiction of certain details between the uncomposited and partly reconstructed views have occurred, but these were not significant. No attempt was made to revise the uncomposited views to make them conform to subsequent interpretations, with one exception which will be duly noted.

The uncomposited drawings are the principal raw data we used in this study, since most of the specimens could not be understood fully from a direct examination of the fossils alone. Those drawings are presented here, unencumbered by the labels that accompany the reconstructed composite view, to allow the reader to examine the spatial relationship of the part and counterpart and to permit an independent assessment of the evidence used to support our interpretations. Through this process, we have striven to make the best use of the imperfect material at hand without overextending the powers of interpretation. In all instances, "left" and "right" refer to the bilateral symmetry of the animal as shown in the composite (labeled) view. In contrast, "above" and "below" refer to the perspective of the viewer, who is assumed to be above the specimen with respect to its original orientation on the depositional interface, as shown in the composite view.

SYSTEMATICS

Class REMIPEDIA Yager, 1981

Diagnosis.—Crustaceans without trunk tagmosis or clearly developed carapace and possessing large, grappling mouthparts. Subrectangular headshield with anterior, lobate projection and cervical groove; antennules large and biramous; protopod indistinctly divided into two segments, the proximal one with aesthetascs, the distal one bifurcate (?); dorsal ramus larger than ventral ramus and consisting of more numerous segments, ventral ramus consisting of twelve or fewer long segments in known species, with short, marginal setae. Antennae biramous. Setose paddles, modest in size, consisting of an anteriorly directed slender protopod of two segments, the second bearing an unsegmented exopod laterally and distally supporting an endopod of three (?) segments arching anterolaterally. Labrum subtriangular, large, and bulbous, at least

partially enclosing mandibles within atrium oris (entognathy). Mandibles well developed, supporting a large, spinose molar process and a small lacinia mobilis (?), lacking palps. Maxillules uniramous, subchelate, with seven segments, spinose basal endites, and terminal fang; robust first endite with at least seven stout spines directed toward mouth. Maxillae uniramous, subchelate, with spinose basal endites, including a tripartite first endite and terminal claw. First trunk somite as maxillipedal segment fused to cephalon; maxillipedes uniramous, subchelate, with terminal claw. Trunk with numerous segments, each bearing a homonomous series of setose swimming appendages; anal segment bearing caudal rami.

Remarks.—This diagnosis includes several characters previously known only from the Nectiopoda (Schram et al. 1986) but now confirmed for the Enantiopoda as well. Chief among these are the details of mouthpart structure and the presence of caudal rami.

Order NECTIOPODA Schram 1986

Diagnosis.—Remipedes lacking pigment and eyes. Cephalon with ventral, spined frontal processes. Antennular aesthetascs with long ribbonlike setae covering antennae; dorsal ramus with several long segments, fewer than twenty in known species. Antennae with long, plumose setae; endopod segmentation complete. Maxillules apparently hypodermic, with subterminal pore on fang connected by duct to glandular tissue. Maxillae and maxillipedes with fewer than nine distinct podomeres in known species. Each trunk segment bearing one pair of biramous limbs, each with a large ventrolaterally directed protopod distally supporting two oar-shaped rami of three (exopods) or four (endopods) elliptical segments with rounded tips and moderate to long marginal setae. Hermaphrodites with gonopores located on bases of eighth (female) and fifteenth (male) trunk limbs. Anal segment with one pair of short, simple caudal rami; gut with metameric diverticulae.

Remarks.—This diagnosis is included here to revise that given by Schram et al. (1986) in light of the revised diagnosis for the class given above. Several of the characters probably pertain to the class as a whole, though their presence in the fossil Enantiopoda cannot be confirmed at this time. The most important of these are the maxillulary fang's being hypodermic, the location of the gonopores (the maxillipedal segment is counted as the first trunk somite), the metameric gut diverticulae, and possibly the frontal processes. The most reliable and significant characters distinguishing this order are the lack of eyes, the long segments of the antennular dorsal ramus, the biramous trunk limbs with similar oar-shaped rami, and the relatively short and simple pair of caudal rami.

Order ENANTIOPODA Birshtein, 1960

Diagnosis.—Anterior headshield bearing a set of large, sessile compound eyes (?); frontal processes unknown; dorsal ramus of antennules finely annulate; mandibles not completely enclosed within atrium oris by labrum. Trunk segments duplopodous, each bearing two pairs of uniramous appendages; anal segment with two pairs of long, uniramous, annulate caudal rami.

Remarks.—The nature of the eyes is unresolved at this time because, although they are very evident on specimens of *Tesnusocaris goldichi*, the eyes are not clearly preserved on any of the specimens at hand of *Cryptocaris hootchi*.

Family TESNUSOCARIDIDAE Brooks, 1955

Diagnosis.—Since there is only one family recognized at this time, the diagnosis is the same as that of the order.

Type species.—*Tesnusocaris goldichi* Brooks, 1955.

Genus *TESNUSOCARIS* Brooks, 1955

Diagnosis.—Adult at least 9.5 cm in total body length. Headshield expanded with length approximately equal to width, partially covering cephalic appendages laterally and first two (?) trunk tergites posteriorly. Trunk with at least 21 tergites; limbs gradually diminishing posteriorly.

TESNUSOCARIS GOLDICHI Brooks, 1955

Diagnosis.—Antennulary aesthetascs bearing relatively short setae; dorsal ramus of antennules with more than 100 short annulae without setae. Marginal setae of antenna relatively short, antennal endopod with incomplete segmentation. Incisor process of mandible unknown; maxillae and maxillipedes with nine podomeres. Mesial trunk limbs (endopedes) developed as flippers including a bell-shaped coxa equally broad as long, a marginal crest laterally, short marginal setae medially, and nine podomeres with the most distal podomere acute. Lateral trunk limbs (exopedes) developed as oars including a bell-shaped coxa broader than long, moderately long marginal setae, and five podomeres with the most distal podomere oval.

Juveniles approximately 2.5–4.0 cm in total body length, not including caudal rami. Headshield small, not covering cephalic appendages laterally or first tergite posteriorly; width exceeding length. Trunk with approximately twelve tergites; most trunk limbs equal in size.

Holotype.—USNMP 124173, concretion with counterparts.

Other Material.—SDSNH 28251a,b,c 28252, 28253, concretions with counterparts.

Type Locality.—29°59'23"N, 102°58'52" (grid coordinates 69478/331915); west of Rough Creek; 4300 ft. S, 51 ft. E of Hill 4334, Dove Mountain Quadrangle, Brewster County, Texas (Fig. 2A, B).

Stratum.—Tesnus Formation, Upper Mississippian.

Remarks.—This diagnosis expands considerably on those by Brooks (1955), Schram et al. (1986), and Schram (1986). These earlier works were based entirely on the incomplete holotype of *T. goldichi* and did not describe the dorsal ramus of the antennule, the protopod and exopod of the antenna, the base of the mandible, the rami of the maxillule, maxilla, and maxillipede, all but the distal end of the exopede, ventral sclerites, the caudal rami, and juveniles. Our understanding of the fundamental structure of nearly all previously described appendages has been completely revised.

We believe it necessary to provide detailed descriptions of the individual specimens given the controversial nature of the anatomy of this species as well as to provide the details concerning the changes we have made in previous descriptions of this *T. goldichi*. Very little has been retained from previous works, aside from the overall form of the species.

Description.—The following examination of the available fossils uses the conventions established under Materials and Methods.

SDSNH 28252 (Figures 4–8)

The concretion that this specimen occupies was found *in situ* near the top of the shale bed. When first cracked open with a hammer, the concretion split so that very little of the animal was exposed on both the part and counterpart (Fig. 4B, shaded area). Subsequent preparation of the part revealed a nearly complete, well-preserved, juvenile individual. The overall body shape and arrangement of limbs indicate a position at burial with the animal resting somewhat obliquely on its left ventral surface, exposing most of the appendages of the right side, and exhibiting little distortion except flattening (Fig. 5).

The most anterior part of the headshield is poorly preserved. The counterpart presents an isolated fragment of the posteromedial

TABLE 1. Measurements of *Tesnusocaris goldichi* specimens in mm. Antennule length for USNMP 124173 is for the ventral branch; antennule length for SDSNH 28852 is for the dorsal branch.

Specimen	Head length	Head width	Body length	A1 length	Length of caudal rami	T1 length	T2 length	T3 length	Trunk segment no.
USNMP 124173	19.7	16.5	82.6+	58.4	—	—	—	—	22+
SDSNH 28851a	4.3	4.7	≈25.5	—	—	—	—	—	13
SDSNH 28851b	≈5.6	5.4	—	—	—	—	—	—	?
SDSNH 28852	7.3	≈7.0	31.0	18.0+	0.95	1.3	1.8	2.2	12

portion of the anterior headshield lobe. On the part, a tenuous outline of the anterior headshield is preserved and is slightly more defined at the right margin, where a faint suggestion of facets may indicate the right eye (Fig. 4B, RE?). An area at the left edge of what appears to be the anterior headshield (Figs. 4B, 6A, AHS?) alternatively might be part of the left antennule.

The part reveals much of the head. The flagellum of the dorsal ramus of the right antennule (RA1D) is poorly preserved on both part and counterpart, but the left dorsal ramus (Fig. 4B, LA1D) is clearly preserved (Fig. 6A). Four segments (.1–.4) appear to constitute the large peduncle, though the first segment may be the dorsal bifurcation of the protopod as it appears in the Nectiopoda (Fig. 25A). An apparent arthrodial membrane between the third and fourth segments may represent an additional podomere. The peduncle supports a distinctive flagellum on which at least 100 annulated joints are well preserved. The annulations are quite distinct, with the distal edges free from subsequent rings. A slight, but distinct, medial ridge extends the length of the flagellum on the dorsal surface. No clear indication of setae is visible, though faintly preserved annular divisions of the right ramus lateral to the dorsal ridge have the appearance of setae. The left flagellum tapers only slightly along its considerable length, and was apparently much longer than the body. The ventral ramus is not clearly preserved but may be present in the confusion of features at the lateral edges of the headshield, especially on the left side.

The main part of the headshield is well preserved only at the anterior and posterior edges and the right posterolateral corner. The overall shape is rectangular, with length slightly exceeded by width. A number of confusing features evident in this area may represent dorsal furrows or ventral structures impressed from beneath. The right side of the cephalon is completely exposed, though structures in this area are poorly defined and appear to have been shifted to the right. The headshield is flexed ventrad slightly in relation to the trunk, despite dorsoventral flattening of the entire specimen.

No clear preservation of antennae, labrum, or mandibles is present. A small, faint object (LM?) appears dark under alcohol immersion at high magnification (100×) is the correct size, shape, position, and orientation to be the lacinia mobilis of the left mandible, since it closely resembles similar structures of nectiopodan mandibles (see Schram et al. 1986). Unfortunately, recent oxidation has made this feature nearly impossible to see, and it soon may disappear completely. The right maxillule (RMx1) is poorly preserved with only the region of primary flexure visible (Fig. 6B). The proximal section of the maxillule appears to be cylindrical, with a blunt ridge on the dorsal surface. The distal section (Fig. 4B, RMx1.5) begins as a similar ridge but flares abruptly on the ventral side. The distal elements are not preserved. The most basal part of the limb is also missing, but under high magnification there is a faint suggestion of short, stout setae beginning at the flexure and extending along the ventral edge of the limb. These reach back to the base of the maxilla in rows approximately indicated by dots on the drawing. The presence of these setae and similar ones on the two succeeding limbs is uncertain, since they are nearly as small as the texture of the matrix and cannot be distinguished reliably from artifacts of preservation or preparation.

The right maxilla (RMx2) is present on both part and counterpart. The first segment is not well preserved, being somewhat obscured by the edge of the cephalon, but appears to be fairly wide and short (Fig. 6B). The second segment (.2) is clearly evident and is barely longer than wide. The third and fourth segments appear fused on the part (where the suture is not preserved) but are separate on the counterpart (where the division is indistinct). The fourth segment (.4) appears to be the longest one on the maxilla and is developed dorsally as a blunt ridge. The ventral surfaces of the third and fourth segments bear several modest spines or robust setae. Two of the spines apparently are borne on the third segment and two on the fourth, followed by two more stout ones at the middle of the fourth segment. Distal to the maxilla's principal flexure, the fifth and sixth (.6) segments are twice as long as wide, strengthened by a dorsal ridge, and armed ventrally with many small or modest spines. Only the proximal portion of the seventh segment (RMx2.7) is preserved, the distal part of the limb being indicated only very faintly.

The form of the right maxillipede (RMxp) closely resembles that of the maxilla (Fig. 6B). The first segment is quite indistinct. The second segment (.2) is well preserved and has both a dorsal ridge (as do all the segments of this limb) and five ventral spines of modest size. The third segment is long and has one or two large spines and four modest-sized ones. The suture with the fourth segment is distinct on the part only, with the fourth segment bent slightly dorsad. As with the maxilla, the third and fourth segments of the maxillipede are fused in nectiopodans. The fourth segment (.4) is relatively short, perhaps because of distortion, and has six small spines along the ventral edge. Distal to the principal flexure, the ventral edge of the limb is not preserved. The fifth segment is quite long and has a faint transverse crease near the proximal end that appears to be diagenetic. The sixth podomere (.6) is twice as long as wide. The seventh segment (RMxp.7) is not preserved distally, nor is the remainder of the limb. The maxillipede is situated in a gap between the posterior headshield and the first tergite. The left side of this gap appears well defined and may indicate the presence of a vestigial tergite, though there is no other evidence to support this possibility.

The first clearly defined tergite (T1) is short and no wider than the cephalon; it apparently lacks well-developed pleura. The left

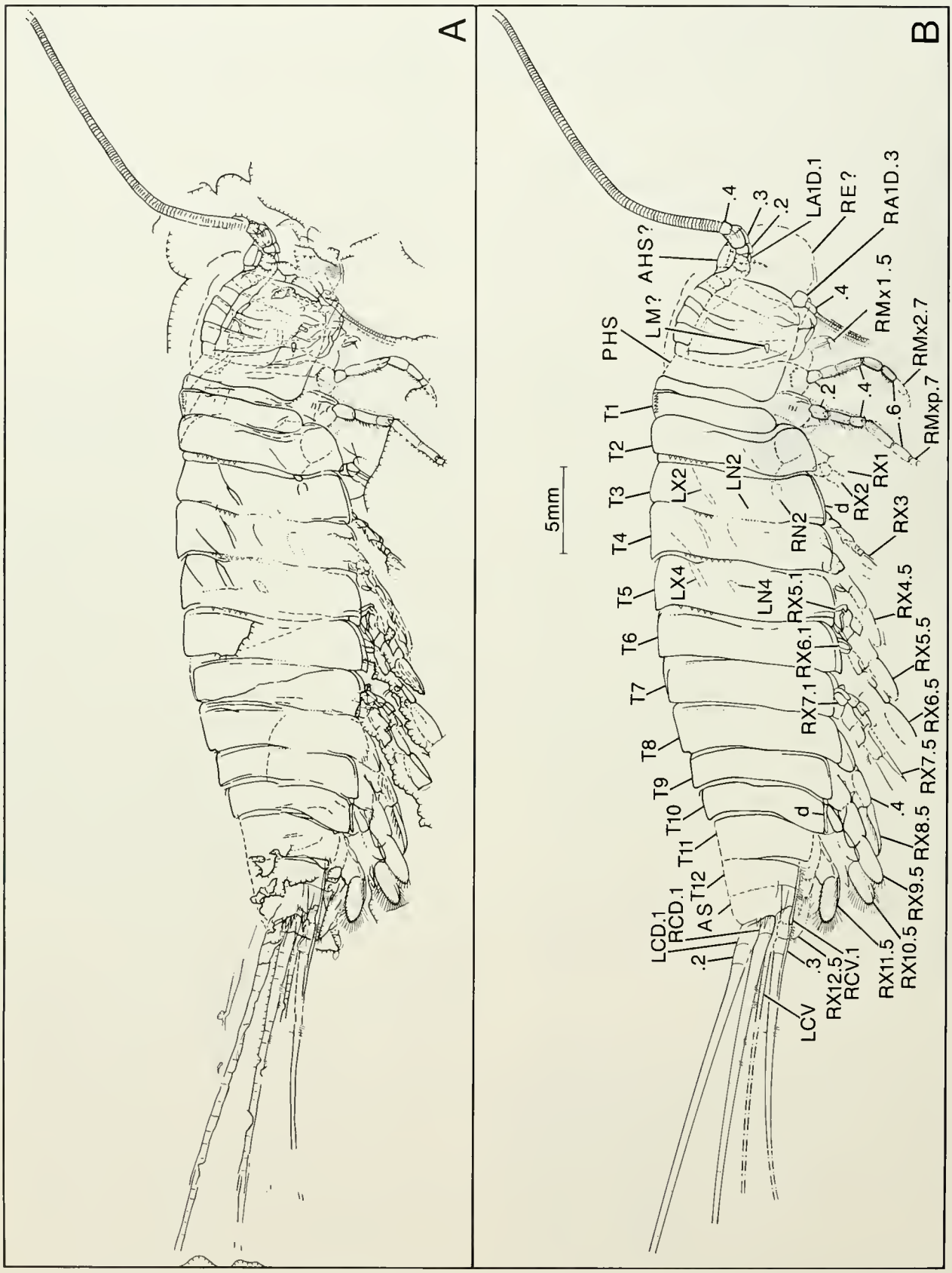

Figure 4. *Tesnusocaris goldichi*, camera lucida drawings of SDSNH 28252. A, part, with shaded areas indicating locations of reddish stain on specimen; B, partially reconstructed, dorsal-oblique view of juvenile Tesnusocaris drawn as viewed at 12× magnification; shaded areas are those preserved on the counterpart.

Figure 5. *Tesnusocaris goldichi*, SDSNH 28252, general view, 1.5×.

lateral margin of this tergite appears to be serrated. Portions of the posterior margins of the next four tergites (T2–T5) also bear faint indications of denticulae. The second through tenth tergites (T2–T10) have well-developed pleura, and several have a distinct marginal ridge laterally (Fig. 7A). Although the preservation of the tergites appears to be nearly complete, the distortion of their left sides suggests that the dorsal surface was slightly convex in cross section, with the pleura directed ventrolaterally. The second through eighth tergites (T2–T8) are much wider than the headshield, but the ninth through twelfth (T9–T12) progressively diminish to a width smaller than the headshield's.

The trunk limbs of *Tesnusocaris* are unusual and require a special terminology. Each trunk segment bears two sets of uniramous limbs, a condition we refer to as duplopody. We have coined the terms "endopede" and "exopede" to emphasize the distinct mesial and lateral positions of these limbs and their probable homology with the rami of the typical crustacean limb, e.g., as seen in the Nectiopoda (Fig. 25B). The nectiopodan trunk limb consists of a ventrolaterally inserted protopod (often divided into a coxa and a basis in other crustacean classes) that distally supports both a mesial endopod and a lateral exopod. In *Tesnusocaris* (Fig. 26B) there appears to be ample evidence of two pairs of distinct uniramous limbs on each trunk segment in each of the available specimens.

The right-hand series of exopedes generally is well preserved. These limbs are broad paddles. The first two limbs (RX1, RX2) are very indistinct (Fig. 7A), and the second apparently overlaps the preceding one. The third exopede (RX3) appears fragmented (Fig. 4A). The coxae (Fig. 7B) seem to be preserved at the posterolateral corners of tergites 4 and 5 (RX4, RX5.1), whereas the coxae are located in a slightly more anterior position on tergites 6 and 7 (RX6.1, RX7.1). These limbs seem to have been shifted slightly to the right, and either exopedes 4 and 5 have been moved posteriad in relation to their tergites, or tergites 6 and 7 have been pushed anteriad; the former condition seems more likely. Because of the angle at which the coxae are preserved, little information can be deduced concerning their overall structure; each appears to have a ridge on the anterolateral surface. The exopedes associated with tergites 8 through 10 (RX8–RX10) appear to insert more ventrally on the body than do the preceding ones, so that only the distal three podomeres are visible on these limbs (Fig. 8A). Since the latter segments are the most clearly preserved examples of the entire series, it is convenient to begin a description of the rami with the distal segments.

The distal three podomeres of exopedes 8 through 10 are of similar size and shape, being flat ellipses nearly twice as long as wide. The distal segment (.5) at least is fringed with moderately long, stiff setae. The anterior margin of this podomere on the eighth and eleventh limbs (RX8.5, RX11.5) is folded back dorsally, indicating that the cuticle was thin and flexible. No setae are visible on the more proximal segments, but their anterior edges bear marginal flaps that appear to be folded back in some instances (Fig. 8A). The posterior edge of each segment broadens distally into a large lobe. This lobe on the penultimate segment of the ninth exopede (RX9) can be seen to narrow proximally, with an articular piece filling the resulting gap between it and the next most proximal segment. The eleventh and twelfth exopedes (RX11, RX12) are progressively smaller in size, and the latter is very poorly preserved, being represented by little more than a few setae at the distal tip of the limb and at the posterolateral corner of the penultimate segment.

The total number of exopede podomeres is not clear from these limbs, since the anterior six exopedes (RX1–RX6) are poorly preserved and the posterior six (RX7–RX12) are basally obscured by the pleura. The anterior exopede series could be interpreted as having six or more segments, and the posterior ones as few as three. Fortunately, there is one limb (RX11) on specimen SDSNH 28251a (Fig. 10) that indicates the actual number is five. Between some of the exopedes (e.g., RX7, RX8) the presence of isolated short segments with pointed corners apparently represents portions of the more ventrally located endopedes, which appear to interleaf with the exopedes to some extent. On the third through sixth tergites (T3–T6), as well as more faintly on the others, the limbs of the two endopedal (LN, RN) and left exopedal (LX) series can be seen impressed through the tergites (Fig. 7C). On the fifth tergite (T5) these appear to represent the proximal sections of the rami belonging to the fourth segment (T4). In this case the limbs seem to insert near the intersegmental junction. These limbs appear to be well separated laterally in evenly spaced rows that have been shifted substantially to the right, suggesting a flexible and convex ventral surface.

SDSNH 28252 is the only specimen of *Tesnusocaris* in which the terminus of the body is preserved. The division between the twelfth tergite (T12) and anal segment (AS) is not clear, except along the right edge (Fig. 8A). The last two segments are short, but the preceding eleventh segment (T11) seems longer. The precise shape of the anal segment is unclear but appears to be a truncated cone, somewhat rounded posteriorly on the dorsal surface. There appear to be at least three dorsal spines of varying lengths at the posteromesial edge of the anal tergite, though these also may be artifacts of compression. There is also a strong lateral ridge with modest spines (?) on the anal and twelfth segments, and this appears to be continuous with a similar ridge on the right ventral caudal ramus (RCV). This may be the result of diagenetic wrinkling.

Four large caudal rami extend posteriorly from the end of the anal segment (Fig. 8B). Although all four are incomplete, it appears that the dorsal pair (LCD, RCD) probably were somewhat longer than the total body length, and the ventral pair (LCV, RCV) may have been nearly equal to the body length. The bases of the rami

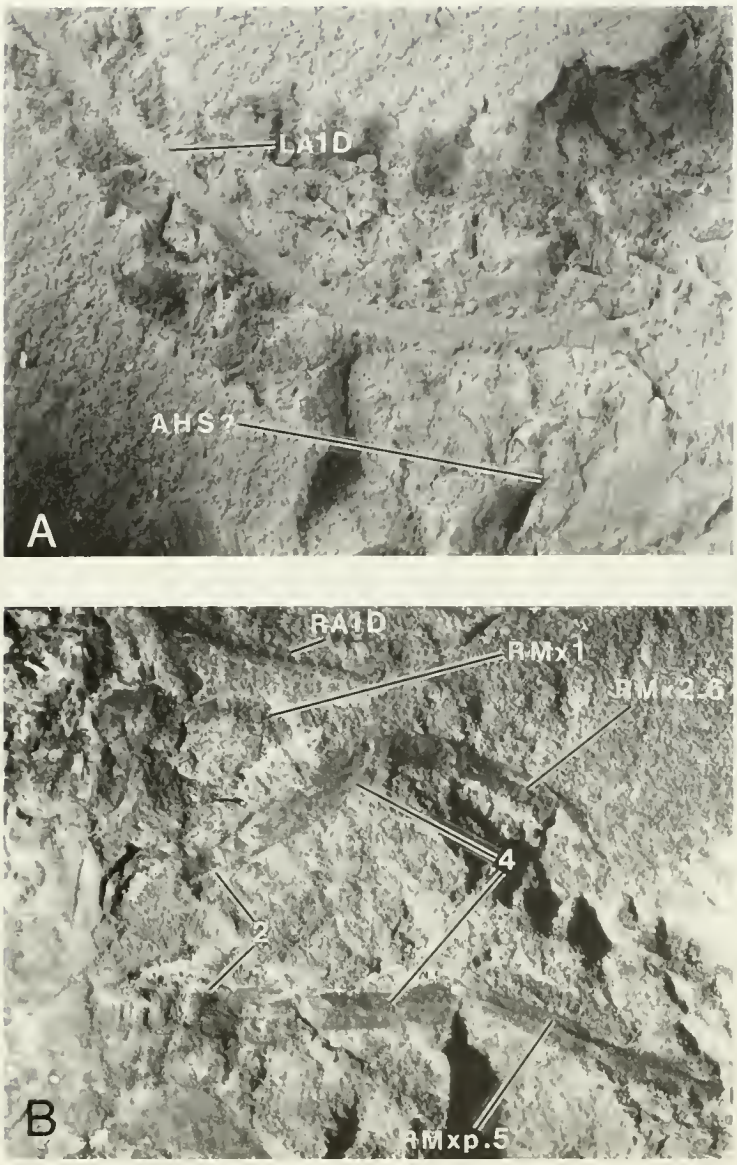

Figure 6. *Tesnusocaris goldichi*, SDSNH 28252. A, closeup of left antennule, 8×; B, closeup of right postmandibular mouthparts, 10×.

converge and are composed of at least one (RCD.1) to three ([RCV].3) large segments. More distally, there are many faint annulations that appear to divide the rami into segments approximately twice as long as wide. Small clusters of short, faint spines on the lateral edges of the right dorsal and ventral flagella (RCD, RCV) suggest that they were spinose throughout their length, at least laterally. A single spine is preserved mesially on the right ventral ramus (LCV). As mentioned previously, these spines appear to be associated with a lateral ridge on the proximal portion of the right ventral ramus.

Areas composed of reddish clay (Fig. 4A, screen) lying along the left margin of the twelfth segment (T12) and parallel to the left dorsal ramus (LCD) are of unknown significance.

SDSNH 28251 (Figures 9–13)

This concretion (Fig. 9) was collected in situ near the bottom of the shale bed 5. It broke into four pieces when cracked; both part and counterpart were fractured along a diagonal line separating two distinct fracture planes. The fortuitous splitting of the concretion on two planes revealed the preservation of at least two and probably three animals (SDSNH 28251a, b, c). The two sections of the part and counterpart were subsequently glued together to facilitate study. Although the overall preservation of the fossils is poor and difficult to interpret, close study and analysis reveal that certain structures are remarkably well preserved and add crucial details to our knowledge of this species. The three animals in this concretion will be described separately.

SDSNH 28251a (Figs. 10–11).—This animal is about 60% the size of SDSNH 28252 (Table 1), which it resembles in providing a mainly dorsal preservation (Fig. 4). The distortion and spatial relationship of the part and counterpart suggest that the animal was lying on its ventral surface anteriorly, leaning slightly on the right side, with the trunk twisting clockwise posteriorly to lie on its left ventral side. The anterior headshield lobe (Fig. 10, AHS) is large but indistinctly preserved (Fig. 11A). The left eye (LEye) is fairly well preserved with a few facets visible around the edges in a reddish stain (Fig. 10, screen). The lobe appears to protrude slightly anteriad, and there are lateral extensions on the posterolateral corners, giving the anterior headshield lobe a broadly triangular outline nearly filled by the enormous eyes. Faint suggestions of limbs protrude from both sides on the counterpart and presumably indicate the presence of the antennules (RA1).

The remainder of the headshield is much broader than long and subrectangular in outline; parts of the right side are indistinct. The anterior margin protrudes slightly between the eyes, and a definite cervical groove is visible about midlength (Fig. 11A). The cervical groove divides the middle (MHS) from the posterior headshield (PHS), though it is unclear just where the mandibles lie relative to the groove. There are suggestions of limb insertions at the level of both the cervical groove (probably indicating the mandibles) and posterior margin of the headshield (probably the maxillipedes). The headshield exclusive of the anterior lobe appears to be somewhat distorted.

The faintly preserved first tergite (T1) appears to be reduced, being short and not nearly as wide as the headshield. Its anterior edge is obscured by the posterior margin of the headshield, and the tergite seems to have been pushed posteriad so that it partly overlies the anterior margin of the second tergite (T2). The latter is indistinct but conforms well to the shape of this tergite in SDSNH 28252 (Fig. 4, T2), with prominent pleura extending beyond the lateral edges of the headshield. The third tergite (T3) is faintly preserved only along the left side, and the fourth (T4) is barely visible. The remaining tergites are not preserved, but the series of preserved limbs suggests that the full length of the trunk is essentially complete.

The most prominent features of this specimen are the distinct tan-colored clay clasts that appear along both sides of the trunk (Fig. 10, screen; Fig. 11B). A careful study of the relationship of these clasts to the few limbs that are clearly preserved and the scarps that appear to connect them with the region of the anterior tergites allows some conclusions regarding the significance of these structures to be drawn. It seems that the scarps define an intercoxal space (IcS) that occupies the ventral midline (Fig. 11B). The left scarp appears to run along the mesial edge of the left endopedal coxae (LN4–LN13). A similar scarp on the right posterior region

Figure 7. *Tesnusocaris goldichi*, SDSNH 28252, 10×. A, right anterior trunk just posterior to maxillipede with endopede pressed from below on the third tergite; B, right side of trunk along the middle of the body showing tergites and laterally extending exopedes; C, left side of trunk with exopede and endopede pressed from below on tergites.

appears to delineate the mesial edge of the right endopedal coxae (RN8–RN13), which are on a slightly lower level than those on the left, especially anteriorly. The clasts appear to be paired and lie immediately anterior and posterior to the posteromesial corner of the coxae. The clasts on the left side thus appear to be associated with the left endopedal coxae (Fig. 11B), those on the right with the right exopedal coxae. Since the left endopedes and right exopedes appear to be preserved on approximately the same level, it can be deduced that the missing left exopedes lie above the fracture plane in the counterpart and the missing right endopedes lie below it in the part. This, in turn, indicates a spatial separation in which the exopedes lie more dorsal than the endopedes and presumably insert on the lateral angles of the ventral body wall. It is also apparent that the left endopedes drop below the fracture plane posteriorly and that the right exopedes and the last few right endopedes (RN12, RN13) rise into it, revealing a clockwise twist to this specimen. The twist and a corresponding curve to the right appear to be strongest in the vicinity of the ninth trunk segment (LN9, RX9).

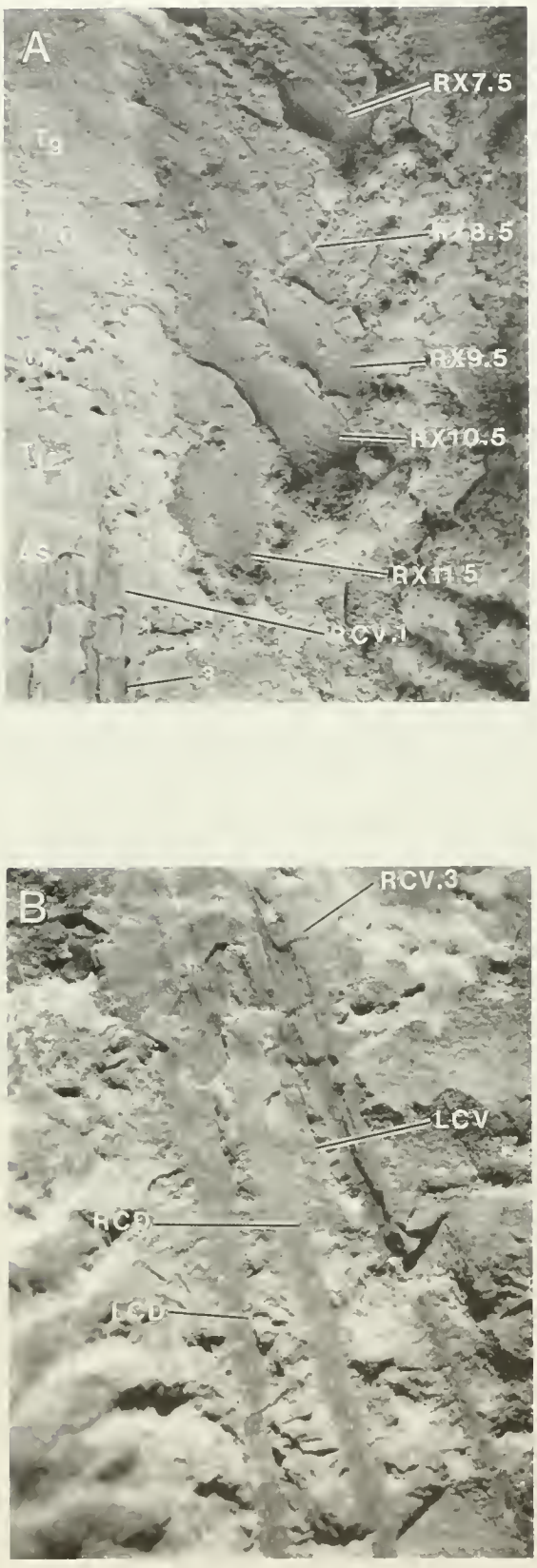

Figure 8. *Tesnusocaris goldichi*, SDSNH 28252, 788.4×. A, right posterior trunk just anterior to the caudal rami, displaying well preserved exopedes; B, most proximal portions of the caudal rami.

The foregoing analysis taken into account, the approximate position of all limbs may be inferred, and consequently the identity of those that are clearly preserved may be reasonably deduced. The leader lines (Fig. 10C) indicate the position of the limb where present and the presumed insertion of the coxa where the ramus is absent (indicated in parentheses). The number of trunk segments inferred on this specimen is thirteen, one more than observed in the larger SDSNH 28252 (Fig. 4). The difference may be the result of either faulty deduction on our part or individual specimen variation. Furthermore, the preservation of the first set of limbs (LX1, RX1) in a position anterior to the first tergite (T1) is reasonable only if the tergite has been displaced posteriorly or the limbs have been displaced anteriorly during preservation. This would indicate that the entire dorsal aspect of this specimen is probably shifted posteriad in relation to the limbs.

Given the rather tentative identity of the few limbs that are preserved, the following conclusions may be drawn. The coxae of the endopedes, with the characteristic bell shape clearly preserved on the holotype (Fig. 14), are apparent on left endopedes 10 and 12 (LN10, LN12), the former with the proximal part of the second podite attached. Endopedal coxae are preserved less distinctly on right endopede 13 (RN13.1) and left endopede nine, the latter with most of the second podite (LN9.2) attached. Although more distal portions of several endopedal rami are preserved, the identity of the segments cannot be specified.

Most of the exopedes on SDSNH 28851A are absent or poorly preserved. On the part, however, right exopede 11 (RX11) presents the clearest view of the proximal portions of an exopede seen on any specimen (Fig. 10A). The mesial part of the coxa is obscured by an overlapping ramus, but the lateral side (RX11.1) is clearly expressed as half of a podite resembling a broader version of the endopedal coxa. The second segment is a short cylinder slightly expanded at each end and probably having a dorsal ridge. The third podite (.3) is larger and broader, with a prominent dorsal crest. On the counterpart, this segment is largely filled by carbonized material, though the exact outline apparently is confused by an overlapping limb. The fourth podite is less clearly preserved but appears to be similar in size and structure to the third. The fifth and last segment (.5) is indicated by the lateral edge of the broad ellipse more clearly preserved on other specimens (Figs. 4, 14). The general outline of this limb is also seen in right exopede 13 (RX13), and the most proximal portion is visible on right exopede 10 (RX10). A carbonized element resembling the third podite is assigned to left exopede 4 (LX4.3?).

SDSNH 28251b (Figs. 10, 12, 13).—This specimen lies very near the terminus of SDSNH 28251a; the two fossils are similar in size (Table 1). At their closest point, the two individuals appear to be in approximately the same plane, and it seems likely that they were in contact at the time of burial. SDSNH 28251b resembles the holotype (Fig. 14) in presenting a view of the ventral surface. The specimen's mouthparts appear to have been exceptionally well preserved, retaining some of their original shape, despite diagenetic flattening. The head and body are slightly curved throughout their length, especially at the juncture of the headshield and trunk, which gives the appearance of twisting clockwise. The greater compression of the animal's left side indicates that the curling was both lateral to the right and ventrad, with the result that the specimen was resting on its right dorsal surface. Considerable distortion and apparent rupture during preservation of this individual have made interpretation of the trunk especially difficult. The most obvious breaks have occurred ventrally between the second and third trunk segments and dorsally between the third and fourth tergites, with the former tergite being pushed up into the fracture plane. Fortunately, the cephalic region is relatively undisturbed.

The anterior headshield lobe (Fig. 10C, AHS) is faintly preserved only on the part, with sections of the lateral and anterior lobe

ERRATA

Grygier, M. J. 1991.

Redescription, Ontogeny, and Demography of Parascothorax synagogoides (Crustacea: Ascothoracida), Parasitic on Ophiophthalmus normani (Ophiuroidea) in the Bathyal Basins off Southern California

Proceedings of the San Diego Society of Natural History 6.

Page 1, column 1, line 3: for five read six.

Page 18, Figure 14, uppermost histogram: partly checkered square above 1 mm mark should be an open square.

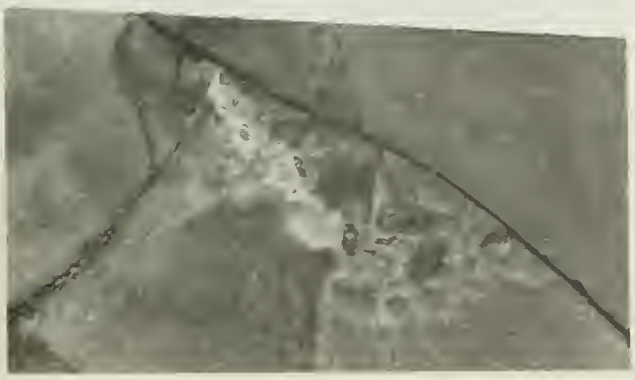

Figure 9. *Tesnusocaris goldichi*, SDSNH 28251, general view, 2.2×.

margins being more defined (Fig. 13A). The eyes (REye, LEye) are poorly preserved and are visible only as relatively small ellipses impressed through the base of the anterior headshield. The anterior region of the middle headshield (MHS) is clearly defined, and its anterior margin protrudes slightly between the bases of the eyes on the part. The right antennule (RA1) extends posterolaterally, but no detail can be seen. The left antennule is faintly preserved in a position that indicates it has been displaced considerably to the rear and possibly detached from its point of insertion. Details are vague, but seem to indicate that the dorsal ramus (LA1D?) is directed posteriorly and the ventral ramus (LA1V?) extends anterolaterally, an arrangement that would require considerable rotation from the position indicated on the holotype (Fig. 14) and the Nectiopoda (Fig. 25A). The actual juncture of the rami is not clearly preserved.

The antennae may be present just posterolateral to the eyes, but their preservation is questionable and the interpretation of this region is not certain. They appear as faint paddle-shaped structures (RA2?, LA2Np?) resembling the antennal endopods of living remipedes, with marginal setae and at least three segments. The left antennal endopod (LA2Np?) appears to overlap distally an even more faintly preserved structure (LA2Xp?) that resembles the large, elliptical, setose exopod of the nectiopodan antenna. If this is the case, and the rami were oriented in life as they are on extant nectiopodan remipedes (Fig. 24A), then the position observed on this fossil would seem to indicate a reversal of the relative positions of the endopod and exopod.

The labrum (Lb) is fairly well preserved (Fig. 13B, C), but it is not as obvious as that on the holotype (Fig. 14, Lb). The labrum is a large subtriangular structure with a bulbous posterior lobe. The [illegible] specimen's mouthparts (Fig. 12) reveals some laterally truncated and appears to have [illegible] mesial end of this structure is hidden, the size, shape, position, and orientation are consistent with the possibility that this represents the base of an incisor process similar to those observed in nectiopodans (Schram et al. 1986). The right mandible also apparently is present on the part, but is largely hidden by the overlapping maxillule (RMx1), from which it is difficult to distinguish separate structures.

The limbs of the posterior cephalon are remarkably well preserved, with the lumina of many individual limb segments lined with black carbon and the sutural septa preserved in solid white quartzite. It seems likely that the carbon residue is associated with remnants of muscle tissue and that the quartzite indicates the distribution of cuticle. The interpretation of this rich detail is admittedly difficult, however, since the basal portions of the limbs are on the part and the distal sections lie on the counter-

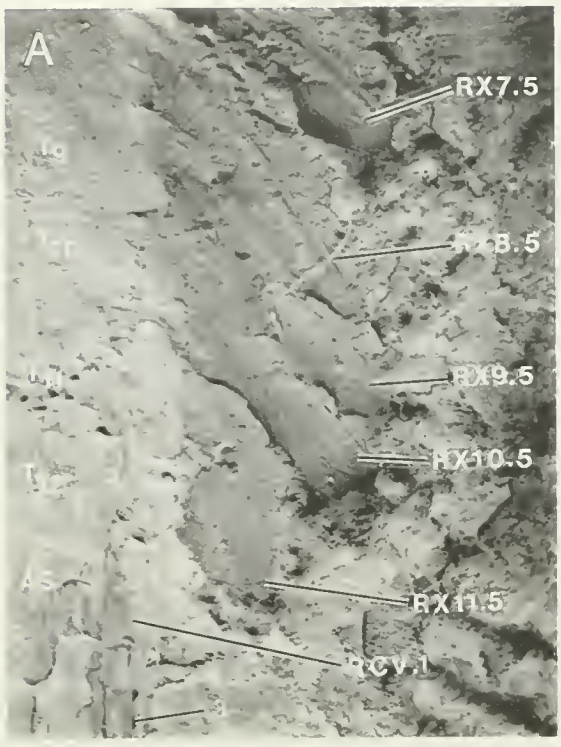

Figure 8. *Tesnusocaris goldichi*, SDSNH 28252, 788.4×. A, right posterior trunk just anterior to the caudal rami, displaying well preserved exopedes; B, most proximal portions of the caudal rami.

The foregoing analysis taken into account, the approximate position of all limbs may be inferred, and consequently the identity of those that are clearly preserved may be reasonably deduced. The leader lines (Fig. 10C) indicate the position of the limb where present and the presumed insertion of the coxa where the ramus is absent (indicated in parentheses). The number of trunk segments inferred on this specimen is thirteen, one more than observed in the larger SDSNH 28252 (Fig. 4). The difference may be the result of either faulty deduction on our part or individual specimen variation. Furthermore, the preservation of the first set of limbs (LX1, RX1) in a position anterior to the first tergite (T1) is reasonable only if the tergite has been displaced posteriorly or the limbs have been displaced anteriorly during preservation. This would indicate that the entire dorsal aspect of this specimen is probably shifted posteriad in relation to the limbs.

Given the rather tentative identity of the few limbs that are preserved, the following conclusions may be drawn. The coxae of the endopedes, with the characteristic bell shape clearly preserved on the holotype (Fig. 14), are apparent on left endopedes 10 and 12 (LN10, LN12), the former with the proximal part of the second podite attached. Endopedal coxae are preserved less distinctly on right endopede 13 (RN13.1) and left endopede nine, the latter with most of the second podite (LN9.2) attached. Although more distal portions of several endopedal rami are preserved, the identity of the segments cannot be specified.

Most of the exopedes on SDSNH 28851A are absent or poorly preserved. On the part, however, right exopede 11 (RX11) presents the clearest view of the proximal portions of an exopede seen on any specimen (Fig. 10A). The

holotype (Fig. 14) in presenting a view of the ventral surface. The specimen's mouthparts appear to have been exceptionally well preserved, retaining some of their original shape, despite diagenetic flattening. The head and body are slightly curved throughout their length, especially at the juncture of the headshield and trunk, which gives the appearance of twisting clockwise. The greater compression of the animal's left side indicates that the curling was both lateral to the right and ventrad, with the result that the specimen was resting on its right dorsal surface. Considerable distortion and apparent rupture during preservation of this individual have made interpretation of the trunk especially difficult. The most obvious breaks have occurred ventrally between the second and third trunk segments and dorsally between the third and fourth tergites, with the former tergite being pushed up into the fracture plane. Fortunately, the cephalic region is relatively undisturbed.

The anterior headshield lobe (Fig. 10C, AHS) is faintly preserved only on the part, with sections of the lateral and anterior lobe

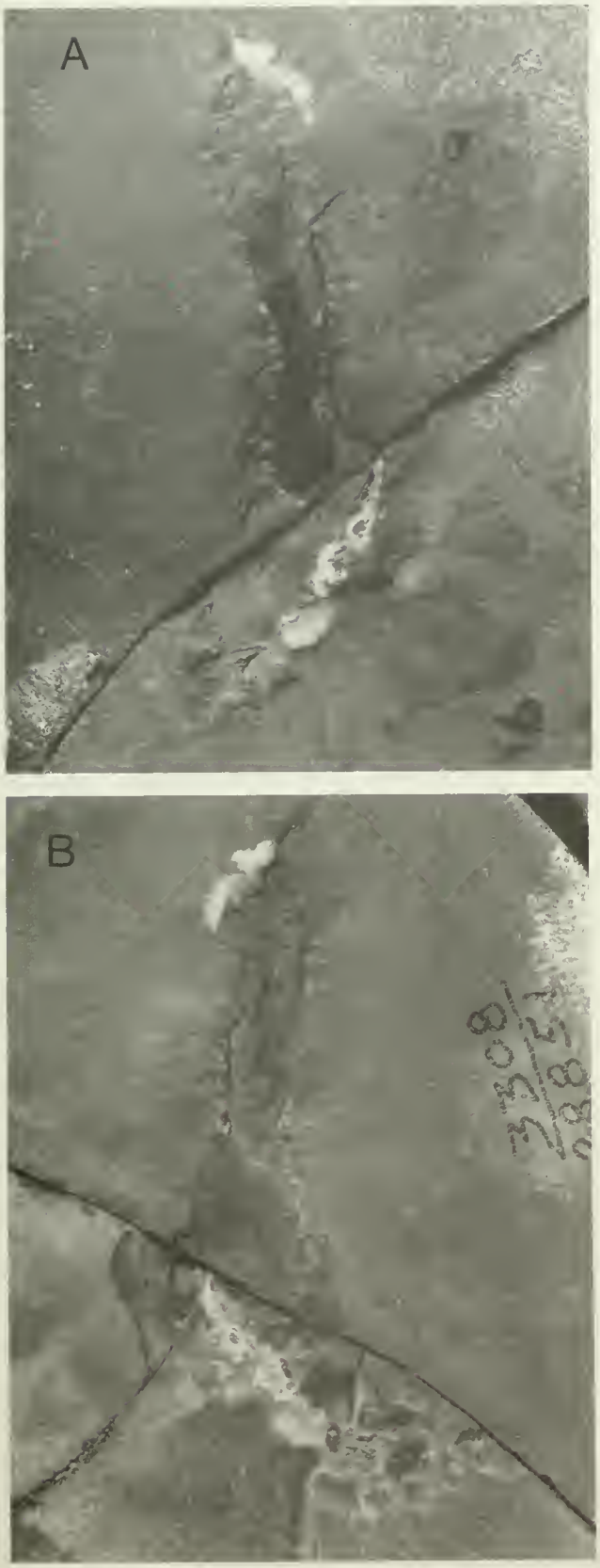

Figure 9. *Tesnusocaris goldichi*, SDSNH 28251, general view, 2.2×.

margins being more defined (Fig. 13A). The eyes (REye, LEye) are poorly preserved and are visible only as relatively small ellipses impressed through the base of the anterior headshield. The anterior region of the middle headshield (MHS) is clearly defined, and its anterior margin protrudes slightly between the bases of the eyes on the part. The right antennule (RA1) extends posterolaterally, but no detail can be seen. The left antennule is faintly preserved in a position that indicates it has been displaced considerably to the rear and possibly detached from its point of insertion. Details are vague, but seem to indicate that the dorsal ramus (LA1D?) is directed posteriorly and the ventral ramus (LA1V?) extends anterolaterally, an arrangement that would require considerable rotation from the position indicated on the holotype (Fig. 14) and the Nectiopoda (Fig. 25A). The actual juncture of the rami is not clearly preserved.

The antennae may be present just posterolateral to the eyes, but their preservation is questionable and the interpretation of this region is not certain. They appear as faint paddle-shaped structures (RA2?, LA2Np?) resembling the antennal endopods of living remipedes, with marginal setae and at least three segments. The left antennal endopod (LA2Np?) appears to overlap distally an even more faintly preserved structure (LA2Xp?) that resembles the large, elliptical, setose exopod of the nectiopodan antenna. If this is the case, and the rami were oriented in life as they are on extant nectiopodan remipedes (Fig. 24A), then the position observed on this fossil would seem to indicate a reversal of the relative positions of the endopod and exopod.

The labrum (Lb) is fairly well preserved (Fig. 13B, C), but it is not as obvious as that on the holotype (Fig. 14, Lb). The labrum is a large subtriangular structure with a bulbous posterior lobe. The enlarged view of this specimen's mouthparts (Fig. 12) reveals some interesting details of the labrum, such as a raised central portion from which several faint ridges extend onto the left side of the posterior lobe; these ridges may represent either sculpturing of the lobe or diagenetic wrinkling of the cuticle. The posterior margin of the labrum is unclear and may be confused with what appear to be underlying mandibular structures.

Only the left mandible (Fig. 12, LMn) is preserved on the counterpart. The spatial relationships involved suggest that this is the interior surface of the mandible, the site of muscle insertions. The anterolateral aspect of this mandible appears lateral to the posterior labral lobe as a rounded structure with a rather complex pattern of carbonization, possibly reflecting sculpturing or diagenetic wrinkling. The mandible is rotated posteromesiad, with the anteromesial edge obscured under the labral lobe. This arrangement confirms the observation that the mandible of *Tesnusocaris* is only partly enclosed in an atrium oris located posterior to the true mouth (Schram et al. 1986). The principal surface structure of the lateral part of the mandible appears to consist of a median ridge extending posteromesially. Posteromesiad, the ridge appears to be continuous with the anterior edge of an uncarbonized structure (IP?), which is laterally truncated and appears to narrow mesially. Although the mesial end of this structure is hidden, the size, shape, position, and orientation are consistent with the possibility that this represents the base of an incisor process similar to those observed in nectiopodans (Schram et al. 1986). The right mandible also apparently is present on the part, but is largely hidden by the overlapping maxillule (RMx1), from which it is difficult to distinguish separate structures.

The limbs of the posterior cephalon are remarkably well preserved, with the lumina of many individual limb segments lined with black carbon and the sutural septa preserved in solid white quartzite. It seems likely that the carbon residue is associated with remnants of muscle tissue and that the quartzite indicates the distribution of cuticle. The interpretation of this rich detail is admittedly difficult, however, since the basal portions of the limbs are on the part and the distal sections lie on the counter-

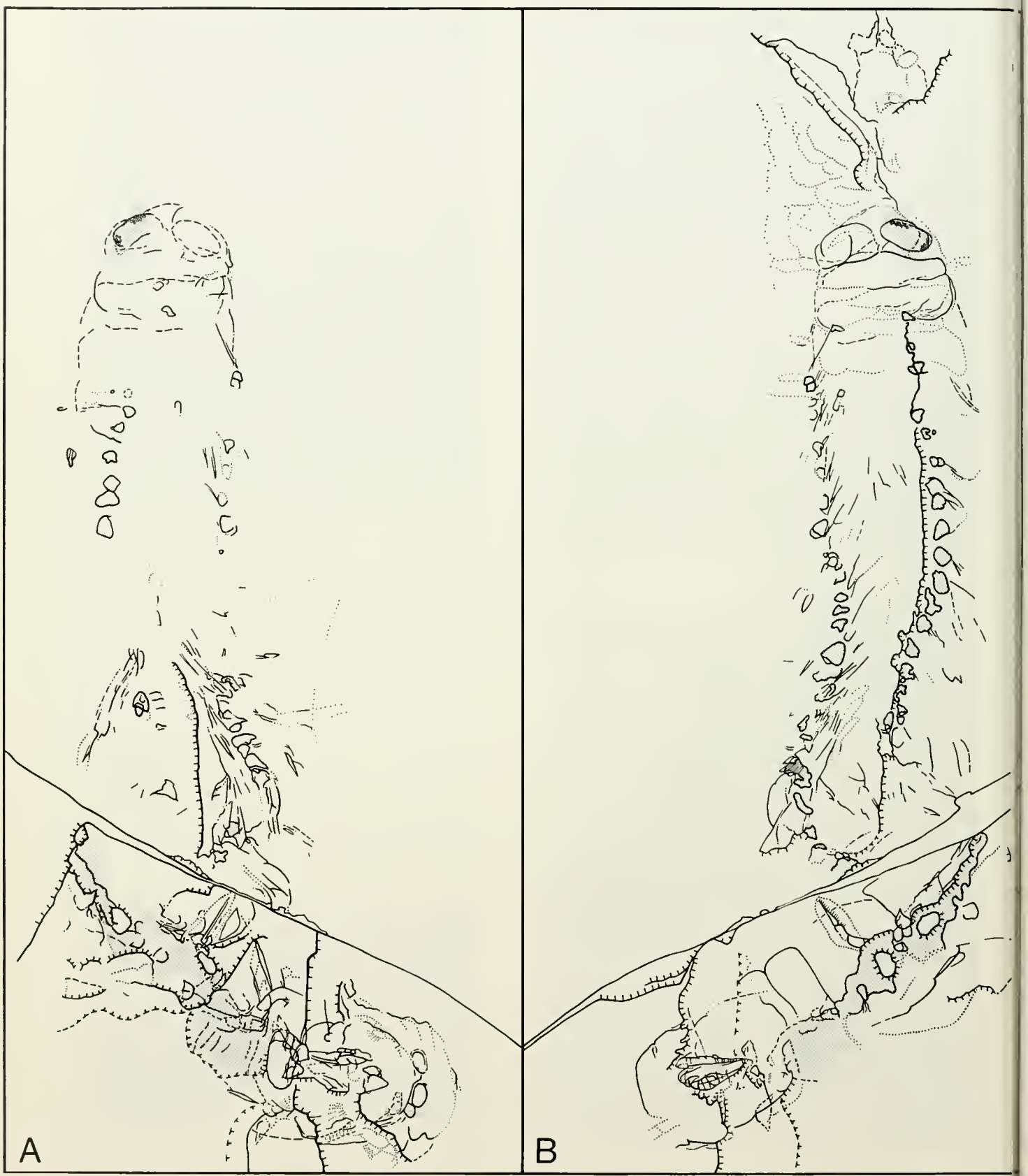
A
B

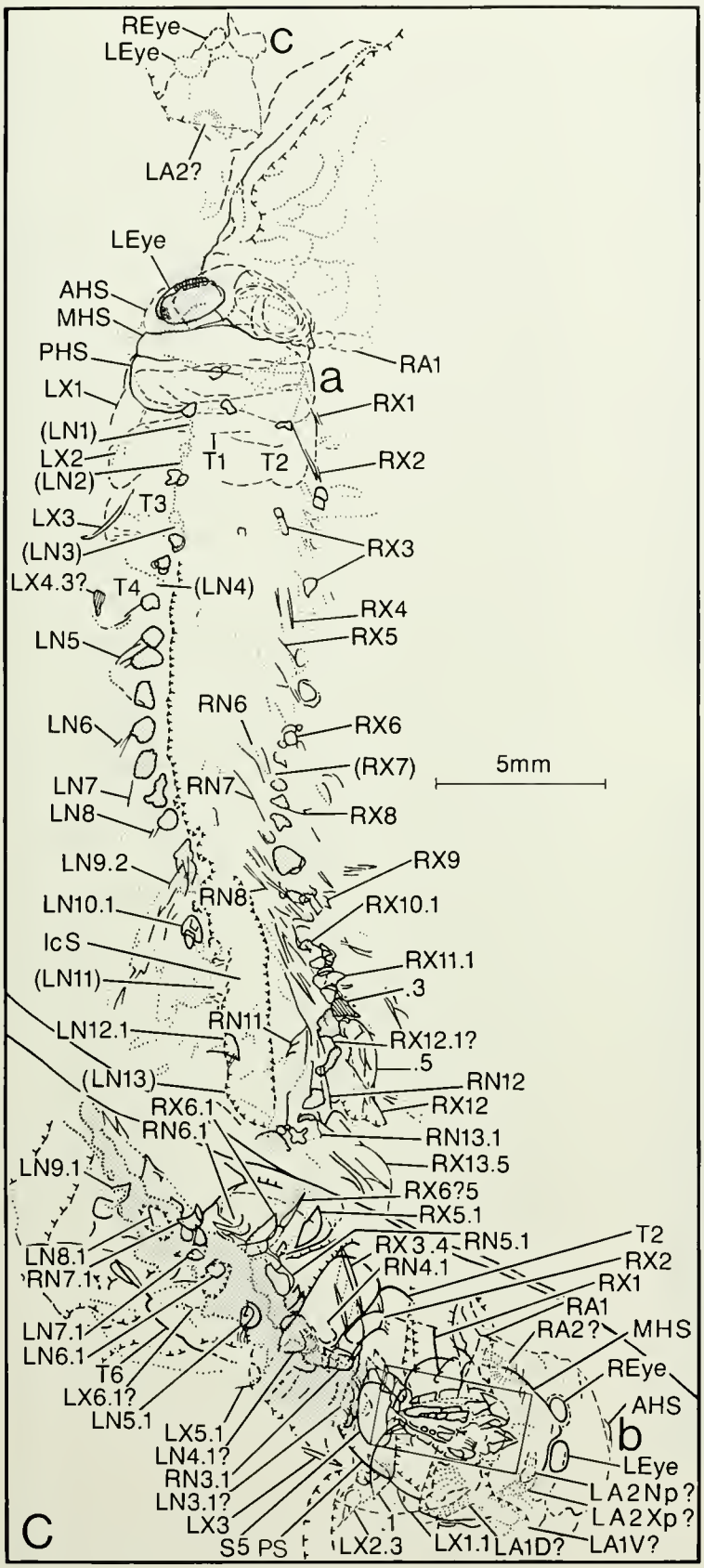

Figure 10. *Tesnusocaris goldichi*, camera lucida drawings of SDSNH 28251. A, part, broken in two sections with 28251a above break and 28251b below the break; B, counterpart, broken in two sections with 28251c visible at the topmost extremity, 28251a just above the break, and 28251b below the break; C, partially reconstructed view of (a) dorsal, (b) ventral, and (c) inverted ventral surfaces of three *Tesnusocaris* juveniles. Shaded areas are areas with reddish stain (around eye) or tan clay clasts; diagonally lined areas have carbonized residue; area enclosed by rectangle (b) is enlarged in Fig. 12.

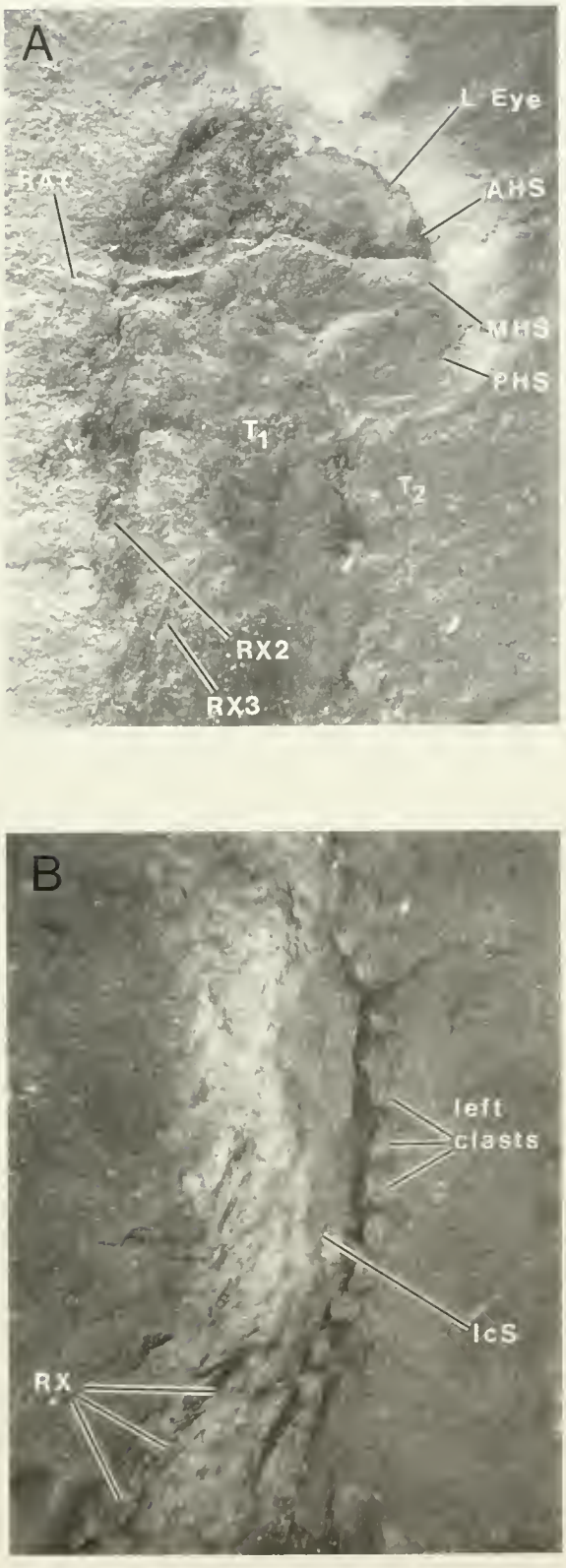

Figure 11. *Tesnusocaris goldichi*, closeup views of SDSNH 28251a. A, head and anterior trunk, 10.8X; B, middle and posterior portions of the trunk, showing clay clasts and leg remnants arranged around the intercoxal space, 6.4×.

part. Only when the two are combined can the structures be interpreted coherently to yield a nearly three-dimensional view of surprising clarity (Fig. 12C). The limbs of the right side are relatively undistorted and are arrayed in a way that the individual components are distinct. The limbs of the left side, however, appear to have projected somewhat vertically at the time of burial, resulting in limbs that overlap each other considerably and that are strongly foreshortened by compaction.

The maxillules are moderate in size. Although the basal segments of the left maxillule (LMx1) are collapsed upon each other, those of the right limb (RMx1) are more clearly displayed (Figs. 12A, C, 13D). The first segments of both limbs meet at the midline as large endites (.1) oriented posteromesially. These endites appear to have a massive rounded base supporting at least six to eight robust spines. The posterolateral edge of the right endite appears to be continuous with a double-edged ventral crest that extends toward the primary flexure or "elbow" of the limb. The second and third podomeres (.2, .3) are short and serve to alter the limb axis from lateral to projecting off the body anterolaterally, with the ventral surface rotated laterally. The second and third segments are not clearly defined, but their presence is inferred by homology with the Nectiopoda. The fourth segment (.4) is large and bears a prominent dorsal ridge; the ventral crest of the second and third podites appears to extend at least to the proximal end of this segment on the right limb. The left limb has a clearly defined septum that appears to divide the fourth segment of the right limb into two equal parts. This may indicate that the fourth segment is an incompletely fused composite of two segments. Since the outline of this septum continues mesiad through the third and second maxillulary segments, it is more probable that this apparent suture is actually related to a structure lying between the proximal and distal parts of the maxillulary ramus. Because of the relative positions of the limbs on the right side, the limb most likely to occupy this position on the left side is the left maxillipede. In this case, the septum is that of the principal flexure between the fourth and fifth podites of the left maxillipede (LMxp.4/5). The principal maxillule flexure is the site of broad articulation between the fourth and fifth podites (RMx1.5, LMx1.5). Beyond the principal flexure, the maxillule is loosely pressed against the more proximal segments, giving the limb a subchelate character. The distal portion of the fifth podomere (Fig. 13D) is large and joins broadly with the shorter, conical sixth podite (.6), which terminates in the short, heavy talon of the seventh segment (.7). The tip of the left maxillule is not clearly visible on the part as shown because it is exposed on a surface that slopes down mesially. To achieve the view shown, the specimen must be tilted considerably before this cryptic structure can be seen. This is the only instance in which we have modified the uncomposited drawings to conform to later interpretation. The most distal portion of both limbs is preserved in the part along with the basal segments, emphasizing the strongly recurved nature of the distal ramus.

The right maxilla is fully preserved (Fig. 13C) distal to the two basal podomeres, which are completely hidden on this specimen but which can be seen on specimen SDSNH 28252 (Fig. 4, RMx2). The third segment (RMx2.3) is long, laterally compressed, and proximally somewhat narrow. This segment is one of the few that is preserved with its outer surface intact. The distal end joins broadly with the fourth podite (.4). These podomeres are fused in modern remipedes (Fig. 25A, Mx2.3), but there appears to be some flexure at this joint on the fossil, and a small projection at the distolateral angle of the third podite may be a condyle. A double-edged crest extends along the lateral edge of both segments, indicating that this is the ventral surface, rotated laterally. The fourth podite is shorter than the third; it is large proximally and tapers slightly distally. The distal aspect angles sharply so that the dorsal (mesial) surface is

much longer than the ventral (lateral) edge, indicating a broad articulation with the fifth segment to form the principal flexure. The nature of this articulation suggests that this limb was subchelate.

The distal portion of the maxilla appears to have been more cylindrical in cross section and oriented with the ventral surface directed ventromesially. The ramus beyond the principal flexure lies on the counterpart and appears to be somewhat foreshortened in comparison with that of SDSNH 28252 (Fig. 4, RMx2), possibly indicating that it was projecting upward at an angle of approximately 40° prior to burial compaction. Beyond the main flexure, the fifth segment (RMx2.5) proximally is broad. It narrows slightly distally and joins the sixth podite with a suture angled so that the ventral edge of the podite is longer than the dorsal. The sixth (.6) and seventh (.7) segments are about as long on the mesial edge as they are wide, with perpendicular sutures between them and subsequent podites. The eighth podite (.8) is shorter than wide and is little more than a ring at the base of the terminal segment. The ninth podomere (.9) narrows abruptly to a point where it curves slightly.

Much of the left maxilla was lost during preparation. Though distorted and fragmentary, the outline of the left maxilla (LMx2.4, .3) conforms well to the description of the right limb. Only the most distal portions beyond the middle of the seventh podomere are clearly preserved. The aspect is apparently more dorsal than on the right limb, giving a different perspective on the terminal segment. In this case, the tip (LMx2.9) appears broad and straight rather than tapered and curved, indicating that the overall shape was that of a wide scoop. At very low angles of illumination under high magnification (100×), a series of distal highlights suggests the presence of two short lateral ridges, the mesial one appearing more robust, and four longer central ridges. These ridges may represent a claw similar to the scooped comblike tip found on the maxilla of the nectiopodan *Speleonectes* (Schram et al. 1986). It should be noted, however, that these structures on the fossils are faint at best, and the authors disagree as to the validity of this observation (FRS questions it).

The maxillipedes appear to resemble the maxillae, though they are larger and less completely preserved. The juncture of what appears to be the first and second podomeres (LMxp.1?, .2?) is incompletely preserved on the left limb. The more distal portion of the limb, except the last two podomeres, is only faintly evident. It seems likely that the carbonized strip partly overlapping the mesial edge of the right maxilla (RMx2.3, .4), preserved on the counterpart, belongs to the right maxillipede. The presence of quartzite bands resembling sutural septa in this area suggests that this strip may represent the mesial edge of the first through third podomeres of the right maxillipede. In any case, the right third podomere (.3) seems to be long and apparently projects just beyond the principal flexure of the right maxilla, where it joins broadly with the next podomere along an angled suture. Parts of the fourth segment of the right limb (RMxp.4) appear to be preserved on the part. Rather wide proximally, this podomere tapers gradually toward the main limb flexure. The overall length appears to be shorter than that of the third segment, and the limb seems laterally flattened in this area, as is the case with the maxilla. A double-crested ridge, resembling those of the more anterior limbs and the ventral endite crests of living remipedes (Schram et al. 1986), extends along the lateral edge and indicates an outward rotation of the ventral surface.

The right maxillipede beyond the principal flexure is undistorted and fairly well preserved laterally. It appears in lateral aspect as a long rigidly curved ramus with angled septa (Fig. 13B). This part of the limb is either extremely narrow or the mesial edge is incomplete. In all of these respects, this part of the limb closely resembles that of the large nectiopodan *Godzillius robustus* (Schram et al. 1986: Fig. 32B), though the two proximal segments are fused in the modern form. This suggests that the maxillipedes of *Tesnusocaris* were subchelate rather than prehensile. The fifth podomere (.5) apparently is the longest, with each succeeding podomere decreasing slightly in length. The eighth segment (RMxp.8) is long in comparison with that of the maxilla. The full length of the eighth podomere is preserved on the left limb (LMxp.8), along with the attached ninth podomere (.9). The terminal segment of the right limb (RMxp.9?) appears to be detached and wedged between the bases of the mouthparts and first trunk limbs. Both are similar in shape to the lateral view of the right maxillary claw, though perhaps slightly more slender.

This is the only specimen in which the first few trunk limbs are preserved with any clarity. The mouthparts and first endopedes appear to have been displaced posteriorly during preservation, with the first pair of endopedal coxae pushed back so that they partly overlap the second pair. It may be that this reflects the natural condition to some extent, in view of the flexure evident at the juncture of headshield and trunk in this and other specimens (e.g., Fig. 4). Similar overlap of endopedal coxae can be seen posteriorly on the holotype (Fig. 14; e g., RN13.1, RN14.1). In any case, it is clear that the mouthparts and first two pairs of endopedes also are crowded together mesially. It would appear, however, that this mesial crowding may be secondary since both SDSNH 28252 (Fig. 4) and the holotype (Fig. 14, IcS) indicate a wider midventral separation between the mouthparts and endopedes.

The first endopedal coxae are preserved incompletely on the counterpart, where the right one (RN1.1) demonstrates the bell shape typical of these podomeres (Fig. 10, Fig. 14; N.1). There appears to be a short point or possible condyle on the posterior margin of this coxa somewhat lateral of center. The posterior margin of the left second podomere (.2) is poorly preserved on the counterpart, followed by five setae that seem to belong to the posterior margin of the third segment, though they partly overlap the posterior of the left second endopedal coxa (LN2.1).

The second pair of coxae are more clearly preserved on the part (Fig. 13C), which demonstrates their position beneath the first pair of coxae. They appear to be slightly longer and narrower than the first pair, and closely resemble the form seen on all other endopedal coxae. A marginal spine or condyle is clearly evident on the left coxa. A similar protuberance is present on the right coxa (RN2.1) and seems to be covered by tissue connecting the coxa and second podomere (.2), though the apparent connection actually may be the edge of the sternite (S5) impressed from beneath. The front of the second podomere (.2) slightly overlaps the posterolateral margin of the coxa, providing contact with the possible condyle. Only the posterior margin of this segment is preserved on the left limb (.2), where four setae are visible mesially. The second and subsequent podomeres are more clearly preserved on the right limb. The coxae lie parallel to the trunk axis, but the right ramus extends posterolaterally. The second segment is slightly wider than long, though the preserved mesial edge may be incomplete. The lateral margin is developed as a prominent crest with a large, posterolaterally directed spine. The third podomere (.3) is also well preserved and similar to the second, though broader mesially. The fourth segment (.4) is not as clearly defined, but appears to be a slightly larger version of the third, with the lateral crest set off from the rest of the podomere by a ridge, a feature prominently displayed on the more distal endopedal podomeres of the holotype (Fig. 14). The remainder of the limb is missing. Although several succeeding endopedal coxae are readily identified by their shape, the trunk segment to which each belongs cannot be determined with certainty, and none has a clearly defined ramus.

Although few of the exopedes are well preserved, important details can be gleaned by studying some of them (Fig. 10). The first exopedes are indistinctly preserved just behind the swept-back antennules (RA1, LA1D?). The right one (RX1) is the better de-

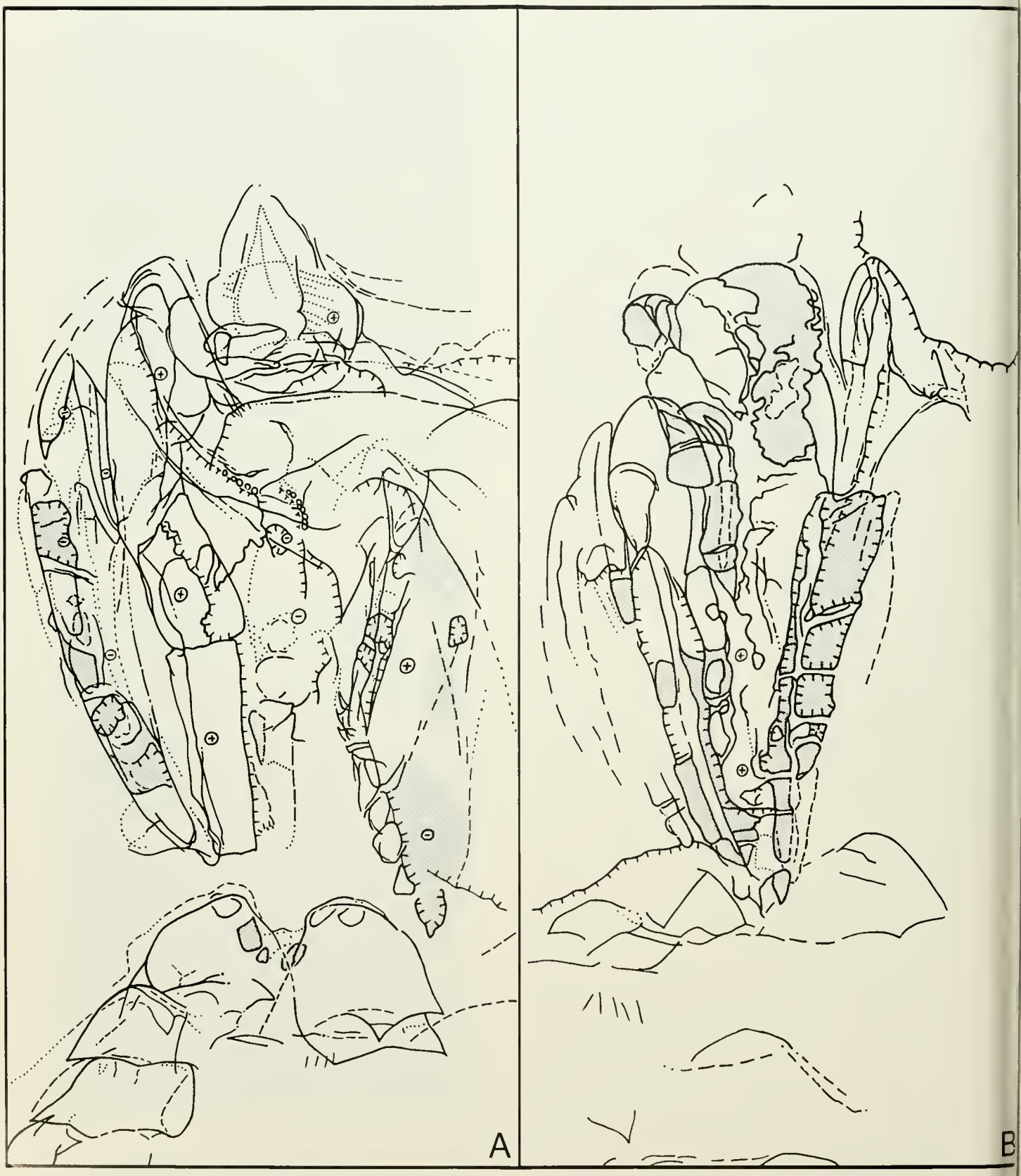
A
B

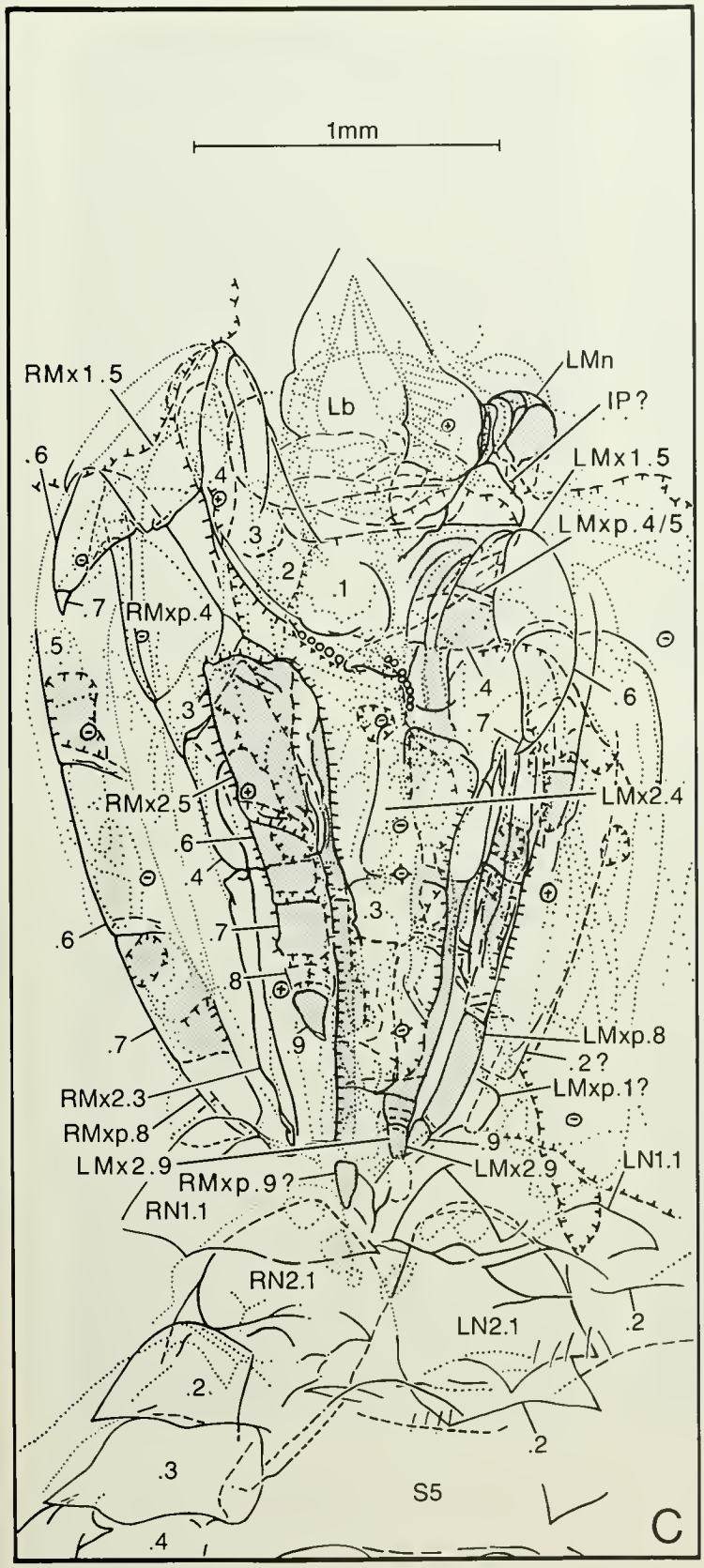

Figure 12. *Tesnusocaris goldichi*, camera lucida drawings of detail of SDSNH 28251b. A, part; B, counterpart; C, partially reconstructed mouthparts and anterior trunk of juvenile *Tesnusocaris* in ventral view. Shaded areas have carbonized residues.

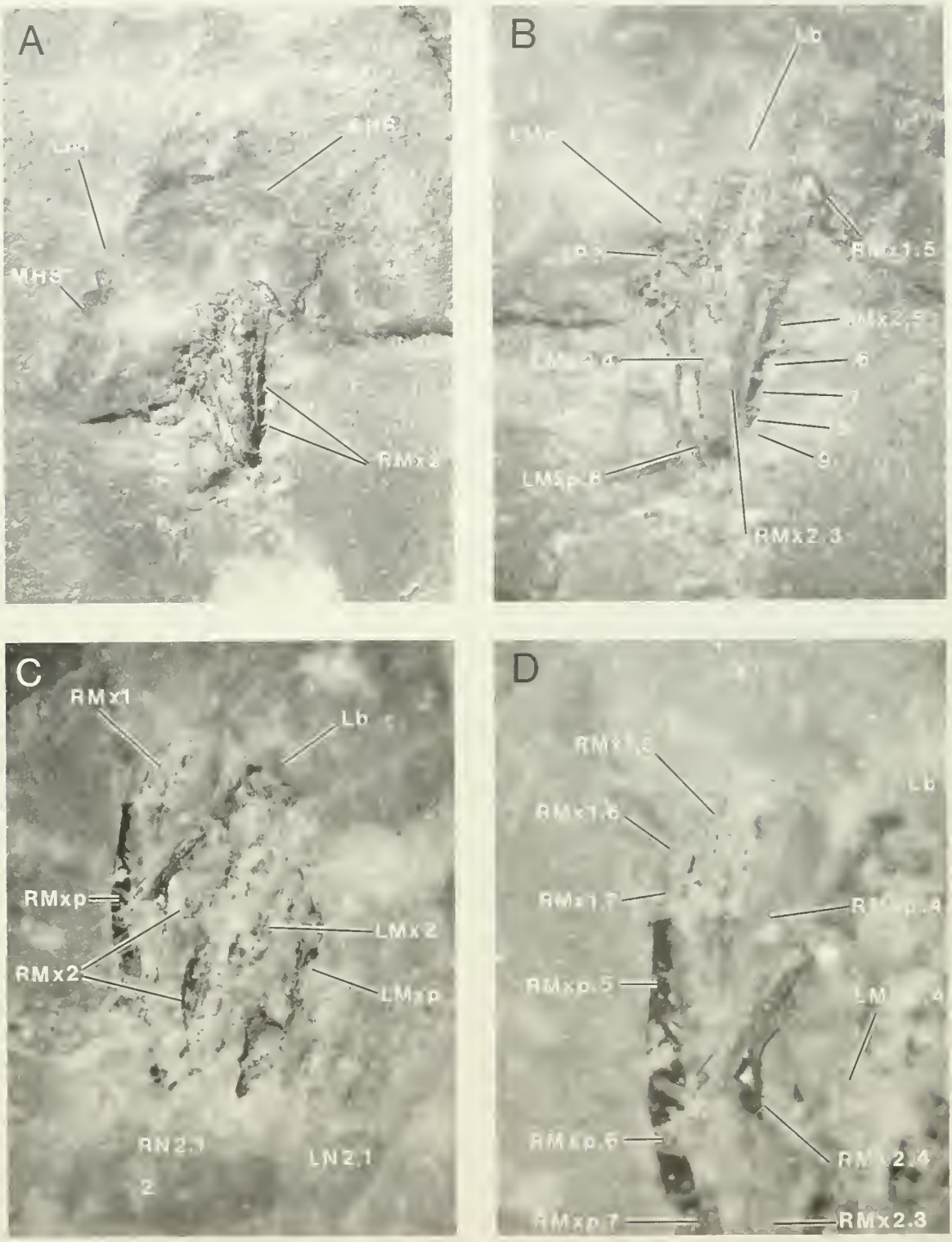

Figure 13. *Tesnusocaris goldichi*, closeup views of SDSNH 28251b. A, general view of counterpart with outline of the headshield and folded mouthparts visible, 12.2×; B, closeup of couterpart, 24.4×; C, closeup of part, under alcohol, 24.4×; D, detail of part, under alcohol, 42×.

fined, with the posterior edges of the coxa and ramus evident. The right second exopede (RX2) is barely visible, but the left limb (LX2) provides more information. The outline of the coxa (.1) is weakly preserved on the counterpart to reveal a bell shape similar to that of the endopede but much broader than long. The next two podomeres are faintly preserved on the part (LX2.3). The angle at which the sutures are distorted and the superior position of the coxa suggest that the limb was inserted on a ventral prominence (the lateral angle of the body) and that the ramus was directed posterolaterally and slightly dorsad, with the principal plane of the ramus angled posterodorsad.

The right third exopede (RX3) is preserved similarly to the limb just described (LX2). The lateral face of the coxa appears to be missing, indicating a somewhat pyramidal shape with only the mesial side visible. The ramus is distorted as with the preceding limb, though an additional podomere is retained (RX3.4). A rodlike structure appears along each margin of the ramus; similar linear objects are clearly preserved on SDSNH 28251a (Fig. 10) and SDSNH 28253. Nowhere does this sort of structure appear to curve around the distal tip of the ramus, where the setae are arrayed as a fan. Although there is no direct evidence of marginal setae on the exopedes proximal to the distal ends of the penultimate (fourth) segment, it seems entirely possible that the proximal section of the ramus supports dense, closely pressed, setose crests that appear as solid rods when preserved on edge.

The fourth pair of exopedes is missing entirely because in this area the fossil is disrupted. The right fifth coxa (RX5.1) is exceptionally well preserved in outline, clearly demonstrating the broadly campaniform shape. Two distinct folds lie just anterior to this coxa, which has been displaced considerably to the right. There is a shallow tooth on the posterior margin similar to the possible condyle articulating the anterior endopedal coxae with their second podomeres. The right sixth exopedal coxa (RX6.1) is in approximately the natural position and exhibits a size and shape similar to that of the preceding one. A ramus, presumably belonging to this limb, appears to have been detached and wraps around the front of the coxa. The last three podomeres of this limb are preserved in apparent sagittal section on the counterpart (RX6?5). The remaining limbs are too poorly preserved to yield additional information.

A number of other ventral structures are discernable on this specimen, especially on the third trunk segment. The most prominent of these is a large, broad, well-defined sternite (S5), which appears to be displaced to the left and rotated slightly counterclockwise. To the left of the sternite is another sclerite (PS), the mesial edge of which is indistinct. Its general outline is bluntly triangular, with the anterolateral corner clearly defined. This part of the sclerite bears several ridges. This sclerite may have originally been more lateral to the sternite and anterior to the exopede. The coxa (.1) of the second left endopede (LN2) partially overlaps this sclerite. [No similar structure is apparent on any other remipede, but the sclerite seems analogous to the "pleura" of several arthropods that are thought to strengthen the ventrolateral body wall (Snodgrass 1952). The use of the word "pleuron" in this case is distinct from its usual application in carcinology, which is used elsewhere in this paper. With reference to crustaceans, "pleuron" indicates the lateral extension of the tergite, and similar structures are referred to as the "epimere" in other disciplines.]

Posterior to the above sternite and mesiad from the posteromesial corner of the "pleural" sclerite is a region that appears to have been poorly sclerotized. The posterior ventral edge of this segment appears to be occupied by a broad low fold or ridge that underlies the coxae of the third endopedes (RN3.1, LN3.1?) and exopedes (RX3, LX3). The ridge appears to extend beyond the exopedal coxae to the posterolateral angles of the segment and perhaps along the ventrolateral edge to some extent. Posterior to the sternite of the third segment, an extensive tan-colored clay deposit obliterates much of the mesial structure. This deposit may represent remnants of the gut, in which case some of the lobes along the left margin may indicate diverticula (e.g., see Schram and Lewis 1988). Several prominent "islands" of cuticle in the clay undoubtedly represent some of the most posterior sternites, such as those of the seventh and eighth trunk segments. Also visible posteriorly are the left lateral edges of some of the tergites (T6).

SDSNH 28251c (Fig. 10).—During our study of SDSNH 28251a, we noticed on the counterpart many faint setalike structures anterior to the right side of the cephalon. In the drawing, the tip of each is indicated by a dot. The setae appear mainly in fan-shaped arrays, though they fade out proximally and do not attach to any defined structure. We doubted the existence of these setae, dismissing them as diagenetic, until subsequently we noticed a patch of what appeared to be fossilized cuticle exposed in the area from which the setae appear to radiate. Closer study revealed two indistinct structures (LEye, REye), similar in size and shape to the eyes of SDSNH 28251b (Fig. 5, LEye, REye), and a very faint ellipse (LA2?) with marginal setae resembling the final segment of the left antennal endopod (LA2Np?) of the same specimen. The inevitable conclusion was that there is a third individual lying somewhat anterior to and above the dorsal aspect of SDSNH 28251a (Fig. 5). The setae probably represent the tips of the trunk appendages, some of which apparently were in contact with SDSNH 28251a. The axis of the body was roughly parallel to that of the latter specimen, though its exact position is unclear.

SDSNH 28253

This concretion was found loose on the ground about 30 meters south of the others, at a point where the shale bed 5 is exposed across a small wash that bisects the locality. All that is preserved of this specimen are some clay clasts and many rodlike structures that apparently are the margins of the leg rami. It is only by comparison with SDSNH 28251a (Fig. 10) that this fossil can be assigned to *T. goldichi*. Although no details are preserved, the length of the field containing structures suggests that the animal was larger than any of the other juveniles. This specimen contains too little information to warrant a detailed description or illustration.

USNMP 124173 (Figures 14–18)

After studying the newly collected specimens closely, we decided to reexamine the holotype. This fossil is remarkably well preserved in most areas except for the posterior cephalon and anterior trunk, the left side of the trunk, and the posterior of the body. What little distortion that is noted seems to indicate that the animal was deposited resting on its right ventral surface. Although this specimen is similar to SDSNH 28251b (Fig. 10) in presenting the ventral aspect, there are many differences in preservation between the two individuals. In the holotype, the posterior cephalic and anterior trunk appendages appear to have been crushed by the compression of the headshield, so that only the structures closest to the plane of the ventral surface are preserved. The poor representation of the left side of the trunk apparently results from compression and the curvature of that side out of the fracture plane.

The anterior headshield (Fig. 14, AHS) conforms well to the form observed in SDSNH 28251. It is much wider than long and is developed on the left side as a large, posterolaterally directed flap. The corresponding right flap appears to be bent dorsad out of the fracture plane by the dorsal ramus of the antennule. The eyes (LEye, REye) are impressed from the dorsal side, and the individual facets are represented on the drawing by dots. The eyes are relatively large (Fig. 15A) in comparison to the similarly situated SDSNH 28251b (Fig. 10, LEye, REye), but do not fill the anterior headshield as completely as do those of SDSNH 28251a (Fig. 10, LEye)

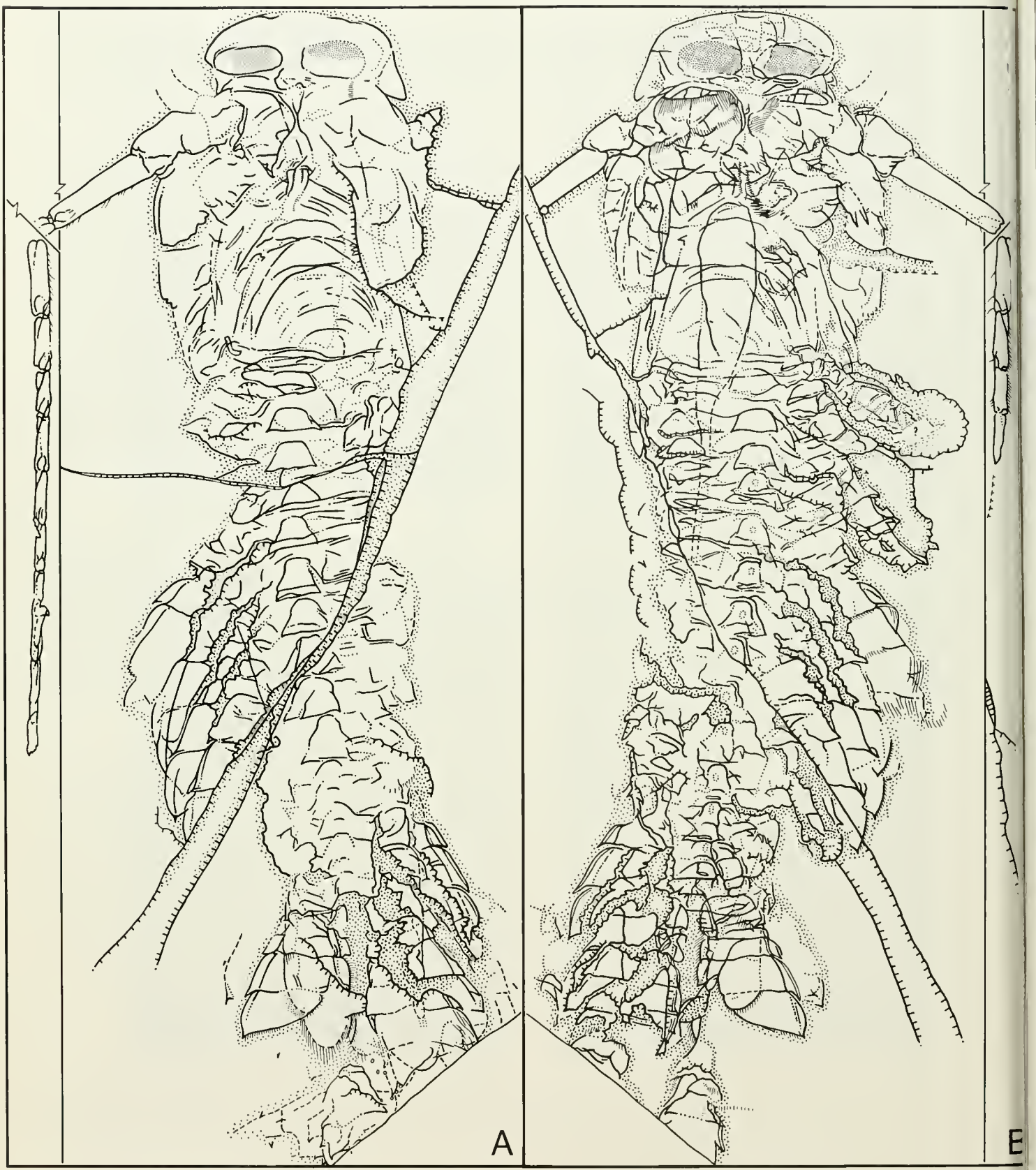
A
B

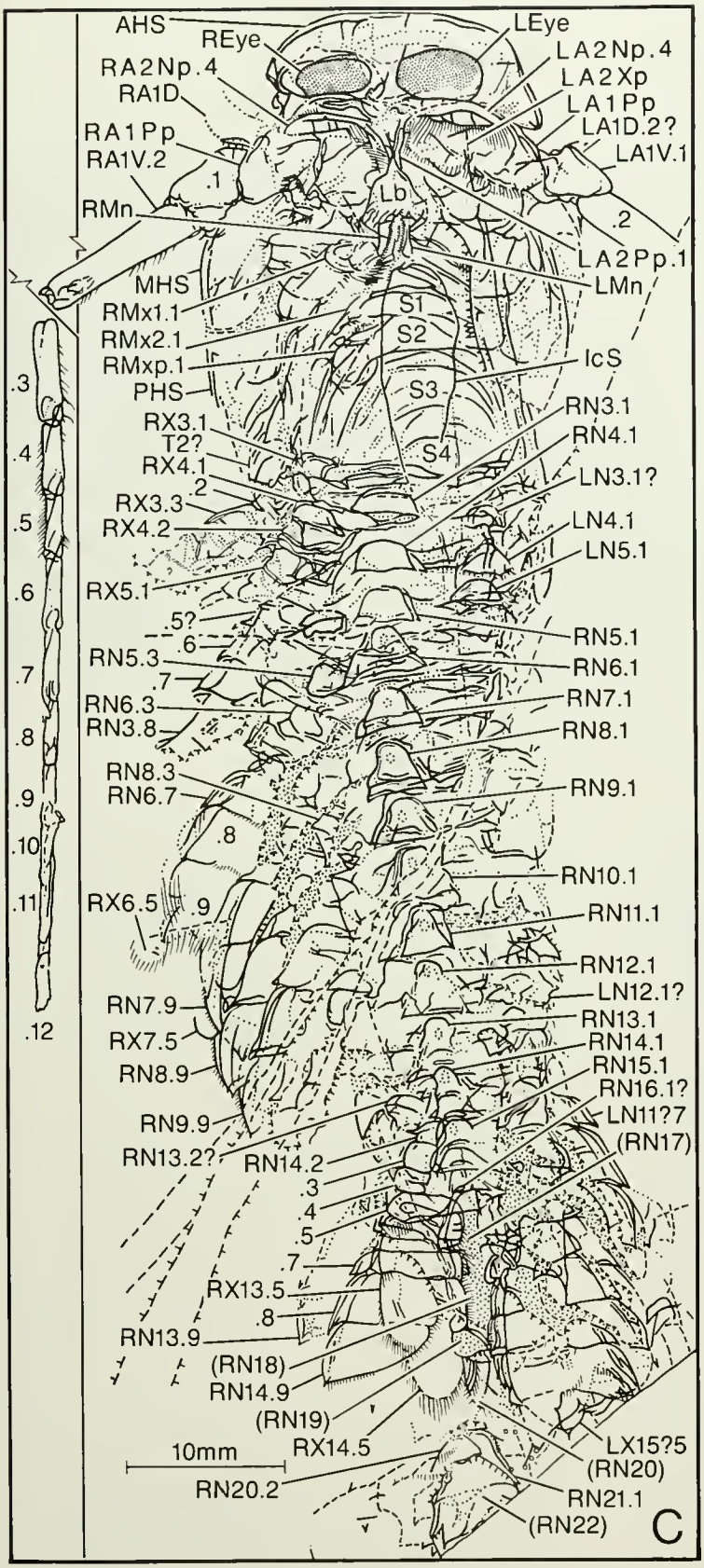

Figure 14. *Tesnusocaris goldichi*, camera lucida drawing of USNMP 124173, the holotype. A, part, showing breaks into three sections; B, counterpart; C, partially reconstructed ventral view of adult *Tesnusocaris*. Stippled areas indicate either rock matrix or facets of eyes.

The large flagella evident on the front of the cephalon are interpreted here as the ventral rami of the antennules (Fig. 14, RA1V, LA1V; Fig. 16A). These rami are not preserved clearly on any other specimen. The base of the protopod is obscure mesially but appears to originate somewhat laterad near the anterior margin of the middle headshield. The protopods (RA1Pp, LA1Pp) are large and appear to be weakly divided into two incomplete segments. A faint outline of the right dorsal ramus (RA1D) projects anterolaterally from the distal end of the right protopod on both part and counterpart, and fragments of the peduncular cuticle of both left (LA1D.1) and right dorsal rami are preserved.

The first segment of the ventral ramus (LA1V.1) is comparatively short and wide and lacks setae. The second segment (RA1V.2) is extremely long and bears several small setae on the posterior margin of the right limb. The next ten segments (.3–.12) of the posterolaterally directed right ramus are progressively shorter and narrower, and some have setae on both margins. The sutures between most of the joints appear to be either straight or angled, presumably depending on their position relative to the fracture plane. The ramus appears to be nearly complete, in which case it is somewhat shorter than the body of the animal.

Posterior to the antennules, the middle headshield (MHS) flares laterally and appears to cover the lateral aspect of the cephalon and at least the proximal parts of the cephalic appendages (Fig. 16A). A narrow marginal thickening is preserved on the right side, and the shield appears to have been fairly rigid, though apparently not mineralized. The appendages preserved on the counterpart (Fig. 15A), which were interpreted by Schram et al. (1986) as the anterior branches of the antennules and by Brooks (1955) as the first cephalic appendages, are reinterpreted here as the endopods of the antennae (LA2Np, RA2Np). This conclusion is supported not only by their apparent positional homology with the antennae of Nectiopoda (Fig. 25A, A2Np) but also by structural details of the fossil that were neglected previously. The general form of these rami is that of a short paddle that narrows at both ends. The anterior edge bears a prominent ridge, which apparently is not divided by the sutures observed along the posterior margin that seem to divide the paddle into four podomeres. Fringing setae are preserved on most margins; these are short anteriorly, moderate posteromedially, and longest along the mesial and distal posterior margin (Fig. 15A). The bases of these appendages appear to arise in front of the anterior tip of the labrum. The slender protopod of the left antenna (LA2Pp.1) is preserved fairly well on the counterpart and appears to be divided into two segments, the second of which supports the two rami.

The outline of the left antennal exopod (LA2Xp) can be traced by using the marginal setae as markers. The presence of various overlapping setose structures in this area makes difficult the determination of just which setae belong to this ramus. The setae that most clearly belong to the exopod underlie the antennal endopod on the part. These short setae do not coincide with the sutures of the endopod but apparently represent the anterolateral margin of the large exopod. A faint indication (Fig. 15A) of the outline of the exopod is preserved posterior to the posteromesial edge of the left antennulary protopod (LA1Pp). Here the posterolateral margin of the antennal exopod ramus appears to be well defined. A series of well-preserved setae defines the posterior margin of the exopod mesially toward the base of the limb, where the setae fan out along the posteromesial angle of the endopod ramus. The mesially directed setae appear short on the left limb but long on the right one. The mesial setae on the left exopod extend anteriad to a small curved structure, which may indicate the posterior extent of the point of insertion on the protopod of this ramus. Although poorly defined, the shape of the exopod appears to be oval, almost subtriangular. An apparent extension of the posterior marginal setae of the exopod laterally along the posteromesial edge of the left antennulary protopod probably indicates the presence of aesthetascs belonging to the latter appendage.

Nothing can be added to the published descriptions of the prominent bell-shaped labrum (Schram et al. 1986; Fig. 15B). The large mandibles (Fig. 15B) also have been described adequately by others. Each consists of at least one row of 13 to 17 mesially directed serrations supported by a distinct ridge. The posterior headshield (PHS) appears to be laterally and posteriorly expanded, and a narrow thickened margin is present.

Only the bases of the limbs associated with the right side of the posterior cephalon are preserved on the counterpart (Fig. 15B). The first endite of the maxillule (RMx1.1) is clearly preserved and conforms well to that seen on SDSNH 28251b (Fig. 12, RMx1.1), with seven or eight long spines directed posteromedially from a rounded base. Parts of the right endite (where the lumina of some of the spines have broken open) were incorrectly interpreted by Schram et al. (1986) as possible mandibular structures. Three small spines just lateral to the first endite presumably belong to the second maxillulary segment. A fragmentary spinous structure located at the posteromesial edge of the right antennulary protopod (RA1Pp) may belong to the more distal parts of the ramus, but it was interpreted by Schram et al. (1986) as part of the antenna. There is no indication of a sternite associated with the base of the maxillule.

The maxillary sternite (Figs. 14, 16B; S1) is preserved along with an indistinct first podomere (RMx2.1) on the part. The latter supports three groups of three modest spines each. The maxillipedal sternite (S2) also is present (Fig. 16B), though the limb base (RMxp.1) is indistinct (Fig. 16C). The rami of the latter limbs appear to extend posterolaterally.

The posterior cephalic region is marked by a well-defined elongate area (lcS) on the counterpart extending posteriad from the maxillules (Fig. 16C). This seems to us to represent the sediment-filled space between the limb bases of the left and right sides, although Brooks (1955) interpreted this area as a stomach. The position of this space in relation to the mandibles and more anterior structures indicates that the ventral surface of the posterior cephalon has shifted considerably to the left. The widest and most distinct part of this intercoxal space is at the level of the posterior cephalic limbs. The width of the intercoxal space anteriorly indicates that the maxillae and maxillipedes arose somewhat laterally on the ventral cephalon. The anterior trunk endopedes appear to have been equally separate mesially, in contrast to their preservation on SDSNH 28251b (Fig. 10, N.1).

Although it is impossible to determine directly the number of anterior endopedes that are missing under the posterior headshield, a reasonable estimate can be made. The sharp definition and continuity of the intercoxal space behind the maxillipedes suggest an unbroken series of structures on each side. In addition, there appear to be two poorly defined sternites (S3, S4) in this region behind that of the maxillipedal sternite (S2), delineated by poorly sclerotized folds similar to that on the third trunk segment of SDSNH 28251b (Fig. 10, S5). Hence, we conclude that the first well-preserved thoracic coxae on this specimen are those of the third post-maxillipedal limb.

The apparent projection of the posterior headshield over two trunk segments (in addition to the maxillipede) is, among all known remipedes, a feature unique to this specimen. It would seem appropriate to compare the enlarged posterior headshield to the short carapace characteristic of some malacostracans, especially the Thermosbaenacea (Schram 1986; Chap. 17). However, since this character is unique to this specimen and poorly preserved, it cannot be considered a true carapace with any certainty. There is a suggestion of a possible trunk tergite (T2?) preserved on the part at the right posterolateral corner of the headshield (Fig. 14), which ap-

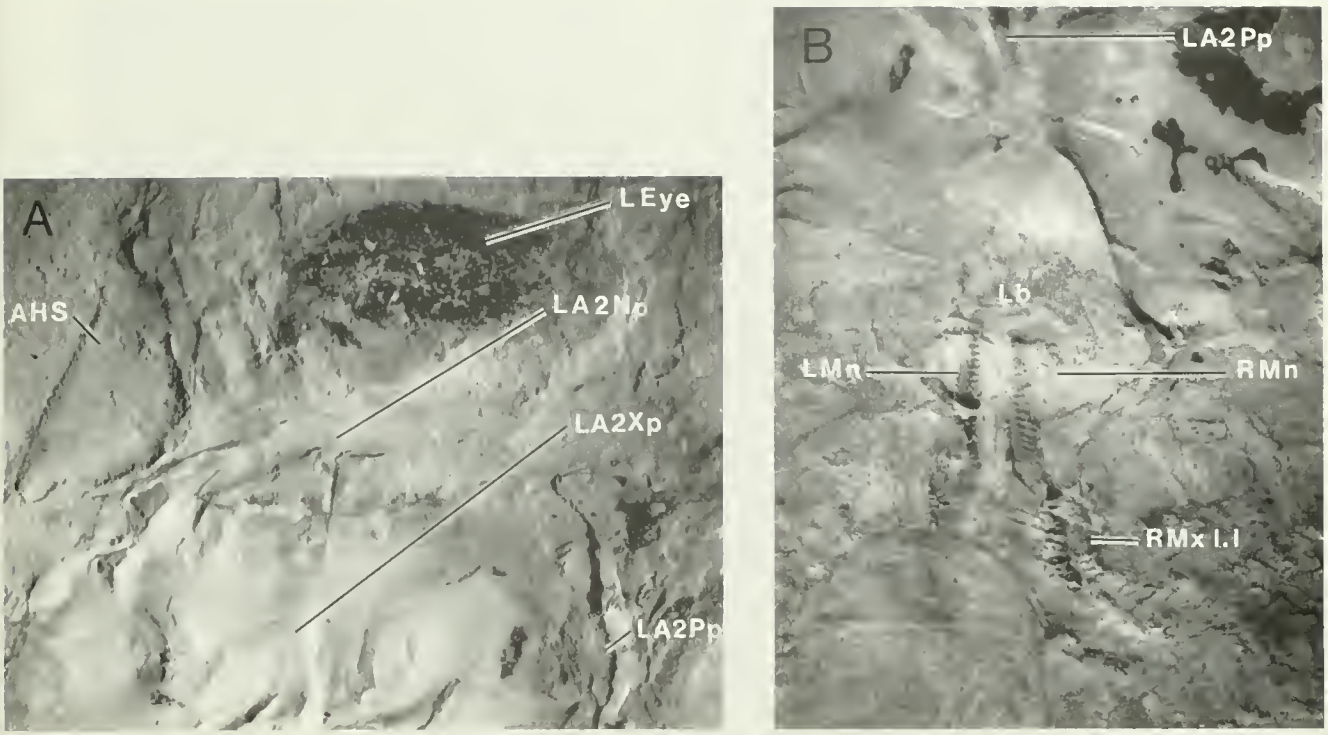

Figure 15. *Tesnusocaris goldichi*, details of USNMP 124173. A, left anterior head with compound eye and portions of the antenna, 8×; B, mouth region with labrum, mandibles, and maxillulary endites, 11.7×.

pears as an indistinct curve of approximately the correct size, shape, and position to represent the right pleuron of the second tergite. If this is the case, the dorsal part of the trunk was only slightly narrower than the headshield.

The structure interpreted here as the right third endopedal coxa (RN3.1) was believed by Brooks to represent the first trunk sternite, and this interpretation was accepted by Schram et al. (1986). In the absence of any other specimens, the asymmetrical and incomplete preservation of the trunk made the original reconstruction of Brooks appear reasonable. An informed reexamination, however, reveals clear evidence of paired endopedal coxae (Fig. 17A) and laterally inserted exopedes (Fig. 17B) consistent with similar structures described for the juveniles. Although Brooks (1955) reconstructed the "endopods" extending symmetrically from the anterolateral margins of his supposed "sternites," there is no evidence on this specimen of any ramus articulating with the left side of any of the clearly preserved bell-shaped structures. Microescarpments to the left of the right fourth and eleventh endopedal coxae (RN4.1, RN11.1), as well as less clearly defined transverse structures associated with the intervening somites, are the only features associated with the left sides of the right coxae. There is no indication of any structures extending posterolaterally to the left, as would be expected if Brooks were correct in his reconstruction. The only endopedal rami apparent on the left side (LN11?, etc.) are not preserved proximally but appear to insert well to the left of the right endopedal coxae. The rami of the right side do articulate with the right sides of the coxae, though not in the manner shown by Brooks. Although he presumed the limbs to be possibly biramous, Brooks did not observe the proximal parts of the "exopods" or their presumed junctions with the "endopods." We will henceforth use only the terminology that we feel describes the actual condition of these structures.

Although Brooks adequately described the bell-shaped form of the right endopedal coxae and the general form of the endopedal rami, we can add a number of refinements and revisions. The part, having broken into three pieces, offers three slightly different views of these coxae, which reveal something of their three-dimensional structure. The fracture plane of the anterior section apparently lies on the epiventral surface of the third through fifth coxae (RN3.1–RN5.1), as evidenced by their convex form. These three coxae are relatively short and broad and lack any marginal, posterior, or median elaborations (Fig. 17A). The fracture plane of the second section appears to have split the next four-and-a-half coxae (RN6.1–RN10.1) on a plane slightly away from the ventral surface, exposing concave impressions of these coxae. These five coxae have a marginal rim, posterior extension, and faint anterior pit (Fig. 18A). The pits are more clearly visible on the counterpart as protuberances on the inner surfaces of the coxae, and would appear to represent a monocondylic articulation of the coxa and ventral surface. The marginal rim is presumably a strengthening feature. Since the anterior, convex portion of the coxae appears solid, the posterior extension, which lies against the ventral surface, must contain the opening through which the muscles pass into the posterolaterally directed ramus. This seems consistent with the condition observed on SDSNH 29251b (Fig. 12, RN2.1), though no possible articulatory condyle appears between the coxa and second podite of the holotype.

Although the coxal impressions of the third section of the specimen are indistinct, the condyles of five or six additional coxae (RN11.1–RN16.1?) can be distinguished on the counterpart. The next four coxae (RN17–RN20) are not apparent in the jumble of overlapping limbs and matrix. The final coxa that reemerges near the broken posterior edge of the concretion appears to be that of the twenty-first endopede (RN21.1), and there is possibly room for one

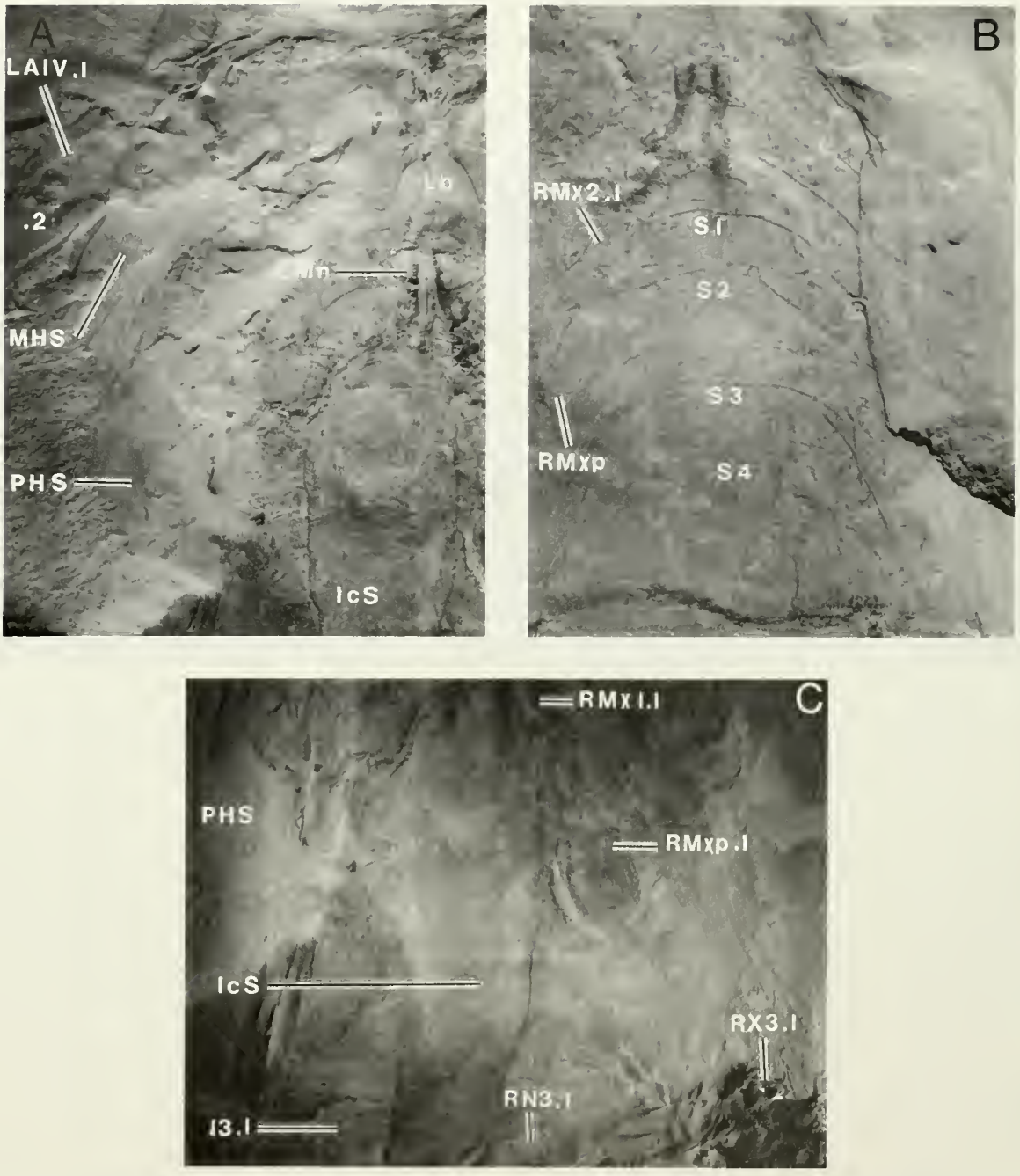

Figure 16. *Tesnusocaris goldichi*, details of USNMP 124173. A, left portion of the head and anterior trunk of the part, 6×; B, anterior trunk showing sternites of the part, under alcohol, 6×; C, detail on the anterior trunk on the counterpart, under alcohol, 10×.

more beyond (RN22). Since all of the fully preserved coxae appear to be subequal in length (though the first ones may be relatively broad), it seems probable that the series is incomplete. If *Tesnusocaris* had as many segments as the maximum number seen on living remipedes (32), then the total length of the holotype animal could be extrapolated to nearly 14 cm. Unlike the juvenile SDSNH 28251b (Fig. 10, N.1), the coxae of this specimen touch or even overlap slightly along the entire length of the body. Nothing resembling the small genital structures associated with the limbs of the eighth and fifteenth trunk segments (in the sense of Ito and Schram 1988) is apparent on this specimen.

At least two of the left series of endopedal coxae are preserved fragmentarily on the counterpart, just to the left of the intercoxal space. These are the anterior portions of the fourth and fifth coxae (LN4.1, LN5.1), which are quite clearly defined. Some indication of the third coxa (LN3.1?) may also be present. A rather clearly defined transverse ridge resembling the post-sternite fold described on SDSNH 28251b connects the fourth pair (Fig. 10, S5).

The only limb that retains a nearly complete ramus (Fig. 18B) is right endopede 14 (RN14). Brooks probably based his reconstruc-

tion of the endopede mainly on this limb, though he apparently thought the ramus was associated with the front of the succeeding coxa (RN15.1), which now seems unlikely. A close examination of the right posterolateral corner of the right seventh endopedal coxa (RN7.1) reveals that on both part and counterpart the adjacent area of the ramus is on exactly the same plane, which would not be the case if the ramus inserted anywhere else. Additional evidence of the posterior insertion of the ramus is found in the apparent structure of the coxae on this specimen as analyzed above, in the right second endopede of SDSNH 28251b (Fig. 12, RN2.1) and in comparisons with similar coxae of other arthropods (Snodgrass 1935, 1952).

The ramus of the right fourteenth endopede apparently has been displaced slightly posteriad, so that the second podomere lies behind the coxa. The second podite (RN14.2) is short and about as wide as long. There is a lateral crest terminating in a prominent spine. The third segment (.3) is slightly larger and also bears an indication of a lateral crest, though no spine is preserved. The fourth segment (.4) appears to be similar to the third but is broken transversely. The next few podomeres are confused with overlapping limbs, but the lateral edge of the fifth podite (.5), exclusive of any presumed crest, seems to be preserved. The next segment cannot be distinguished from the overlapping podites, but appears to be similar in size to the preceding ones. The seventh podomere (.7) is well preserved laterally as an elaborate crest set off by a narrow sharp ridge and by having a similarly defined groove along its outer margin. The overall shape of the crest is lanceolate and terminates in a fairly short straight spine. The eighth segment (.8) is much longer and wider than the preceding ones. The crest is similar to the preceding one but terminates in a long, slightly hooked spine. The ninth and terminal podite (RN14.9) is about the same length laterally as the preceding one but its posterior edge narrows abruptly to a short stout terminal spine. The lateral edge of this segment bears what apparently was a flexible flap unlike the more proximal spinous crests. Short setae extend mesiad along the posterior margin from the tip at least onto the eighth podite (though the setae in this area are confused with those of the overlapping exopede) and perhaps more proximally, as indicated by Brooks. It should be noted that the segmentation of this endopede is not clear at midlength, and, as a result, Brooks interpreted the ramus as consisting of seven fairly equal segments rather than six short and two long ones.

A few additional details can be gleaned from the other, more fragmentary, endopedal rami. The right seventh through ninth rami clearly demonstrate that the lateral flap of the terminal segment (RN7.9–RN9.9) is fringed with short setae. None of the more proximal crests shows any indication of setation, since the setae associated with the crests of the sixth ramus (RN6) are of the long form characteristic of the exopedes, suggesting that setae of the underlying exopede (RX6) have wrapped around the anterior edge of the endopede. This ramus does have clearly setose intersegmental margins. The third right endopede (RN3) shows parts of the more proximal crests. The crest of the sixth podite (.6) ends in a slender, hooked spine, and that of the fifth (.5?) in a straight, anterolaterally directed one. A similar spine is preserved indistinctly on the anterodistal angle of the fourth podomere. Thus, it appears that each

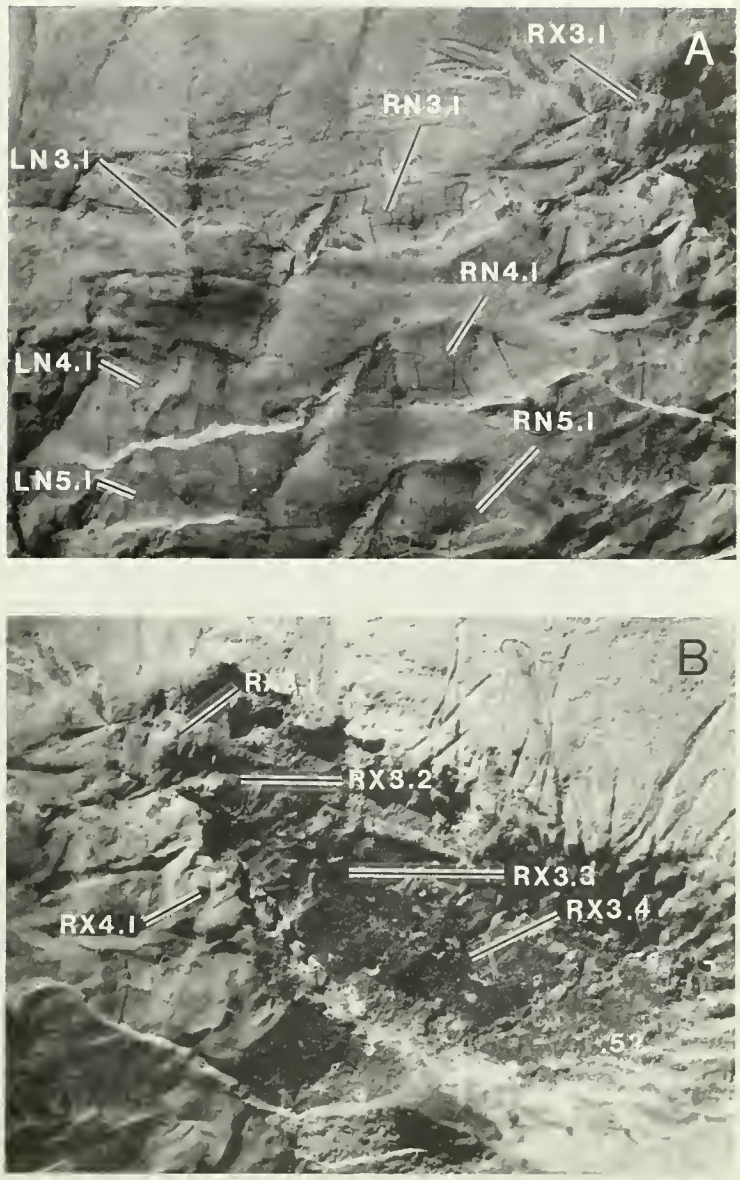

Figure 17. *Tesnusocaris goldichi*, details on the anterior trunk of USNMP 124173. 7×. A, midline of the trunk showing the right and left endopedes; B, right side of the trunk just lateral to (A) showing the third right exopede.

segment of the endopedal ramus except the last supports a prominent crest terminating distally in a strong spine, as indicated by Brooks. Although not generally preserved, it is likely that the characteristic short setae line all of the segmental margins of the endopedes except along the spinose crests and coxae. This conclusion is supported by the preservation of marginal setae on the proximal segments of the first two left endopedal rami of SDSNH 28251b (Fig. 12, LN1[.3], LN2.2).

Three exopedal coxae are clearly preserved on the right side of the counterpart (Fig. 17A). The right third coxa (RX3.1) lies just behind the headshield and is fairly well preserved except laterally along the mesial angle. The outline is similar to those of the exopedal coxae of SDSNH 28251b (Fig. 10, RX5.1, RX6.1), being broadly bell-shaped. There seems to be a medial ridge that divides the surface into mesial and lateral aspects. A similar ridge is pre-

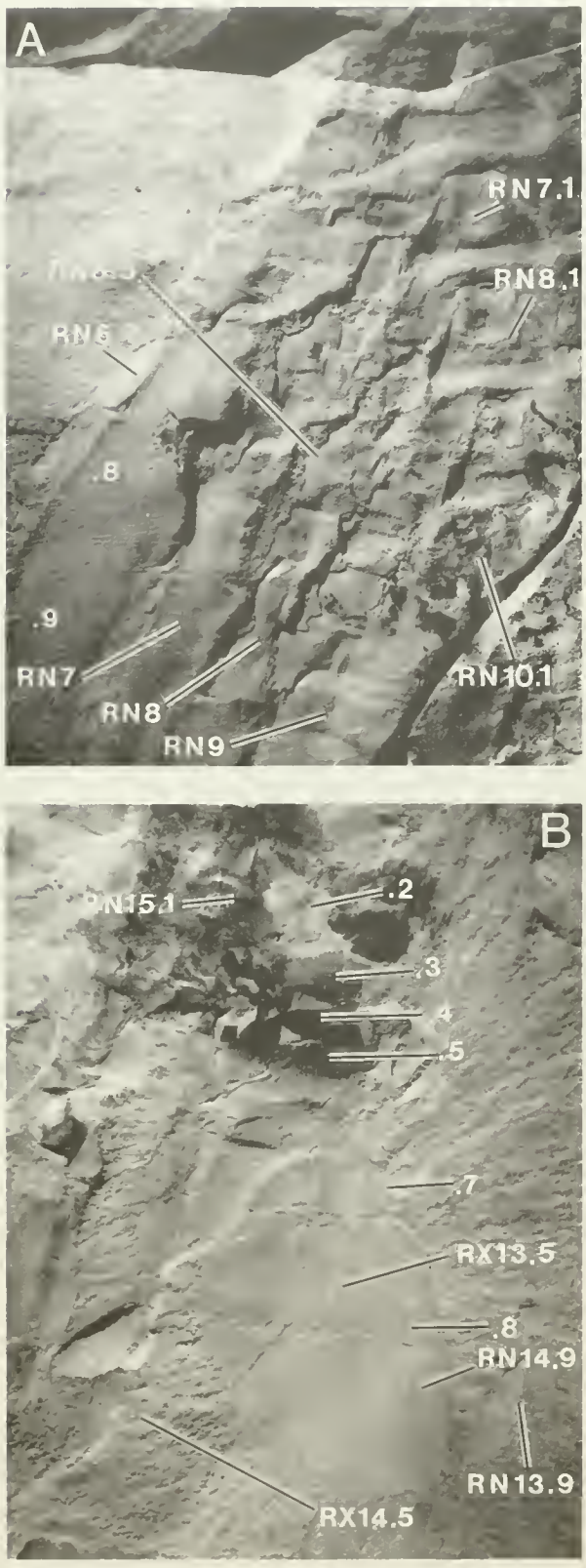

Figure 18. *Tesnusocaris goldichi*, details of USNMP 124173, 5.5×. A, Right side of the middle region of the trunk displaying the serial arrangement of the endopedes; B, posterior right exopedes.

served on SDSNH 28252 (Fig. 4, RX5.1–RX7.1). The fourth and fifth coxae (RX4.1, RX5.1) are similar to the third in all respects, though the fourth is more complete and the fifth is mesially incomplete. What appears to be a narrow ridge on the posteromesial edges of the third and fourth coxae is more likely part of the opening through which the musculature passes into the ramus. The lateral corner is obscured on each, disappearing behind the preceding exopedal ramus. The third exopedal coxa is closest to the ventral midline, its posteromesial corner lying very close to the presumed position of the posterolateral corner of the missing second endopedal coxa. The next two coxae are inserted progressively more laterally. The evidence from the other specimens suggests that the normal position is lateral (Figs. 4, 5; X.1), the third and fourth coxae apparently having been displaced slightly mesiad by the compression of the posterior headshield and twisting of the trunk.

The proximal section of the right third exopede ramus (RX3) was uncovered by our preparation of the counterpart (Fig. 17B). The limb projects obliquely off the venter with the anterolateral edge angled toward the viewer, an orientation also indicated on SDSNH 28251b (Fig. 10, LX2, RX3). The second segment (.2) is badly preserved but appears to conform to the relative size and shape observed on SDSNH 28251a (Fig. 10, RX11). The third segment (RX3.3) is well preserved proximally on the anterolateral margin, which appears to be strengthened by a narrow ridge (possibly a setose crest). The other edges are not clearly defined, but the distal intersegmental margin appears to be lined with short setae similar to the intersegmental setae of the right sixth endopede (RN6). The more distal portion is not preserved.

The distal ramus of the right fourteenth endopede (RN14.9) lies between the rami of the right thirteenth (on the part) and the fourteenth (on the counterpart) exopedal rami (RX13.5, RX14.5), demonstrating the interleaving of the limbs when held near the body axis. The distal tip of both exopedes is broadly rounded and fringed with the long setae characteristic of the exopedes of SDSNH 28252 (Fig. 4, RX9.5–RX11.5). These setae appear to extend at least onto the distal margins of the penultimate segment.

The relative positions of the distal tips of the endopedes and exopedes provide some useful confirmation of the separation of their bases. The terminus of the right sixth endopede (RN6.9) is surrounded by the long setae of the right sixth exopede (RX6.5), which appear to extend beyond the tip of the former. The tips of the somewhat more posteriorly directed right rami of the seventh trunk segment (RN7.9, RX7.5) are nearly coincident. The right limbs of the thirteenth (RN13.9, RX13.5) and fourteenth (RN14.9, RX14.5) trunk segments demonstrate that as the exopedes come to lie alongside the body, they appear shorter than the endopedes. This reversal of the apparent relative lengths of endopede and exopede is undoubtedly a consequence of their laterally distinct insertions, the rami probably being equal in length.

As noted by Brooks, the endopedal rami, exclusive of their coxae, diminish in size posteriorly. Specifically, the right fourteenth endopedal ramus (RN14) is 78% the size of the third (RN3). Therefore, on the average, each succeeding ramus diminishes by 2%. By extrapolation, the ramus of the last coxa preserved, the twenty-first (RN21.1), was 64% as long as the third, and the first two (RN1, RN2) were presumably larger than the third. Although no exopedal rami are fully preserved, the portions that are visible appear to diminish posteriorly in approximately the same proportion as do the endopedes.

Since the coxae do not diminish posteriorly, it seems unlikely that the length of the tergites did either. If it is assumed that the exopedal coxae also did not diminish significantly posteriad, it is improbable that the body width tapered to the extent figured by Brooks. The lines lateral to the right ninth through seventeenth endopedal coxae (RN9.1–RN17) that appear on both the part and

counterpart, though giving the impression of a tapering trunk, more likely represent the mesial edges of exopedal rami lying near the body axis, the outlines of which have been impressed through the overlapping endopedal rami.

Some indication of the freedom of movement possible for the limbs may be derived from an analysis of the angles between them and the main axis of the body. The main axis of the endopedal coxae, as measured by taking the perpendicular of the straight posterior edge, typically is parallel to that of the body. Using an arc measuring 0° anteriad, 90° laterad, and 180° posteriad, it can be seen that the coxae of the right side exhibit very little movement. The presumably displaced third one (RN3.1) excluded, the movement of the endopedal coxae ranges from 174° to 186° in an apparent slight rocking movement pivoting about the anterior condyle. The more distal parts of the endopedal rami range through only 11° of lateral movement, from 142° to 152° in relation to the trunk axis. The angle between the endopedal coxae and rami (measured as if all the coxae were perfectly aligned with the body) shows slightly more variation, through 17°, ranging from 131° to 148°. The podites of the ramus appear to be fixed, so the ramus probably functioned as a single unit articulating on the coxa.

The few exopedal coxae in evidence on the right side (RX3.1–RX5.1) are all angled at about 157° and appear to have been capable of little or no movement. The more distal parts of the rami, however, range through more than 70° from 114° to 185°. Another way to consider this range of movement is relative to the axis of the coxa, with 0° being the ramus doubled anteriad over the coxa; 90° extending laterad, perpendicular to the coxal axis; 180° being the ramus directly in line with the coxa, and 270° being the ramus held mesiad, perpendicular to the coxa. Using this scale makes it easier to compare the relative movement of the endopedal and exopedal rami on their respective coxae. The exopedal rami extend from 43° to 208° in relation to their coxae. Very similar figures apply to the anterior exopedes of SDSNH 28251b (Fig. 10), though the right first exopede (RX1) achieves a slightly greater anteriad reach. The segments of the ramus appear to be capable of some folding, especially the ultimate one, as seen on the right eleventh exopede of SDSNH 28252 (Fig. 4, RX11.5).

Genus *CRYPTOCARIS* Schram, 1974

Diagnosis.—Adults averaging 3.1 cm in total body length. Headshield somewhat wider than long, not demarcated into regions nor marked with strongly developed cervical groove, posteriorly not covering free trunk tergites. Antennule ventral branch with only short to moderately long segments. Trunk with about 15 tergites.

CRYPTOCARIS HOOTCHI Schram, 1974

Diagnosis.—Since the fossils at hand are not very well preserved and there is only one species, the diagnosis is the same as that of the genus.

Holotype.—P 32053, concretion with counterpart.

Type locality.—Peabody Coal Company, Pit 11, Will County, Illinois.

Stratum.—Francis Creek Shale, Carbondale Formation, Westphalian D, Desmoinesian, Middle Pennsylvanian.

Remarks.—In 1988, while sorting and identifying Mazon Creek crustaceans in the Field Museum, we encountered specimens that were similar to specimen P 32053, the holotype of *Cryptocaris hootchi*. This specimen had been designated originally as a tanaidacean malacostracan (Schram 1974). However, as a tanaid, the holotype was always the odd specimen out, and the original description of the tanaidacean and a subsequent review of all fossil tanaids (Schram et al. 1986) focused exclusively on specimens in private collections that were unquestionably tanaidacean. The new specimens in the Field Museum are obviously not tanaids, prompting Schram (1989) to select a new holotype and name for the Mazon Creek tanaidacean. Study of the holotype, P 32053, and the new specimens reveals that they are related to *T. goldichi*. *Cryptocaris hootchi* is, therefore, now placed within the Enantiopoda.

Several specimens mentioned or illustrated by Schram (1974) also may be attributable to *C. hootchi*. All of these specimens, however, are either lost or are unavailable for study (Carman 1990): SLM 6 apparently still exists (Carman 1990), but Stephen LeMay has not acknowledged our requests to study the specimen and thus we can not verify its identity; two very nice specimens, LS 1366 and LS 1995, that were in the collection of the late Levi Sherman are now lost (the latter being very unfortunate since old photographs of that specimen reveal what may be remnants of sessile eyes).

Description.—The following review is based solely on the available fossils at hand (Table 2).

P 32053 (Figure 19)

Although this is the best preserved of the available specimens of *C. hootchi*, its quality is not as good as that of specimens of *T. goldichi*. The arrangement of the fossil on the concretion indicates that the animal was preserved on its side through most of its length (Fig. 19A). The posterior segments are twisted into a dorsoventral orientation, displaying both the right and the left sets of caudal rami.

The headshield is well preserved dorsally and posteriorly, but the ventral and anterior aspects are not well expressed (Fig. 19B,C). The dorsal ramus of one of the antennules is clearly discernable extending from the anterior part of the head (Fig. 19A) and displays the small joints of its finely annulate flagellum. Only two of the peduncular segments can be seen. The total length of the flagellum is at least 4.43 cm, longer than the 3.33 cm of the body, and there are remnants of what appear to be segments of the associated ventral branch of this antennule near the base of the limb (Fig. 19B).

It appears that the ventral branch of the other antennule is partially preserved and projects from the ventral part of the head as seven moderate-sized segments (Fig. 19 B,C), but these represent only a portion of the total ramus. Fragments of appendage segments can be found just posterior to this ramus on the ventral aspect of the head (Fig. 19C) and probably are parts of incompletely preserved mouthparts.

TABLE 2. Measurements of *Cryptocaris hootchi* specimens in mm. Antennule length for P 32053 is for the dorsal branch.

Specimen	Head length	Head width	Body length	A1 length	Length of caudal rami	T1 length	T2 length	T3 length	Trunk segment no.
P 32053	7.2	—	33.3	44.3	≈21.1 ≈13.0	1.5	1.8	2.3	15
PE 29406	8.7	9.5	≈32.4	—	—	1.0	1.3	1.3	17 (?18)
PE 37731	≈7.3	≈8.0	≈32.5	—	—	1.5	1.9	2.2	14 (?15)
PE 37759	5.3	≈6.4	27.4	—	—	0.9	1.2	1.7	15 (?16)

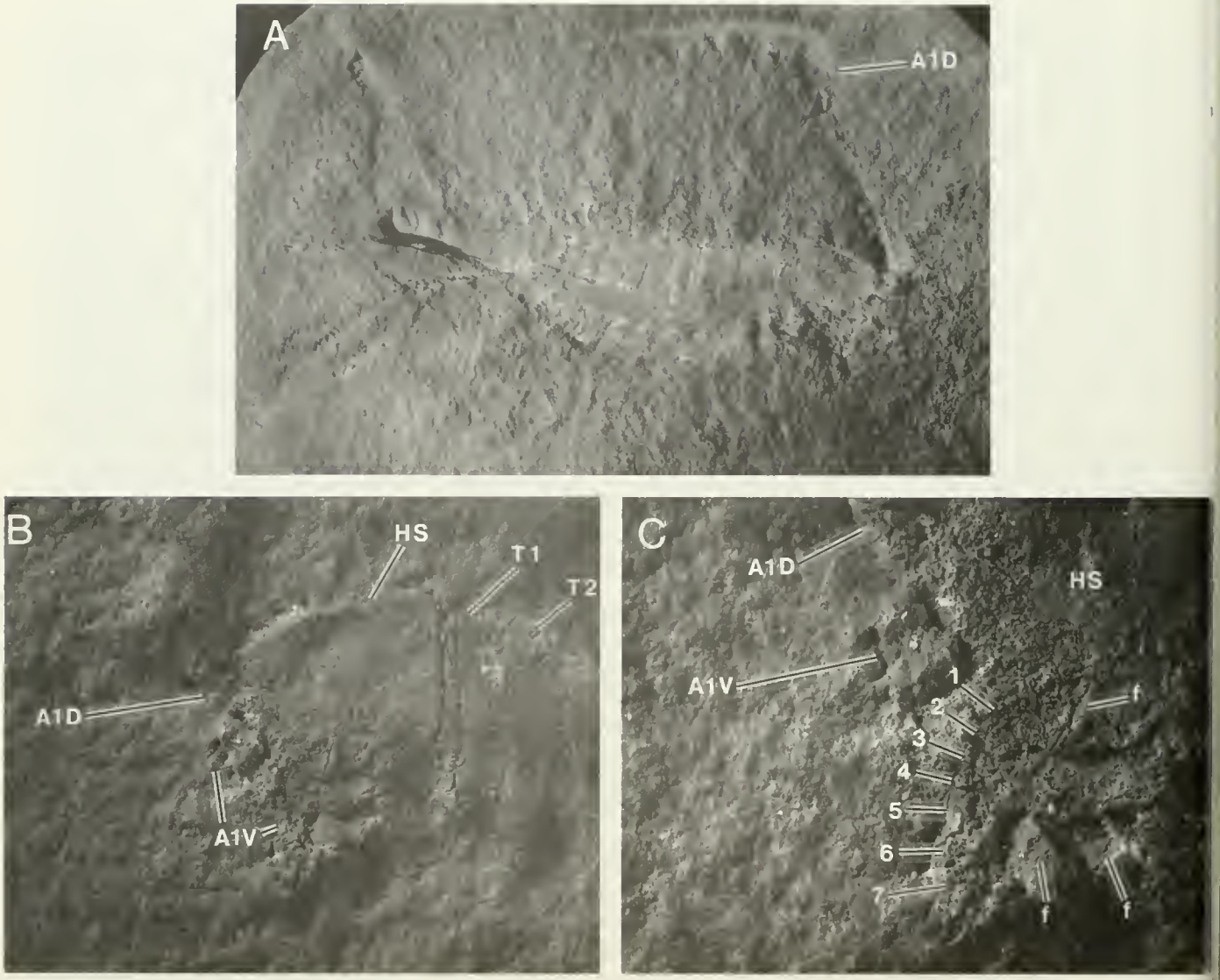

Figure 19. *Cryptocaris hootchi*, P32053, the holotype. A, lateral view of body with head to the right and tail to the left. 1.8×; B, the head on the counterpart, 5×; C, detail of (B) under alcohol showing the proximal segments of the ventral branch of one antennule and the most basal segment of the other, 10×.

The first tergite of the trunk is short and completely exposed (Fig. 19B). The other trunk tergites immediately behind it are longer and subequal, the second somewhat less so, until the most posterior portion of the trunk, where the segments gradually become shorter and smaller. The trunk pleura are broadly rounded anteriorly and posteriorly. Scattered fragments of what appear to be the exopedes can be seen ventral to the trunk, but details can not be discerned. Two sets of long, thin, finely annulate caudal rami are preserved (Fig. 19A), and a portion of the detritus-filled gut can be seen towards the posterior portion of the body.

PE 29406 (Figure 20A)

This specimen is preserved along its entire length in dorsoventral aspect. The 17 (possibly 18) trunk tergites are moderately well preserved, but the head has only a few features visible.

The headshield is discernable only in rough outline. Some remnants of the ventral rami of the antennules are just barely visible with very low-angle lighting at higher magnifications; these rami consist of a row of moderate-sized segments folded back over the cephalic midline. There is a faint suggestion of some long, laterally directed limb segments on the posterior half of the head, and these are probably the basal elements of the raptorial mouthparts.

None of the trunk tergites appears to be covered by the headshield. The first segment is somewhat shorter than those that immediately follow. The anterior and middle segments are somewhat better preserved than those more posterior, but there appear to be 17 or 18 tergites in the trunk. The full width of these is not preserved, although it seems clear that the trunk tergites at about the level of segment 10 begin to decrease in width and length as the body terminus is approached.

PE 37731 (Figure 20B, C)

This fossil is largely a color difference in the concretion, a common preservation among Mazon Creek fossils. Nevertheless,

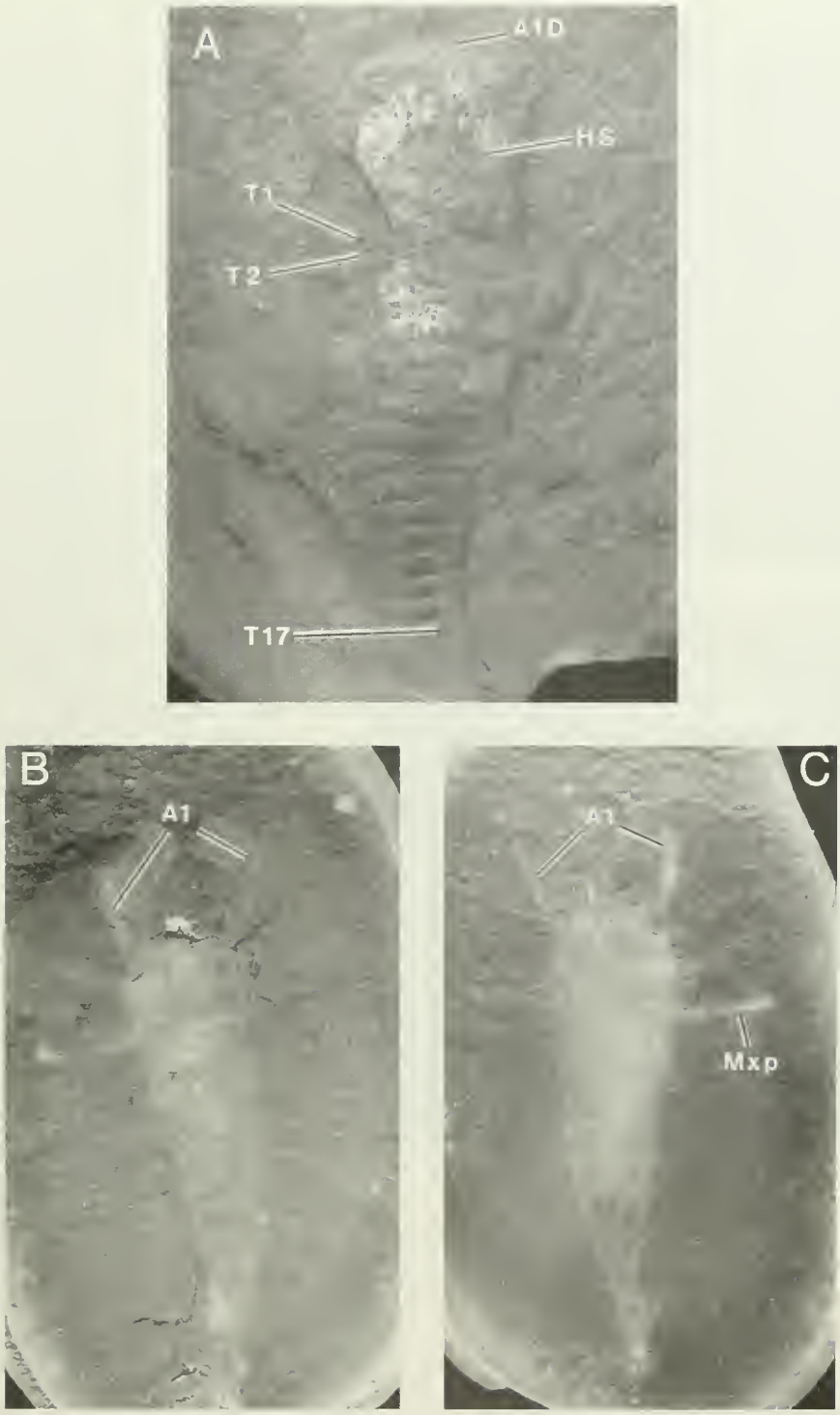

Figure 20. *Cryptocaris hootchi*. A, PE 29406, dorsal view of body, 2.5×; B, C, PE 37731, part and counterpart, specimen exists as a color difference on the rock, 2.3×.

some cephalic limbs are noticeable and a few segment boundaries are preserved.

The anterior end of this fossil is incomplete, especially on the counterpart. However, what appear to be the maxillipedes and one of the maxillae are visible and extend laterally from the head/trunk boundary. In addition, what appear to be the proximal parts of the antennules extend forward from the anterolateral aspect of the head. What may be a cervical groove is evident on the part, just posterior to where the antennules arise.

The trunk is not clearly preserved, especially in the posterior region, but there appears to be 14 or 15 tergites.

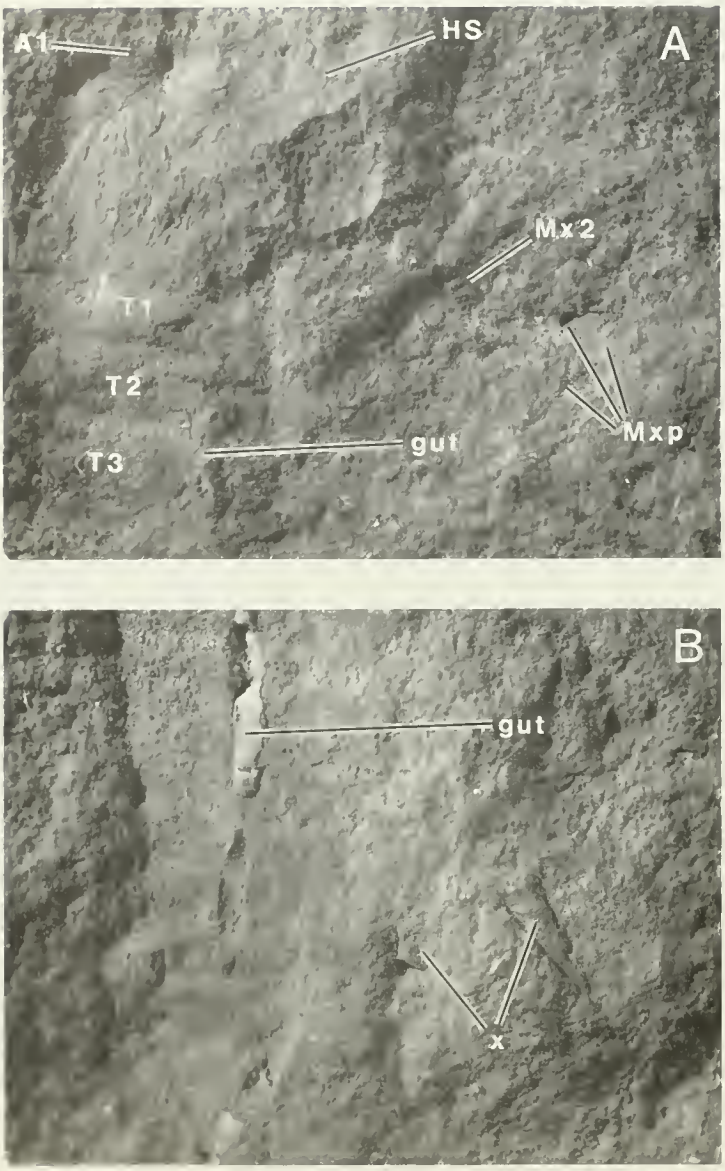

Figure 21. *Cryptocaris hootchi*, PE 37759. A, head and anterior trunk, 7.3×; B, posterior portion of the trunk, showing sediment-filled gut and remnants of exopedes, 8.5×.

PE 37759 (Figure 21)

In some respects this is one of the more interesting specimens at hand. Preserved in dorsoventral orientation, the outline of the subquadrangular headshield is fairly complete. What appear to be remnants of antennules are just visible extending forward from the shield boundary, and the part preserves portions of the raptorial mouthparts, probably the maxillae and maxillipedes (Fig. 21A), that extend laterally from the posterior portion of the headshield.

The trunk is well preserved, with some 15 tergites visible, and contains traces of the gut filled with detritus. Although only vaguely discernable, several pieces of the trunk limbs lie lateral of the trunk tergite margins and extend toward the posterior (Fig. 21B).

Remarks.—From the above information, a tentative reconstruction of *Cryptocaris hootchi* can be put forth (Fig. 22). The unregionalized trunk and simple headshield, combined with the large antennules with distinctly different segmentation on the two rami, the large raptorial mouthparts, and the very long, annulate, caudal rami seem to place this species clearly within the Remipedia. Unfortunately, we can discern at present very little about the form and arrangement of the trunk limbs on *Cryptocaris*, features which would allow some definitive affinity with the Enantiopoda to be established. A few characters, however, such as a finely annulate dorsal branch of the antennules and the bifurcate, annulate caudal rami, are similar to conditions seen in *Tesnusocaris*.

DISCUSSION

The incomplete preservation of *Cryptocaris hootchi* precludes any effective and detailed consideration of this species at this time. Consequently, most of our discussion will focus on the better known species of the Enantiopoda, *Tesnusocaris goldichi*.

The first question that we address before using the new specimens to reconstruct *T. goldichi* is whether or not the new materials at hand belong to the same species as the holotype. Because the differences in size and preservation are wide, there is a possibility that the smaller specimens are not conspecific with the holotype. In addition to the geographic and stratigraphic similarities between the specimens, however, we believe that congruence in the structures preserved in the fossils is sufficient to warrant assigning them all to the same species. Among the structures shared by USNMP 124173 and at least one or more of the new specimens are large sessile compound eyes on an anterior lobe of the cephalon, a subrectangular headshield ventrally bearing two biramous preoral appendages followed by a large subtriangular labrum and three pairs of raptorial limbs with spinose bases, a long series of similar trunk segments, each apparently bearing two pairs of uniramous appendages with bell-shaped coxae, and exopedes with rounded tips and long marginal setae. The body proportions of USNMP 124173 are different from those of the smaller SDSNH specimens, which could indicate a pattern of differential growth from juvenile to adult. It is interesting to note that although most dimensions increased by a factor of approximately 3, others grew much less. For example, it appears that the tergites grew much more rapidly in width than in length. A similar difference is apparent between juveniles and adults in the Nectiopoda, e.g., *Lasionectes entrichoma* (Fig. 23). In *Tesnusocaris*, this restriction of the axial growth of somites resulted in an increase in crowding of trunk limbs, while the width of the body remained proportional to the size of the cephalon.

Most of the scaling up and down to match specimens in making the composite reconstructions was done mechanically by matching positionally homologous features preserved in different specimens and using the resultant proportions to extend the reconstructions to adjacent features. For example, we graphically enlarged the mouthparts of SDSNH 28251b (Fig. 13) to match those of SDSNH 28252 (Fig. 4) to achieve a partial reconstruction. We then graphically enlarged the reconstructed juvenile mouthparts so that the size of the labrum matched that of USNMP 124173, resulting in the proportions shown for the mandibles, maxillules, maxilla, and

Figure 22. *Cryptocaris hootchi*, partial reconstruction.

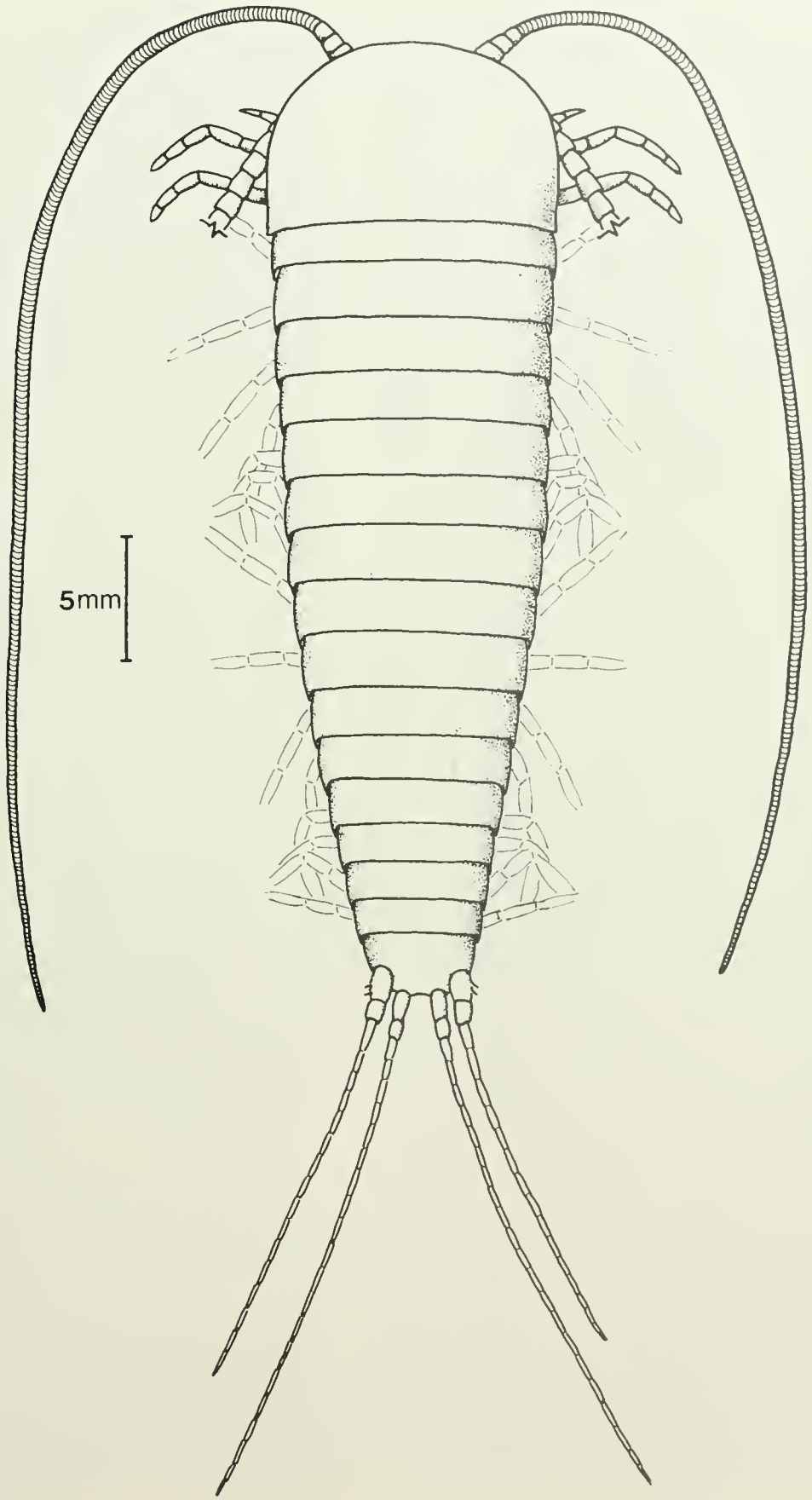
5mm

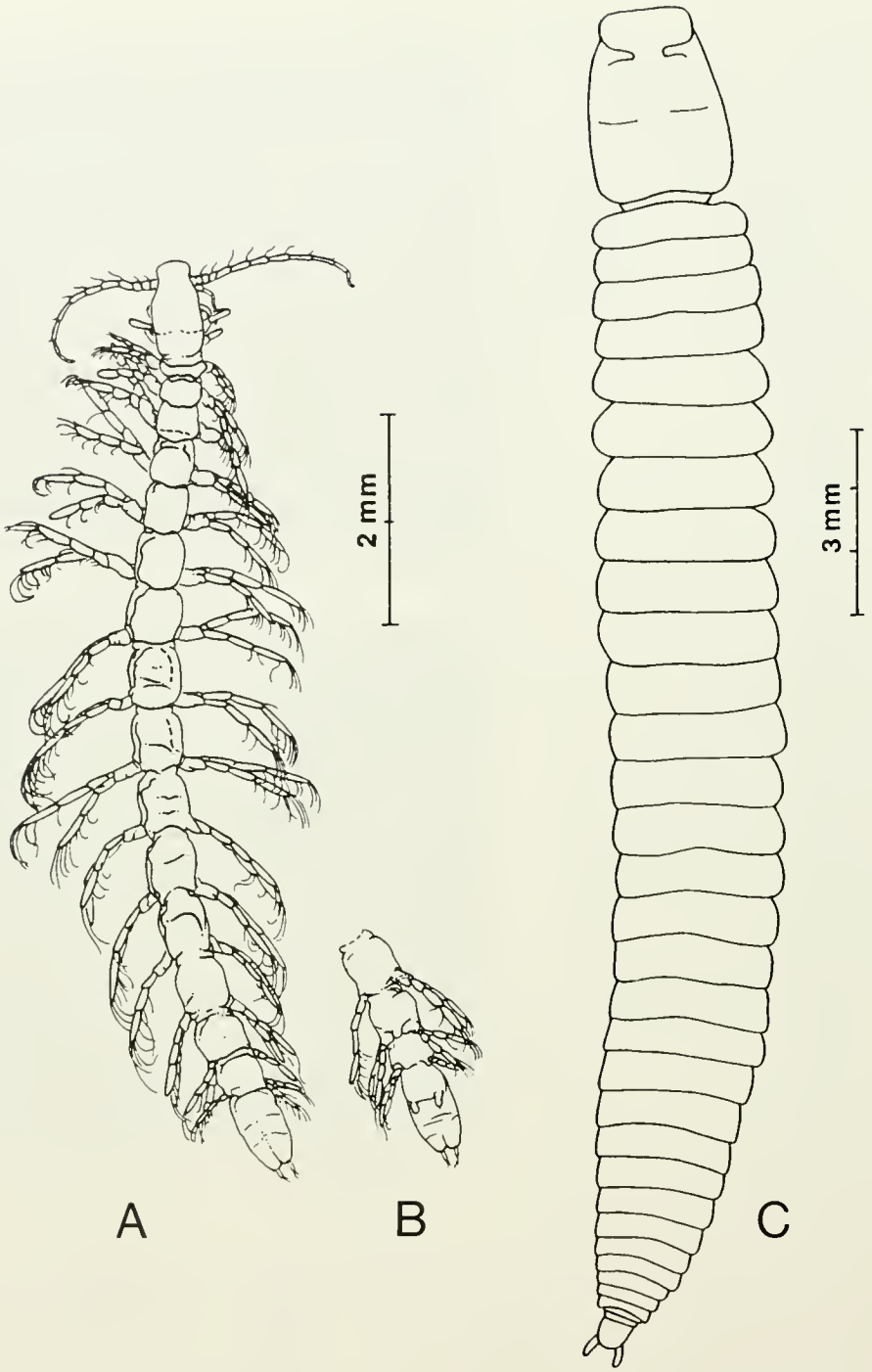

Figure 23. A, B, probable juvenile *Lasionectes entrichoma*, A, dorsal view, B, ventral view of anal segment showing limb buds and caudal rami; C, dorsal view of and adult L. entrichoma with appendages removed (from Schram et al. 1986, fig. 14A).

maxillipedes in reconstructions of the adult (Figs. 26, 27). The results seem satisfactory with a few exceptions, such as the adult's relatively large molar process of the mandible and first endite of the maxillule (compare Figs. 24, 26, Mn and Mx1.1). We concluded that the pattern of allometric growth that emerges is generally consistent with the interpretation that the small SDSNH specimens are conspecific with USNMP 124173.

The second major question that must be addressed is whether or not it is appropriate to use the nectiopodans as models to assist in the reconstruction of the enantiopodans. In some instances, we interpreted features that are preserved ambiguously on the fossils as being similar to homologous structures on the Nectiopoda. The apparent circularity of this process can be justified only because specific and unambiguous comparisons between other structures

not in question can be made. The features that are shared by nectiopodans and at least one of the fossils are listed in the diagnosis of the Remipedia under Systematics, and the morphological differences between them are listed in the diagnoses of the respective orders. It is clear from these diagnoses that important aspects of the overall body form, the shape of the headshield, the possession of large uniramous grappling mouthparts (especially the distinctive first endite and talon of the maxillules), and the absence of trunk tagmosis are shared by the Carboniferous and Recent species. Without considering for the moment whether these structures are plesiomorphic or apomorphic, taxonomically significant or not, the presence of such morphologically similar details in positionally homologous structures seems to justify to us their use in reconstructing the fossils. As a result of our comparisons between the extant and fossil remipedes, we freely admit our reconstructions of *Tesnusocaris* are biased to some degree in that similarities with the nectiopodans are emphasized perhaps more than would have been the case if the Nectiopoda were not known.

Reconstructions

The reconstruction of *Tesnusocaris goldichi* is made difficult, but not impossible, by the paucity of specimens, their generally poor preservation, the wide range of size of the individual fossils, and their unique morphology. Factors that have made the task possible include the availability of the nectiopodans as models and the fact that nearly every detail of the morphology of the fossils can be found adequately preserved on at least one if not more of the specimens. The following general description of the species draws from the best features of each specimen. Detailed presentation of the material evidence for each feature can be found in the descriptions of the specimens cited. The reconstructed illustrations include the appendages of a juvenile (Fig. 24), the ventral cephalon and anterior trunk of an adult (Fig. 26A), a ventral view of a juvenile trunk segment (Fig. 26B), a ventral view of an adult (Fig. 27), and a dorsal oblique view of a juvenile (Fig. 28).

The anterior headshield (AHS—USNMP 124173, Fig. 14; SDSNH 28251a, Fig. 10; 28251b, Fig. 10; 28252, Fig. 4) is a distinct lobe (Figs. 26A, 27, 28) that is much wider than long and may or may not have a slight anterior protrusion. There is a distinct flap at each posterolateral margin, giving the lobe a subtriangular shape. The AHS bears two large sessile compound eyes with a large number of facets. The eyes occupy much of the dorsal surface of the AHS. The middle headshield (MHS) and posterior headshield (PHS) together form a subrectangular unit divided by a cervical groove. This part of the headshield is wider than long in the juveniles and approximately square in the adult. The adult headshield is extended posteriorly, apparently covering the first two trunk tergites. The lateral margins of the adult headshield are extended ventrolaterally, covering at least the bases of the cephalic appendages.

The trunk tergites (T—SDSNH 28252, Fig. 4; SDSNH 28251a and SDSNH 28251b, Fig. 10; questionably on USNMP 124173, Fig. 14) are generally much wider than long and are developed laterally as pleura (Fig. 28), except for the first tergite, which is reduced and lacks well-developed pleura. There are denticulae on the lateral and posterior margins of some or all of the tergites. Except for the first one, most of the juvenile trunk tergites are uniform in size. The last few tergites are reduced gradually, and the last one may lack a pleuron (Fig. 24J). Although the tergites of the adult are not preserved clearly, the trunk somites are uniform in length throughout.

The anal segment (AS—SDSNH 28252, Fig. 4) is short, wide, and slightly tapering in diameter posteriorly (Figs. 24J, 28). There is a suggestion of large, posteriorly directed spines on the median, dorsal margin. Four large caudal rami extend posteriorly; their bases are clustered proximally and the flagella are splayed distally. None of the flagella are preserved completely, but the two dorsal caudal rami (CD) appear to be longer than the body of the animal, and the two ventral rami (CV) apparently are shorter (as in *Cryptocaris*, Fig. 22). The dorsal and ventral caudal rami are otherwise very similar in form, being divided by distinct segments proximally and by faint annulations distally. The rami appear to have a laterally directed row of spines, possibly matched by a mesially directed row. On the proximal section of the ventral ramus, the ventrolateral margin seems to be developed as a ridge that supports the spines and extends onto the anal segment and possibly onto the last trunk segment. Resembling the cerci of insects and other arthropods (Snodgrass 1952), the caudal rami of *Tesnusocaris* find their closest analog among crustaceans in the uniramous caudal rami of notostracans and in the biramous flagellar uropods of some tanaids (e.g., see Schram 1986). They differ from all these examples, however, in details of number, position, and structure. The Nectiopoda bear a single pair of short, simple, uniramous caudal rami (Fig. 23C).

Two sternites (S1, S2—USNMP 124173, Fig. 14) appear to be associated with the maxillae and the maxillipedes (Figs. 26A, 27), and each trunk somite also bears a sternite (Figs. 26B, 27). The sternite (S5) of what appears to be the third trunk segment (SDSNH 28251b, Figs. 10 and 12) appears to bear a lateral sclerite (LS), as well as a large sternal bar (SB) connecting the coxae of the endopedes (Fig. 26B), similar to that seen on some nectiopodans (Fig. 25B). The sternite proper appears to be separated from the sternal bar and lateral sclerite by weakly sclerotized cuticle. The sternites and sternal bars occupy a clearly defined midventral space, lying between the coxae from the maxillae to the end of the trunk and defining an intercoxal space (ICS—USNMP 124173, Fig. 14; SDSNH 28251a, Fig. 10).

The antennule (A1) is inserted somewhat laterally on the ventral surface of the cephalon at the juncture of the MHS with the AHS. The protopod (Fig. 24A, A1Pp—USNMP 124173, Fig. 14) consists of a large basal segment with short, posteriorly directed aesthetascs (Aes), possibly separated by an indistinct suture from a distal area lacking aesthetascs that supports the two rami. The first segment of each ramus actually may be the bifurcated tip of the protopod (Fig.25A, A1Pp), as it is in the Nectiopoda (Schram et al. 1986). The ventral ramus (A1V) is directed ventrally and posterolaterally (USNMP 124173, Fig. 14). Eleven elongate segments of the ventral ramus are preserved, many of them with short marginal setae, and the ramus probably is somewhat shorter than the body of the adult. The dorsal ramus (A1D) has a peduncle (SDSNH 28252, Fig. 4; 28251b, Fig. 10) of four or five broad articles. The peduncle is directed anterolaterally and supports a long, annular flagellum with more than 100 rings. A low ridge extends the length of the flagellum on the dorsal surface. There are no setae preserved on this ramus. The dorsal ramus, though incomplete on all specimens at hand, appears from the relative proportions of the various elements of the preserved rami to have been much longer than the body.

The antenna (A2—USNMP 124173, Fig. 14; faintly on SDSNH 28251b and SDSNH 28251c, Fig. 10) has a slender protopod (A2Pp) that inserts medially just anterior to the labrum. The protopod is divided near the point where its orientation changes from anterior to lateral. The second segment of the protopod appears to be longer than the first and is continuous with the undivided anterior ridge of the adult endopod (Figs. 24B, 26A, 27). The endopod (A2Np) is a relatively small paddle lying near the base of the antennulary protopod. Marginal setae of variable lengths line the edges. Although the anterior marginal ridge of the endopod appears undivided on the adult, the antennae of the juveniles show no such ridge. The segmentation of the endopod, incomplete on the

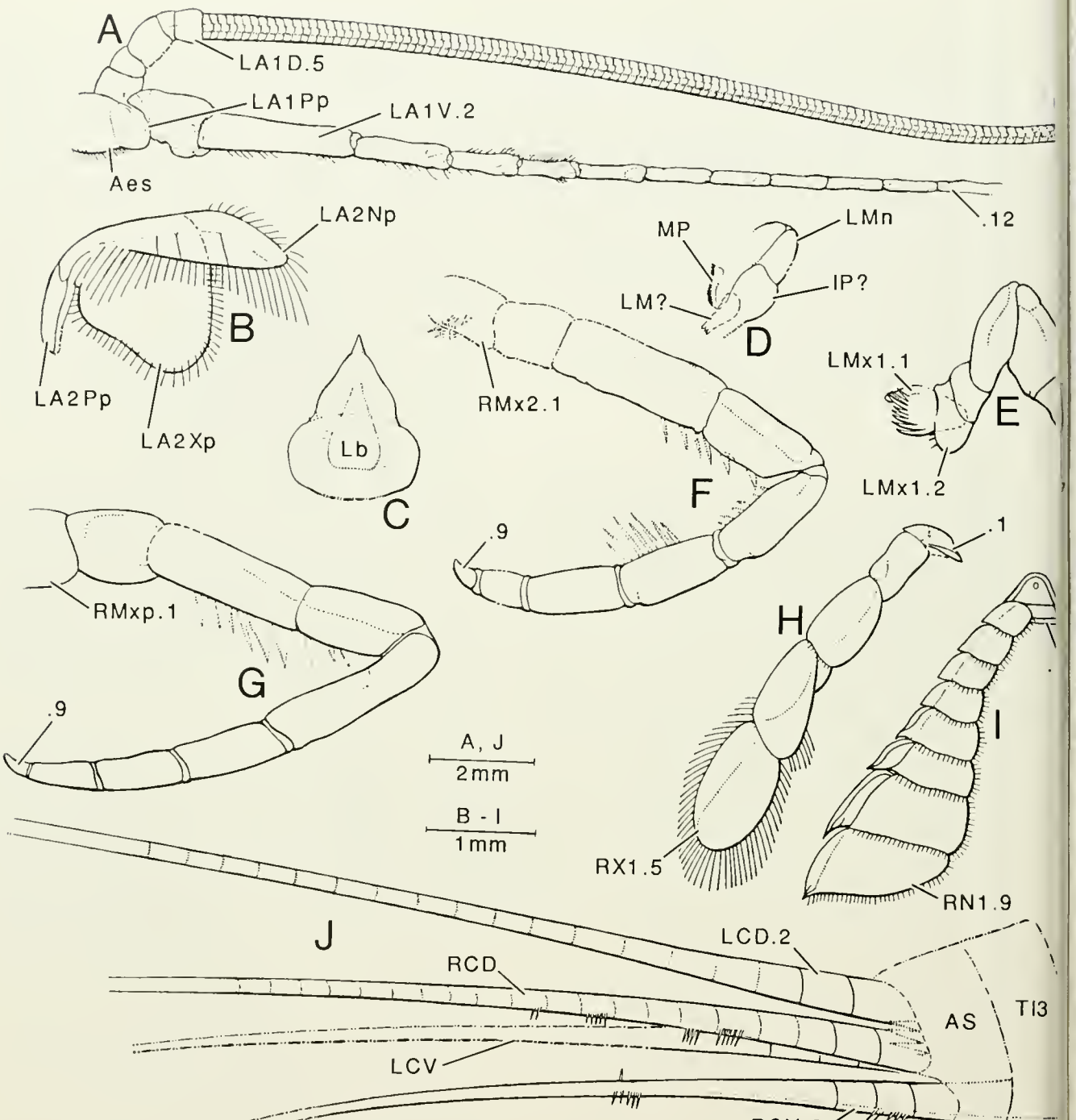

Figure 24. Reconstructions of dissected *Tesnusocaris goldichi* appendages. A, left antennule, anteroventral view; B, left antenna, ventral view; C, labrum, ventral view; D, left mandible, anteroventral view; E, left maxillule; anterior view; F, right maxilla, posterior view; G, right maxillipede, posterior view; H, right third exopede, ventral view; I, right third endopede, ventral view; J, right dorsolateral view of the posterior trunk showing the anal segment and caudal rami.

adult and apparently complete on the juveniles, divides the ramus into at least three podomeres. A possible fourth podomere at the base of the adult endopod appears to be the distal part of the protopod. The exopod (A2Xp) inserts laterally on the second segment of the protopod; the point of attachment is covered by setae. The exopod ramus itself appears to be a fairly large ovoid scale that lies partially under the endopod. The margins are setose at least along the posterior edge, and setae appear to be continuous around all the margins of the ramus.

The configuration of the preoral limbs (Figs. 25A, 26A) appears to differ slightly from that of the Nectiopoda (Schram et al. 1986). In the modern remipedes, the antennae are held so that the exopods project ventrolaterally with the endopods tucked behind them, the entire limb being nearly hidden by the long aesthetascs of the anteriorly positioned antennulary protopod (Aes). In *Tesnusocaris*, the antennal endopod appears to overlap the antennal exopod and possibly the antennulary aesthetascs, though the relative positions of the latter elements are unclear. Aside from this rearrangement of elements and the annulate dorsal ramus of the antennule, however, the general structure of the enantiopodan preoral appendages closely resemble that of the nectiopodans, in contrast to earlier interpretations of the fossil species.

The labrum (Lb—USNMP 124173, Fig. 14; SDSNH 28251b, Figs. 10 and 12) is a fairly large bell-shaped structure with an enlarged, bulbous posterior lobe (Figs. 24C, 26A, 27) and is virtually identical with that of nectiopodans (Fig. 25A). The apparent anterior projection actually may be the gap between the bases of the antennal protopods of USNMP 124173. The raised median plateau of the juvenile labrum appears to have some sculpturing or wrinkling.

The mandible (Mn—USNMP 124173, Fig. 14; SDSNH 28251b, Figs. 10 and 12) is exposed at its base lateral to the labrum but inserts a portion of its distal components beneath the posterior lobe of the labrum (Figs. 24D, 26A, 27). A medial ridge appears to extend the length of the mandible, connecting posteriorly with the anterior edge of a structure that may be the base of the incisor process (IP). On the adult, the mandibles appear as large serrated molar processes (MP) that are covered at least partly by the labrum. A small lacinia mobilis (SDSNH 28252, Fig. 4) may be present on the left mandible (LM) and in size and shape is strongly reminiscent of nectiopodan lacinia (Schram et al. 1986).

The maxillule (Mx1—SDSNH 28251b, Figs. 10 and 12; less so on SDSNH 28252, Fig. 4, and USNMP 124173, Fig. 14) possesses a large endite with a rounded base supporting seven or eight slender spines (Figs. 24E, 26A, 27). The spines are directed medially or posteriorly. The second podomere is developed as a posteriorly directed rounded endite with at least three small spines along the mesial edge. The second and third podomeres are poorly defined but appear to be fairly short. The fourth podomere is large and has a ridge on the anterodorsal surface. A similar ridge is found on the proximal end of the large fifth podomere, which is strongly flexed in relation to the fourth in a subchelate form. The sixth segment is joined broadly to the fifth and tapers in a cone shape to the talon of the seventh podomere. The nectiopodan maxillule has a terminal fang, which appears to be hypodermic, apparently injecting a glandular secretion of unknown composition and probably functioning in feeding (Schram and Lewis 1989).

The maxilla (Mx2—SDSNH 28252, Fig. 4; SDSNH 28251b, Figs. 10 and 12; indistinctly on USNMP 124173, Fig. 14), has three groups of three spines directed posteromesially apparently representing an endite. The second podomere is a short segment. The next four segments bear a dorsal ridge and ventral spines. The third and fourth podomeres are broadly joined and may or may not be fused (as they are in nectiopodans where only a slitlike crease in the cuticle remains as a vestige of that fusion). The principal flexure occurs between the fourth and fifth segments, forming a subchelate limb (Figs. 24F, 26A, 27). This limb is strikingly similar to the nectiopodan maxilla (Fig. 25A). The seventh through ninth podomeres (SDSNH 28251b) lack details such as spines and ridges. The terminal segment appears to be a slightly recurved claw similar to that of the Nectiopoda (Schram et al. 1986), though little detail is apparent on the fossils.

The maxillipede (Mxp) is similar in form to the maxilla (Figs. 24G, 26A, 27), as in the Nectiopoda. No endites or spines are visible on the first two podomeres or on the distal parts of the ramus. The maxillipede is larger than the maxilla.

Each trunk somite appears to bear two pairs of uniramous swimming appendages. [The reader is referred to the descriptions of the trunk limbs of USNMP 124173 (Fig. 14), SDSNH 28252 (Fig. 4), SDSNH 28251a and SDSNH 28251b (Figs. 10 and 12) for the details of how we came to our interpretation of these limbs.] The trunk rami of the juvenile specimens appear to be fairly uniform in size on most of the somites, with the limbs of the last few somites becoming abruptly smaller. The trunk rami of the adult, however, form an evenly graded series, with each succeeding ramus smaller than the preceding one.

The endopede (N—USNMP 124173, Fig. 14; incomplete on SDSNH 28251a and 28251b, Figs. 10 and 12; poorly preserved on SDSNH 28252, Fig. 4) arises from a bell-shaped coxa that is approximately as long as wide (Figs. 24I, 26A, B, 27). There is a monocondylic protrusion on the inner surface of the anterior section of the coxa, and the marginal rim has a raised border. The coxa inserts ventrolaterally with the straight posterior margin generally prependicular to the long axis of the body. The structure and preserved positions of the endopedal coxae indicate little freedom of movement beyond a slight rocking about the anterior condyle. The articulation of the first and second podomeres seems to have allowed a freedom of movement greater than at any other point on the limb. The second through fifth segments of the endopede are similar to each other, being slightly wider than long, with an anterolateral crest that ends distally as a sharp spine. The sixth and seventh segments are similar in length to the preceding ones, but their width is greater, and the crests are more elaborately developed with ridges and grooves. The eighth podomere is much longer and somewhat wider than the preceding ones. The ninth and terminal segment is nearly as large as the eighth, but its mesial edge is very short, resulting in a subtriangular shape. The anterolateral edge lacks a spinose crest and instead has a flexible flap that folds back along the dotted line in some instances. Short setae apparently line all of the margins except for the spinose crests. The limb terminates in a short, sharp spine that appears to have been heavily sclerotized. All of the podomeres of the ramus are broadly joined.

The exopede (X—SDSNH 28252, Fig. 4; SDSNH 28251a, Fig. 10; USNMP 124173, Fig. 14; partially on SDSNH 28251b, Fig. 10) has an anteriorly rounded coxa with a nearly straight posterior edge (Figs. 24H, 26A, B, 27). The exopede coxa is considerably wider than long. The insertion of the coxa on the lateral body wall appears to have been fixed at an angle such that the posterior edge faces posterolaterally. There is a medial ridge on the outer surface of the coxa that divides the mesial and lateral portions. It terminates in an apparent condyle on the posterior margin that seems to articulate freely with the second podomere. The second podomere is fairly short and cylindrical, and there is a suggestion of a partial ridge on the anterodorsal surface. The third podomere is large and flat; its distal margin is fringed with short setae. The fourth podomere is similar to the third in size, but the posterodistal end is much larger than the proximal end. An articular piece is developed proximally at the juncture with the third podomere. There are moderately long setae at the distal extremes of the anterior and posterior margins. The articulation between the fourth and fifth segments is broad and

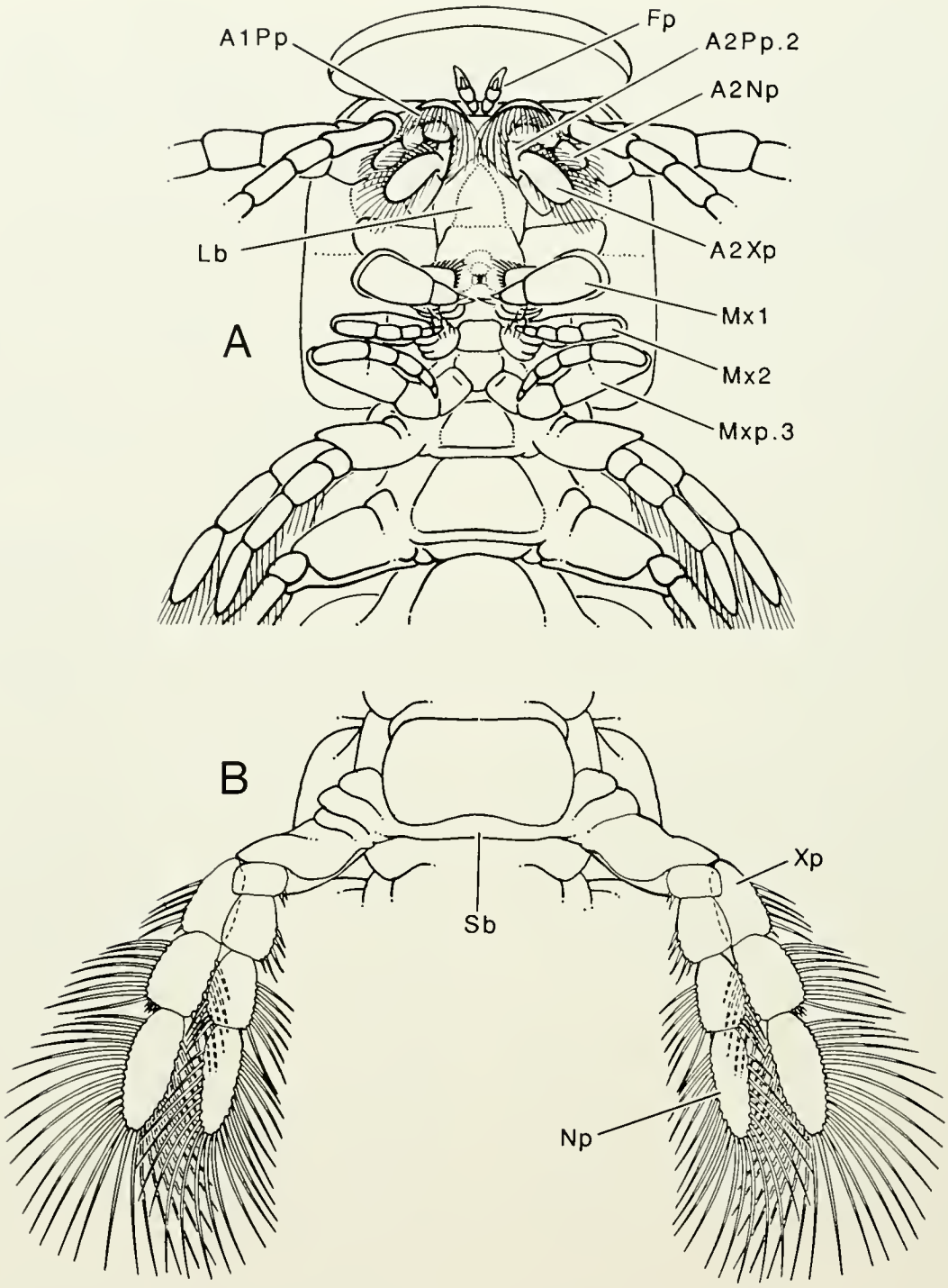

Figure 25. Ventral views of generalized nectiopodan remipedes. A, head and anterior trunk; B, generalized trunk segment with biramous limbs.

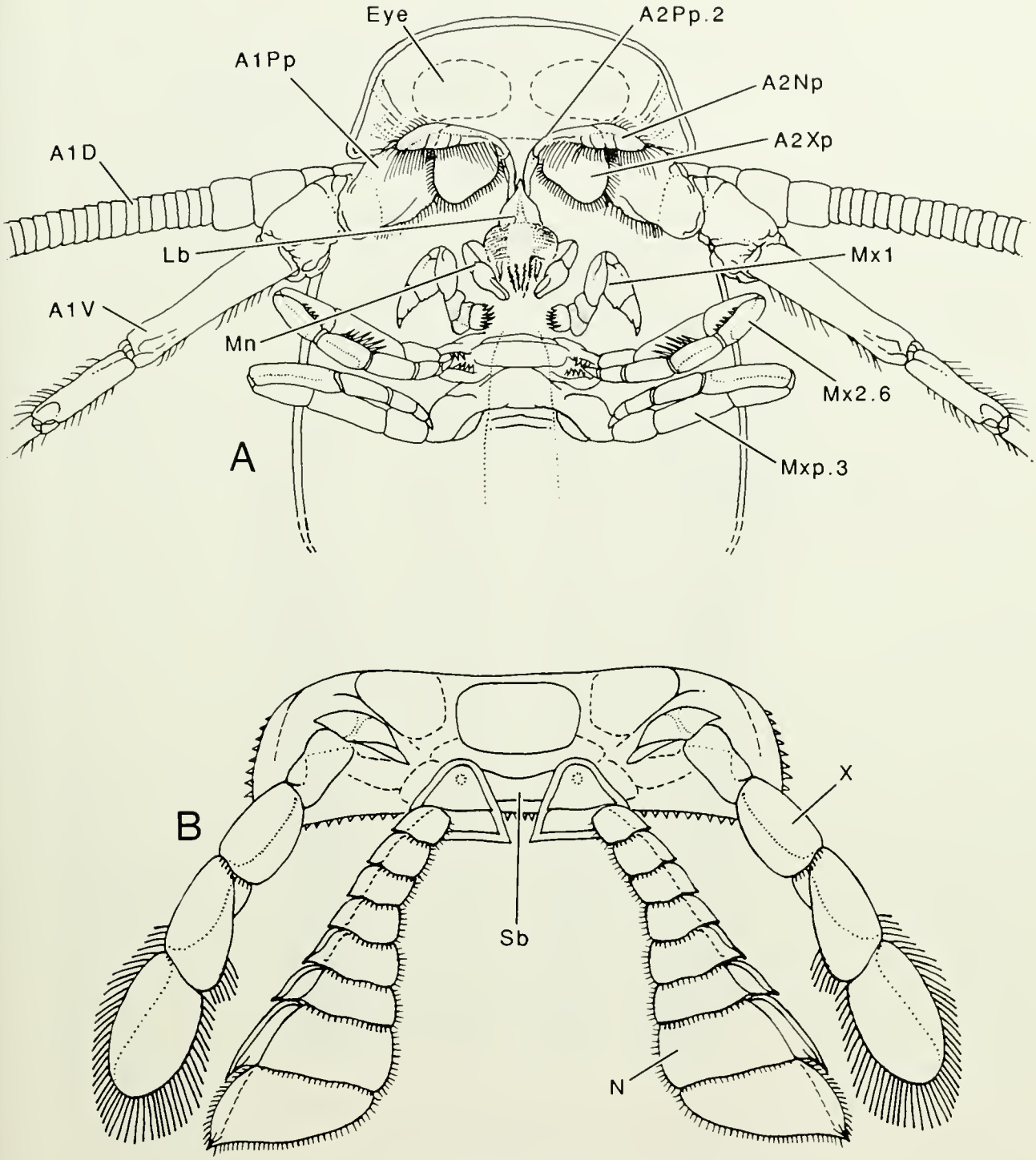

Figure 26. Ventral view of *Tesnusocaris goldichi*. A, head; B, trunk segment with two sets of uniramous limbs.

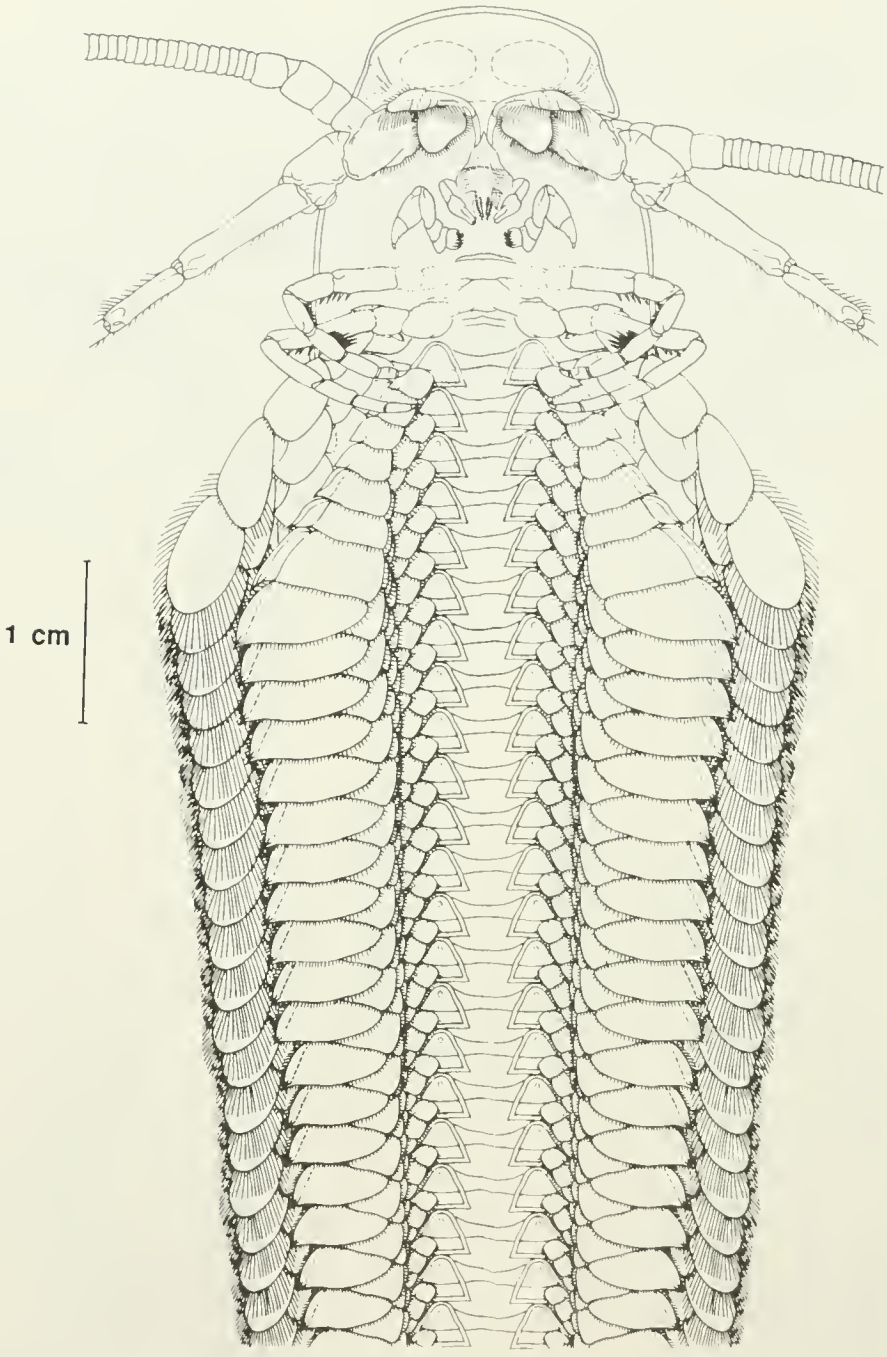

Figure 27. *Tesnusocaris goldichi*, ventral reconstruction of an adult.

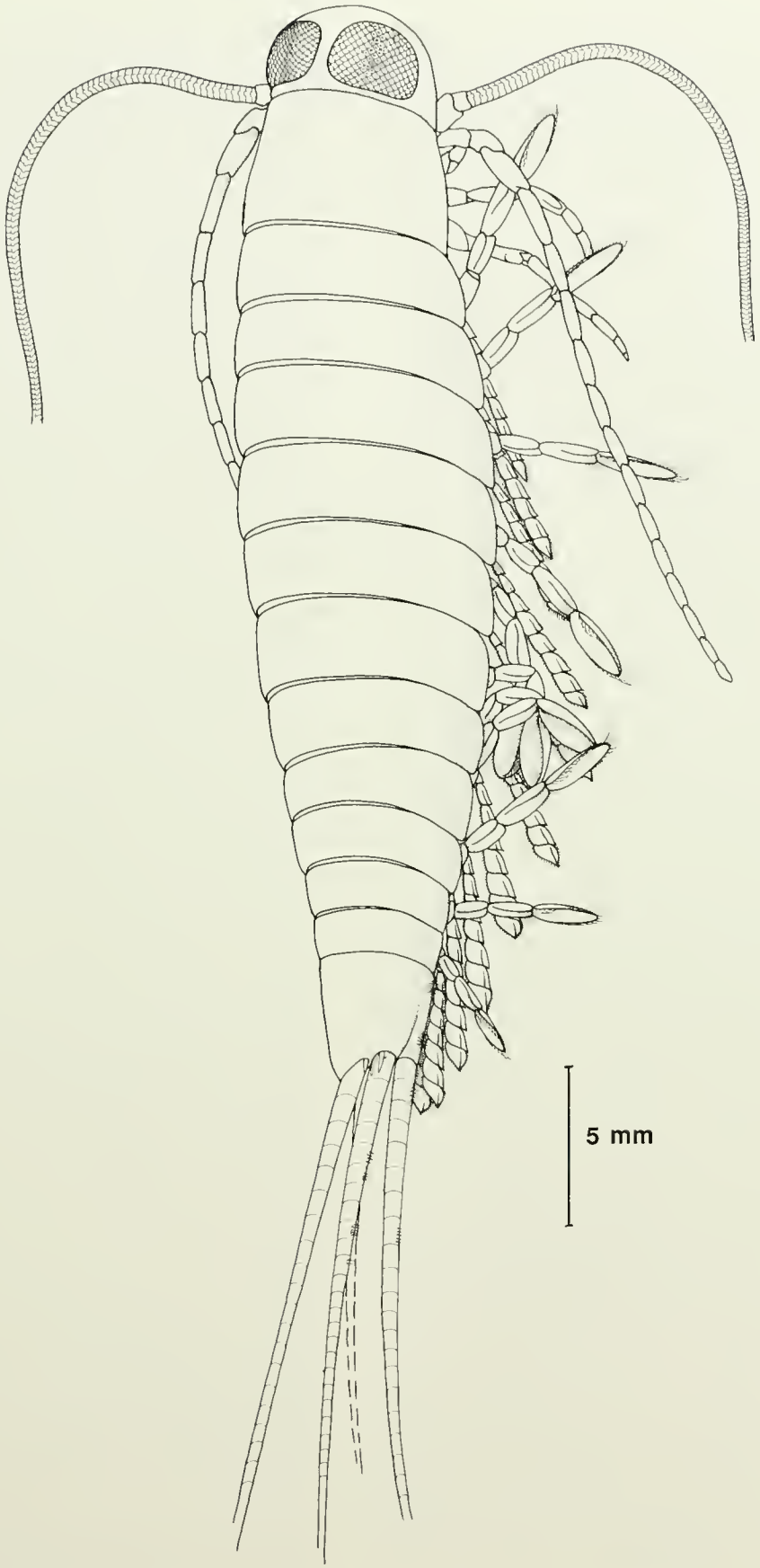

Figure 28. *Tesnusocaris goldichi*, dorso-oblique reconstruction of a juvenile.

appears to have permitted less freedom of movement than the more proximal joints. The terminal fifth podomere is the largest and is developed as a flat, oval plate with long, marginal setae. The anterior margin is folded back dorsally in some instances (to a position indicated by the dotted line, Figs. 24H, 26B 27, 28; the dotted lines on the third and fourth podomere reconstructions may represent a similar capacity, surface sculpturing, or diagenetic wrinkling).

Functional Morphology

An interesting analysis of the functional morphology of the Remipedia can be based on the descriptions of the fossils. Aside from the loss of sight in the Nectiopoda, it is clear, because of structural similarities, that *Tesnusocaris* used the cephalon in a manner similar to the nectiopodan *Lasionectes* in locating, obtaining, and processing prey items (Schram and Lewis 1989). (L. G. Abele, personal communication, however, believes from extensive field observations of individuals in Yucatan caves that *Speleonectes tulumensis* subsists on carrion rather than live prey.) The posterior cephalic limbs, therefore, probably played no role in normal locomotion.

In modern remipedes, the trunk limbs provide the sole propulsive force, and the creatures apparently swim ceaselessly (J. Yager, personal communication). The trunk limbs of *Tesnusocaris* seem to be adapted for swimming. The flattened shape of both the endopedes and exopedes would have served them well in that regard, though some fossorial function cannot be ruled out. Before an attempt to reconstruct the functional morphology of the trunk, the mechanical options available to swimming organisms are worth considering. The following discussion is synthesized primarily from the works of Alexander (1982), Clancy (1975), Plotnick (1985), Robinson (1975), Selden (1981), Tricker and Tricker (1966), and Whittington and Briggs (1985). The reader is referred to these discussions for more detailed information on the mechanics and hydrodynamics of swimming.

The primary habitat of the Crustacea is aquatic, and a wide variety of swimming techniques are evident within the group (Lochhead 1977, Hessler 1981). Although a given organism may employ more than one locomotory action, the range of possibilities is inevitably limited by the biomechanical specializations that evolved to exploit particular options (Robinson 1975). The result is an organism in which form and function are linked so closely that it often is possible to deduce one from the other. In the case of a fossil species such as *Tesnusocaris*, for which it is impossible to observe function directly, the logical approach is to analyze carefully preserved structural specializations to deduce possible function.

The following discussion is limited to a consideration of techniques for achieving steady forward movement in the horizontal plane, since this presumably is the principal component of locomotion for a free-swimming pelagic organism. Useful work in these terms is that which counteracts drag with thrust, and weight with lift. These forces are perfectly balanced in steady horizontal movement forward so that momentum is constant. In reality, limb movements undoubtedly create "unsteady effects" that are poorly understood (Clancy 1975, Plotnick 1985) and will be ignored in this discussion. The principle of conservation of momentum states that an object can give itself momentum only by giving equal and opposite momentum to the surrounding medium. In order for *Tesnusocaris* to move forward at a given rate, the animal had to displace backward a mass of water equal to the weight of the volume of water displaced by its body, plus sufficient water to balance the various forms of drag produced by fluid resistance to its movement. It also had to displace downward a mass of water equal to its weight, if it was negatively buoyant.

A swimming organism must generate thrust to overcome drag, a force opposite to the direction of travel. The sources of limiting drag vary with the size of an object and its speed in relation to the medium in which it is moving. One of the most fundamental relationships of fluid dynamics is expressed in the Reynolds number, in which inertial forces are divided by viscous forces. For very small objects existing in a realm of low Reynolds numbers water is a highly viscous medium, and the main source of drag is skin friction. For larger objects in a realm of high Reynolds numbers water is a relatively turbulent medium, and the main source of drag is the formation of eddies in the wake of the body or its moving parts. An additional source of drag that is more important at higher Reynolds numbers is the pressure drag that develops in front of a moving object. Every swimming organism has evolved structural features not only to minimize the particular forms of drag that hinder its movement through water, but also to exploit the characteristics of the medium that allow it to move more efficiently.

Of the various forms of swimming employed by different organisms, several probably did not apply to *Tesnusocaris*. The fossils reveal no mechanism that could have effectively enclosed a mass of water so that it would have been ejected backward to achieve hydraulic locomotion, such as employed by cephalopods and a few crustaceans (Barlow and Sleigh 1980). *Tesnusocaris* has no obvious modifications of the trunk or tail that suggest axial undulations were important in its locomotion. The use of axial undulations of the body or tail to propel the organism forward is common among worms and vertebrates, rare among crustaceans, and unknown in living remipedes. The remaining option is the most likely one: the use of paraxial oscillation of paired trunk limbs to drive water downward and backward.

There are two principal methods of swimming using paired appendages: rowing and sculling. Although both of these types of swimming involve the oscillation of paired paddle-shaped limbs that operate as levers, there are numerous differences in the functional morphology of each that allow them to be distinguished with considerable accuracy (Robinson 1975).

Rowing is familiar to anyone who has used a rowboat or similar craft, though submerged organisms do not produce surface waves and they must execute the recovery stroke under water. Rowing is a drag-based mechanism in which an oar exerts backward force on the water by maximizing turbulence and drag near the tip of the blade so that it remains stationary in the water as nearly as possible while the shaft levers the body forward. The oar blade is a flat plate that typically is broadest distally to increase drag. Force is imparted to the water only during the propulsive stroke, when the blade is moved anteroposteriorly while being held perpendicular to its direction of travel. This provides a brief but powerful thrust that derives from pushing a distinct mass of water backward. During the recovery stroke, the blade is rotated 90° or otherwise feathered and usually collapsed in the plane of the limb to minimize drag while the limb is drawn forward to the starting position. The recovery stroke creates drag, lessening the propulsive efficiency of rowing in maintaining forward momentum, but no thrust.

Because rowing depends on drag, it is efficient for organisms generally operating at Reynolds numbers ≥ 100. These include many crustaceans, including the Nectiopoda, and many secondarily aquatic and semiaquatic insects and vertebrates. Terrestrial mammals generally adopt rowing movements when in water, perhaps because the mechanics of rowing and walking are similar. Otters and freshwater turtles are among the largest animals that typically use rowing. Turbulence created in both the power and recovery strokes probably limits the effectiveness of rowing for larger animals.

Limbs used for rowing are usually modified to increase their efficiency as biomechanical oars. Because the oar functions as a

lever of body mass, it is most effective if inserted near the plane of the center of gravity. The typical rowing limb is characterized by a narrow shaft that is just large enough to house the intrinsic locomotory muscles and provide structural strength. The principal propulsive force is generated by the extrinsic muscles associated with the limb base. Because the base of the shaft is close to the body and therefore limited in the relative velocity of its swing, the proximal section usually has no special modifications to increase propulsive drag. The thickness of the shaft in the direction of motion must be kept to a minimum to reduce drag on the recovery stroke. The shaft should be jointed in such a way as to function as a strong lever on the power stroke and then either rotate 90° or collapse and overlap the segments on the recovery stroke. The distal part of the shaft supports the oar blade, a broad thin plate designed to create maximum turbulence and friction drag on the propulsive stroke. An efficient oar blade has a shape that is the opposite of streamlined. Drag is increased by the expansion of effective surface area by structures such as webbing or long marginal setae. An efficient oar is widest near the tip, which is rounded or squared off to increase drag distally. Since the oar blade functions nearly perpendicular to the flow of water during the power stroke and the resultant forces are similar around the margins, its outline generally is symmetrical on the dorsal and ventral edges. Because the oar describes an arc as it pivots about its point of attachment, the blade of a rigid oar is perpendicular to the water flow (Robinson 1975). At the more anterior and posterior positions, most of the water is pushed sideways, and relatively little forward thrust is generated. As a result, an efficient oar has a short quick stroke confined to 45° from the lateral position. The musculature and joints of the limb should reflect the need for greater power and mechanical efficiency in the propulsive stroke (Robinson 1975).

In sculling, a hydrofoil accelerates water backward by moving rapidly through the water. The hydrofoil is designed to create lift and minimize drag and turbulence at all times. A typical hydrofoil is a cambered plate, streamlined in cross section, and tapering toward its distal end. Force is imparted to the water during both the upstroke and downstroke. The foil is held at a small angle of attack from the direction of the fluid flowing past it, creating lift on the forward surface.

Unlike aircraft wings, which are fixed at a constant angle of attack, oscillating limbs can serve to propel a body as well as to suspend it in the medium. Sculling is a kind of subaqueous flying similar to aerial flying except that water is a fluid some 800 times more dense than air. Despite this difference, the principles involved are the same, and some birds (such as alcids) use their wings to "fly" both above and below the surface of the water. The flapping wing operates much as a propeller in generating thrust by accelerating a mass of water backward and drawing the body forward by the creation of lower pressure on the forward-facing side of the foil. The cross section of the backward-moving column of water is the wing disk, which is defined by the sweep of the foil. Unlike a rotary propeller, an animal wing must change direction twice in each cycle. In contrast to rowing, swimming by the use of hydrofoils involves holding the plane of the limb slightly inclined to the flow of water and moving the limb perpendicular to the direction of travel. Sculling operates on a lift-based mechanism that can propel the body forward on both the up and down strokes of a freely oscillating foil. Lift is produced by the difference in pressure on the upper and lower surfaces of the wing and by pressure exerted directly by the oncoming flow. Lift operates perpendicular to the incident stream of fluid over a foil. For an aircraft wing fixed parallel to the flow of the medium, the leading edge of the wing encounters the air approaching horizontally, and lift is produced vertically. During the interphase between sweeps this is also true for an oscillating foil. When a hydrofoil is oscillating actively, however, it encounters the flow at an angle between its own direction of motion and that of the body to which it is attached (Robinson 1975). Since lift is dependent on a foil's angle of attack, a flapping wing must adjust its orientation to maintain lift throughout the stroke. On the downstroke, the leading edge of the wing is angled down slightly and lift on the upper surface pulls the animal forward and upward. The angle of attack is usually reversed on the downstroke so that lift on the lower surface pulls the body forward and downward. The upward and downward components of lift cancel each other out through the cycle, and the net result is forward movement.

The lift and drag produced by any particular hydrofoil are dependent on its angle of attack and on the velocity of the fluid, expressed in the Reynolds number, so these factors must lie within narrow limits for swimming to be efficient. If velocity is too low or angle of attack too high, a stall will occur when the low-pressure cell above the foil breaks down, resulting in an abrupt loss of lift. Although there is no distinct recovery stroke, the relatively static interphase between up and down strokes provides little or no thrust, but may give some lift. During the interphases, the limb is usually drawn forward slightly so that the power strokes can be directed somewhat posteriorly with an increased angle of attack. As a result, the path of the wingtip seen from the side describes a figure-eight stroke in relation to the body. At all speeds, a narrow stroke form is more efficient than a wide one (Robinson 1975). In rapid flight, the figure-eight is nearly horizontal, the wing's angle of attack remains shallow throughout the stroke cycle, and the front of the foil is the leading edge at all times. In slow flight and hovering, the figure-eight becomes nearly vertical and the wing must rotate considerably to maintain a favorable angle of attack during its cycle. Some of the resulting stroke forms may resemble rowing at certain points (Plotnick 1985), but functional hybrids are generally inefficient (Robinson 1975). In the sculling motion that is the simplest form of hovering, the front and back of the foil alternate as the leading edge, and the foil is relatively symmetrical. Because sculling does not require a distinct recovery phase, it is much more efficient than rowing.

Sculling is also most efficient for large animals, since the viscosity of water at low Reynolds numbers prevents smaller organisms from building momentum by this means. The smallest extant swimmers using foils apparently are the portunid crabs, which use their last pair of pereiopods in a highly modified, sideways form of sculling, in addition to rowing, digging, and walking (Lochhead 1977, Plotnick 1985). A more typical use of hydrofoils in forward locomotion can be found in sea lions, penguins, sea turtles, and other highly aquatic vertebrates. The extinct plesiosaurs apparently are the sole example of vertebrates that used both pairs of limbs in sculling; other vertebrates use only the anterior limbs as hydrofoils. Sculling by a long series of paired limbs has been proposed for only one fossil invertebrate, *Anomalocaris*, the largest creature of the ancient Burgess Shale (Whittington and Briggs 1985). The two species of this unique genus had broadly overlapping folds that apparently functioned as continuous fins running the length of the body. Cuttlefish and several true fish, such as certain eels, swim by undulating long fins that are not derived from paired appendages, though the mechanical principles involved are similar. The tails of such rapidly swimming vertebrates as whales and tunas also function as hydrofoils.

Biological hydrofoils share certain morphological characteristics that distinguish them from oars. Because the hydrofoil can serve to lift the mass of the body, it is most effective if inserted below the plane of the center of gravity (Whittington and Briggs 1985). The typical wing has a hydrofoil cross section throughout its length—the leading edge is rounded and the trailing edge is tapered. This asymmetry results in a streamlined cross section that reduces turbulence in the wake of the wing. The center of lift on a hydrofoil

lies on a line approximately one-third of the distance back from the leading edge of the wing. In a biomechanical foil composed of a relatively flexible material that oscillates through the water, the hydrofoil cross section has the further advantage of stiffening the critical leading edge so that the center of lift can maintain a favorable angle of attack, while allowing the trailing edge to bend passively and reduce turbulence caused by the moving foil. The tip of the foil should be abruptly narrowed to a point to reduce the wingtip vortex often observed trailing aircraft wings, a major source of turbulence drag. The foil is also usually cambered; one side (usually the upper surface) is more convex than the other, which increases the water flow on the convex side and creates lower pressure on the cambered side, resulting in lift. In a flapping wing, it is advantageous to change the camber of the wing so that lift is created on both the up and down strokes. Although the trailing edge may be "softened" with short, thin structures to reduce turbulence, there is no mechanical advantage to be gained in expanding the margins with structures such as long plumose setae.

An efficient wing will have a high aspect ratio: the distance from wingbase to wingtip (span) will be maximized, and the width of the wing (chord) will be minimized. This results in relatively high lift in relation to friction drag, which is a function of surface area. To maintain the maximum aspect ratio, the foil should be rigid enough to resist passive bending, folding, or collapsing during movement against the water. Although rigidity of the foil is important, control over the shape of the foil to achieve favorable camber and a smooth transition from upstroke to downstroke is also advantageous. The base of the flapping limb should have a joint that allows pivoting and some rotation of the ramus to provide a favorable angle of attack on both the up and down strokes. The joints of the ramus itself should permit little twisting and no collapsing in the plane of the limb, only controlled flexing perpendicular to the plane of the foil. Ideally, either the joints will be reduced to just the articulation with the body, or the ramus may be divided by broad sutures that permit only vertical movement. The greater the vertical range of the foil or scull, the greater the potential velocity of the scull at midstroke, the greater the volume of water that can be swept back, and the more efficiently the animal will move. The optimal relationship of blade area to the area of sweep is between 1:5 and 1:6, which maintains a uniform flow of water through the foil disk (Robinson 1975). Another way to increase efficiency is to enlarge the foil disk by lengthening the scull, though this results in greater drag and mechanical stress. The rate of flow through the foil disk can be increased by increasing foil speed, decreasing drag, or increasing the angle of attack. Of these options, the last is incompatible with the first two. In a buoyant medium such as water, where gravity does not exert as strong a downward force as it does for large animals in the air, the dorsal and ventral limb muscles both should be strongly developed.

An analysis of the functional morphology of the trunk limbs of *Tesnusocaris* suggests that the endopedes and exopedes were used in very different modes of locomotion. The exopedes were well adapted to rowing, as evidenced by their oarlike shape (slender shaft, expanded blade, blunt tip), adaptations to increase distal surface area (long, marginal setae), preserved range of movement from anterior to posterior (165° as described above), and jointing of the ramus (allowing collapse on the recovery stroke and rigidity on the power stroke). In each of these respects, the exopedes closely resemble the limbs of many rowing invertebrates, including the biramous trunk limbs of nectiopodans (Fig. 25). The endopedes, however, show none of these adaptations for rowing. All the modifications of the endopedes would make them more efficient as hydrofoils: the hydrofoil cross section of the entire ramus, the stiffened leading edge and presumably flexible trailing edge, high aspect ratio, the acute tip, preserved range of movement (little or no anteroposterior component), and jointing (broad transverse sutures allowing only limited vertical flexing that would direct water backward). The strongest asymmetrical cross section, swept-back position, and apparently limited capacity for rotation and horizontal movement (11° to 17° as described above) are consistent with the interpretation of the endopedes as hydrofoils adapted for continuous, rapid swimming.

The locomotory specializations of *Tesnusocaris* would appear to be unique. Until now, no other creature has been described as having distinct series of limbs adapted for both rowing and sculling. The closest approximation may be the enigmatic animal *Anomalocaris*, which also had a ventrolateral series of "limbs" that apparently served as hydrofoils (Whittington and Briggs 1985). In the latter case, however, the foils of each side were joined very broadly to the body and only could have functioned as long, continuous fins. The lateral series of limbs in *Anomalocaris* do not appear to have been adapted for locomotion, but may have functioned as gills. A similar arrangement has been noted in another enigmatic creature from the Burgess Shale, *Opabinia* (Whittington 1975), though the locomotory mechanisms used are less clear. In addition, we propose an interpretation varying from that of Briggs (1976) for the Cambrian arthropod *Branchiocaris pretiosa* (see Emerson and Schram 1990a), a pattern of limb structure with laterally inserted flaplike exopedes and medioventrally inserted flipperlike endopedes, virtually identical to that described here for *Tesnusocaris*. Although *Anomalocaris* and *Opabinia* bear little resemblance to *Tesnusocaris* and may not have been arthropods, along with *Branchiocaris* these three apparently unrelated animals are the only organisms other than the Enantiopoda known to have had separately inserted lateral and ventrolateral appendages, and they are the only known metameric creatures that may have used their limbs (the ventral series in each case) as hydrofoils.

The presence of four well-developed limbs on each of 21 or more relatively wide trunk segments yields a total of at least 84 locomotory limbs on the adult *Tesnusocaris*, half of which were rowing horizontally and half of which were sculling vertically. The limbs overlapped extensively (Fig. 29A), further necessitating the close coordination of limb movement to prevent excessive turbulence. This overlap is also true for nectiopodans such as *Lasionectes* (Fig. 29B), but to a lesser extent since they have only one set of limbs on each relatively elongate segment. To understand the nature of the coordination of all these limbs, we have reconstructed one possible version of swimming in *Tesnusocaris* in Figure 30.

We assumed as a possibility that the endopedes and exopedes beat simultaneously in a metachronal wave involving eight segments (the latter number is a somewhat arbitrary convention adopted in similar studies but also corresponding to the actual case in nectiopodans). Although the reconstruction shows the metachronal beat of the limbs as a freeze-frame of a series of limbs, the illustration also can be thought of as a temporal description of the motions of a single limb in a repeating series. In other words, X6 corresponds both to the exopede of the sixth somite shown in the series and to the sixth stage in the eight-beat metachronal wave. In Figure 30, three repeating waves are indicated, involving eight somites each; they are distinguished by the designation of prime and double prime. We began our reconstruction of *Tesnusocaris* swimming with the exopede cycle, basing it on the model used by Selden (1981) to describe eurypterid swimming. Although the validity of this model for eurypterids has been called into question (Plotnick 1985), it seems to describe the rowing of nectiopodans quite well [e.g., see Schram et al. 1986 (frontispiece) and cinefilms by Dennis Williams, Freeport, Bahamas] and is probably adequate in illustrating the function of the enantiopodan exopedes.

At X1' the exopede is extended anterolaterally (Fig. 30) and the ramus is in the vertical attitude. The latter positioning could be accomplished mainly by the passive force of the oncoming stream. Active control of rotation by limb muscles could have an effect on

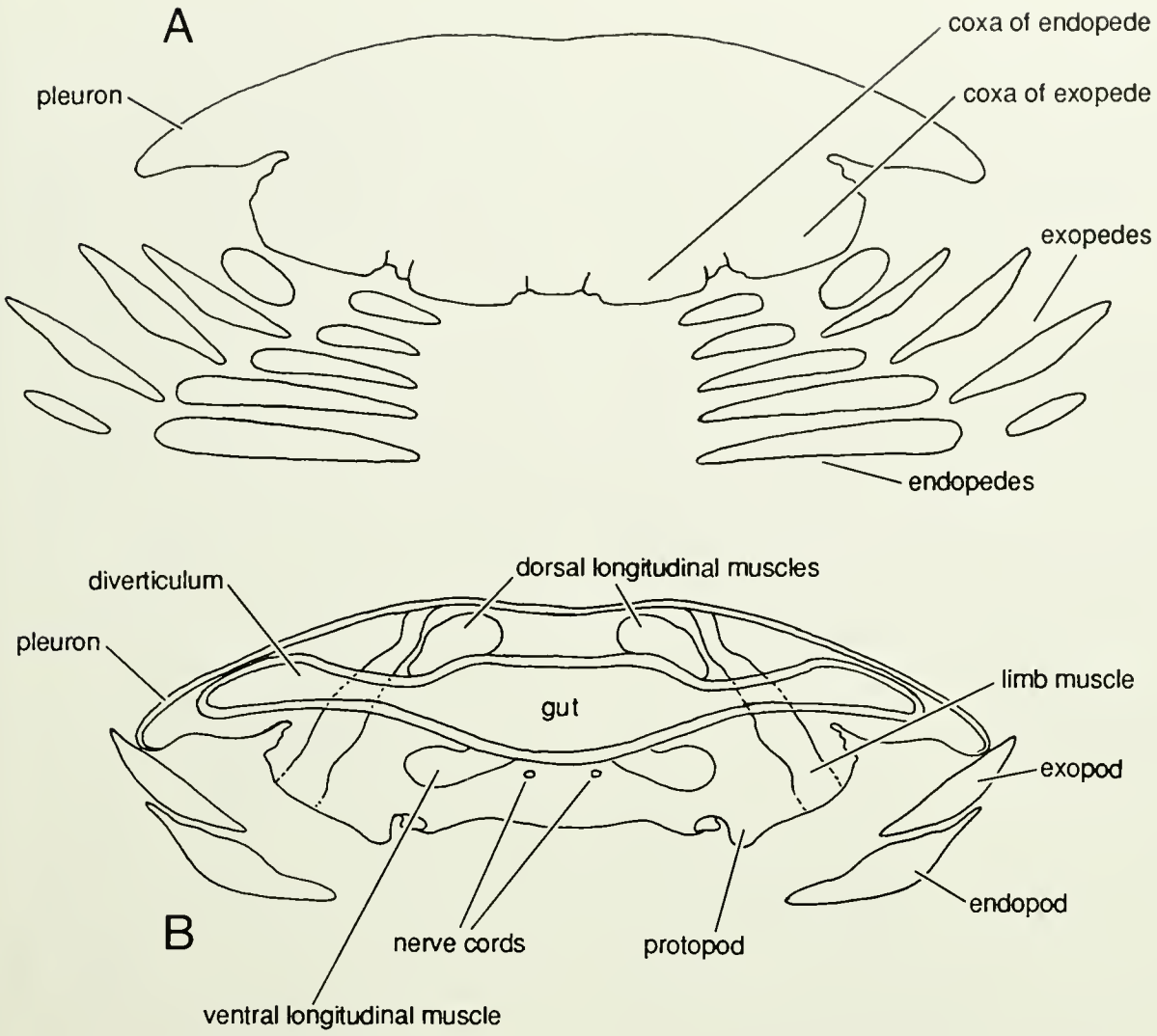

Figure 29. Cross-sections of remipede trunks. A, *Tesnusocaris goldichi*, reconstructed from the study of external anatomy of the fossils; B, *Lasionectes entrichoma*, based on stained serial sections of live materials.

momentum. Relative to the oncoming stream, rapid rotation would create a slight downward thrust, and slow rotation would allow upward lift at the expense of increased drag. From this point through the power stroke, any posterior movement slower than the current (or anterior movement of any kind) would serve as an effective brake. From X1' to X4' the exopede swings back in the power stroke, which provides the maximum propulsion between X2' and X3' when the oar blade extends laterally. X4' extends posterolaterally and is feathering into the recovery position.

At X5' the plane of the ramus is held horizontally, and the proximal shaft is beginning to draw forward. The recovery stroke continues through X7' as one podomere after another is extended forward individually by the progressive collapse and straightening of the ramus joints. Note that the anterior marginal flaps of the two distal podomeres and their setae fold back dorsally during the recovery stroke (Fig. 30, lateral view), affording several potential means to reduce drag. First, the limbs assume a more streamlined shape as the leading edge becomes smooth and rounded, reducing turbulence, and the effective surface area and resulting friction drag are reduced. Second, the rami could have overlapped and nested together in such a way as to draw forward as a single unit, which would have combined the pressure drag, friction, and turbulence of the individual limbs into a single, reduced value. In cinefilms of living nectiopodans made by Dennis Williams, the recovering wave appears as a distinct unit that moves forward along the body. The recovery is completed from X7' to X1" as the distal podomeres extend forward and the limb positions itself to begin a new propulsive stroke.

We perceive that there are two ways in which the endopedes could have functioned: one active, the other more passive. In the former, the endopede wave corresponds on a unitary basis with the exopede wave (as shown in Fig. 30), so that a single cycle occupies eight body segments. It is possible that the endopedes beat more rapidly than the exopedes, particularly during rapid acceleration. In fish, such as rays, that use lateral fins for sculling, slow swimming occupies the entire fin, and acceleration is accomplished by means of several short waves rippling through the fin. Since we are considering steady movement, the assumption of unitary correspondence seems to be a justifiable simplification. The range of sweep shown for the endopedes corresponds to a wingtip speed twice the

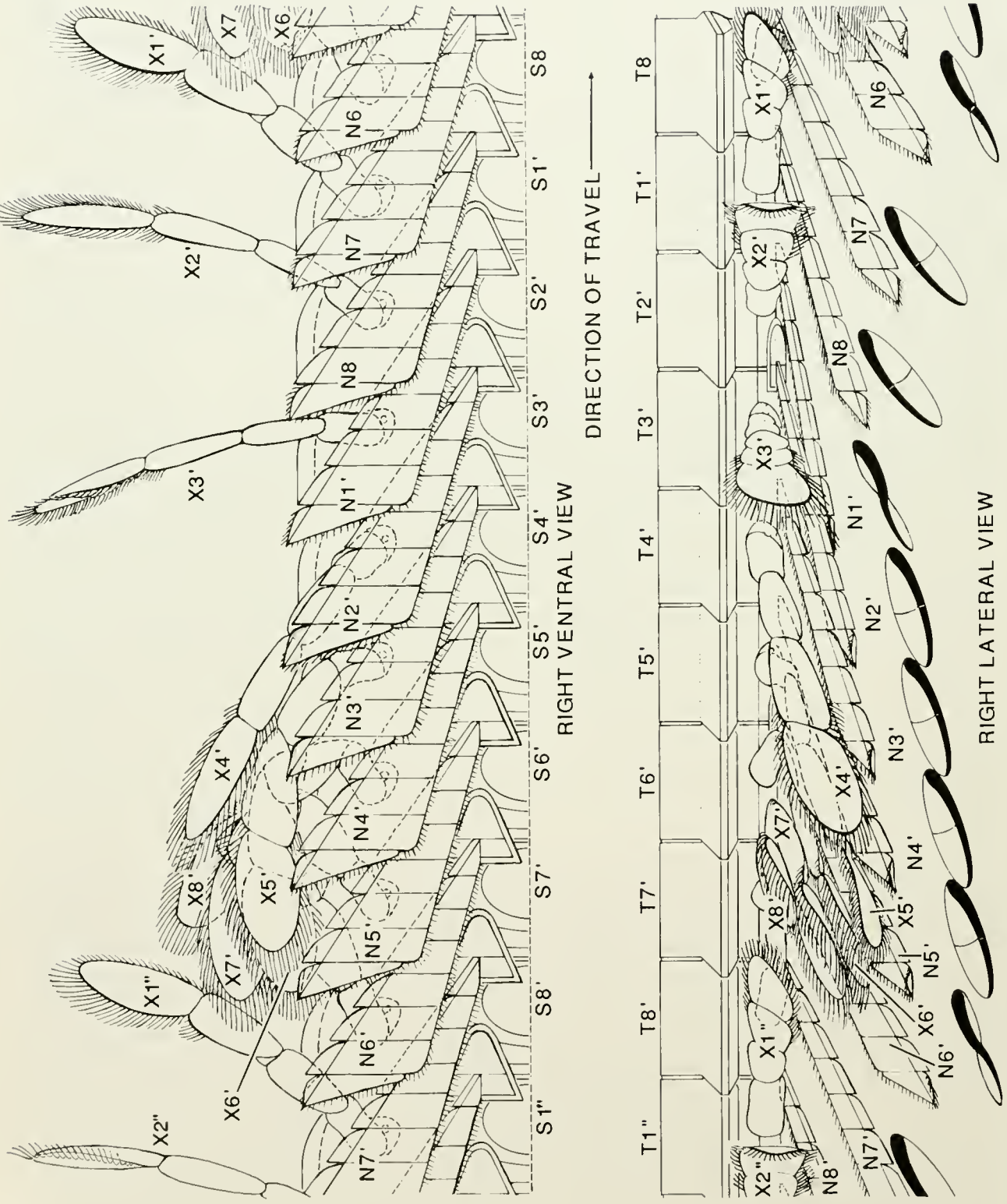

Figure 30. Diagrammatic reconstruction of swimming in juvenile *Tesnusocaris goldichi* spanning all or parts of three cycles (designated by unprimed, primed, and double primed callouts). A, right ventral view; B, right lateral view with cross-sectional profiles of endopedes. See text for explanations.

forward speed of the body, a value that is arbitrary but reasonable. A pronounced increase in the amplitude of the wave would have resulted in greater efficiency and speed, but the mechanical principles would have been the same. The upper limit of the endopede sweep is set by the overlap of the limbs and the need to avoid interference with the exopedes. We have shown the endopede cycle with an emphasis on the downstroke to compensate for the weight of the animal. However, a need to compensate for weight may not have been an important factor, since many aquatic arthropods store lipids, waxes, and light skeletal elements that help achieve neutral buoyancy. The density of soft-bodied crustaceans is only somewhat greater than that of seawater. For example, the density of the copepod *Labidocera trispinosa* is 1.082 g/cm^3 and that of the mysid *Hemimysis lamornae* is 1.104 g/cm^3, while the density of seawater is 1.024 g/cm^3 (Hargreaves 1981). Since water is more dense than air, the emphasis on the downstroke is less in sculling, or "aqueous flying," than in aerial flying by vertebrates. Although an assumption of slight negative buoyancy might seem justified, other sources of lift may have eliminated the necessity of emphasizing the downstroke. For example, the ventral insertion and principally subventral sweep of the endopedes would have tended to increase the upward component of lift, though certain mechanical considerations resulting from the overlap of the limbs might have reduced the lift from these sources.

The active endopede cycle (Fig. 30) is shown as a simple flapping of the limbs. It is possible that there was a small anteroposterior component, but the fossil evidence suggests that this was slight. Indeed, it is possible that the endopedes were relatively fixed in position and functioned as passive hydroplanes. At N1' the endopede is near the top of its cycle. The ramus could not have risen vertically much more than shown because of the overlap of the succeeding endopede, which is beginning to move downward. N1' is shown with the ramus twisting as the base of limb rotates slightly, decreasing the angle of attack. The outward twisting is facilitated by the transverse joints of the ramus and permits a smooth transition from the upstroke to the downstroke. Although this is one of two points in the cycle that provide the least potential for thrust, the backward sweep and transverse joints of the limb would tend to translate the progressive twisting of the ramus into a slight thrust. From N1' to N2' the limb completes it rotation and twisting and begins to move down. The overlap of the endopedes results in the closure of the gaps between them so that from N2' to N5' the endopedes function as a single surface, at least distally. The overlap of the endopedes would have prevented them from rotating forward sufficiently to achieve a favorable angle of attack in the downstroke, so their capacity to provide thrust as individual wings would have been greatly reduced. Instead, the continuous surface presented to the oncoming stream would have functioned more like a sail or a long undulating fin. As the endopedes moved down, the anterior spinose crest of each limb may have hooked onto the posterior setae of the preceding endopede. This would have reinforced the surface in much the same way as the barbs on the pinnules of a bird's feather hook together to create a continuous sheet. The lengthwise flexibility of the rami afforded by their transverse joints would have permitted the adjustment of this surface to achieve favorable camber, resulting in considerable lift and acceleration.

At the bottom of the downstroke, the base of N6' rotates the leading edge upward so that the ramus twists into position for the upstroke, again providing a smooth transition and some thrust as the trailing edge flips into place. The gap created by the twisting of the limb widens as N7' and N8' pivot up and back, so that the endopedes function as individual wings on the upstroke, just as the primaries of a bird's wing "feather" on the upstroke to present less resistance to the oncoming stream. The upward movement of the endopedes may have been either largely passive, caused by the current, or actively powered by limb muscles. Although the upstroke of a bird's wing is believed to be mainly passive, and the flight feathers are not individually muscled, there is some evidence that the individual primaries function as separate wings, providing some lift on the upstroke. There is a strong possibility that the endopedes were capable of providing lift on the upstroke by controlling their movement, camber, and angle of attack in relation to the incident flow of water, though probably not as much as during the downstroke. The large angle of attack shown is consistent with the short, quick upstroke described earlier. From N8' to N1" the limb finishes the upstroke and begins to twist into position for another downstroke.

The coordination shown between the endopede and exopede cycles is based on the assumption that the system would have evolved to provide continuous propulsion by lessening the negative effects of the cycle and by heightening the positive aspects to achieve maximum lift and thrust at each stage. Enhancing interactions between the endopedes and exopedes would have been limited by the fairly small overlap of the two series as seen in the ventral view. Since the weakest link in the entire locomotory chain is the recovery stroke of the exopede, we synchronized the endopede and exopede cycles in Figure 30 in a manner that seemed to minimize the negative effects of the recovery phase. By placing the downstroke of the endopedes (N1'–N6') directly beneath the recovering exopedes (X4'–X1"), the anteriorly moving low-pressure cell created by the endopedes would have helped draw the exopedes forward with a minimum of resistance. Additional enhancement of hydrodynamic efficiency may have occurred during the upstroke of the endopedes (N6'–N1") and the power stroke of the exopedes (X1'–X4'). The main loss of thrust in the exopede power stroke would have resulted from the turbulent movement of water around the edges of the oar blade, which may be thought of as a vortex ring expanding from the margins of the limb. The rising endopedes would have fed water into the path of the exopedes and helped channel the downward part of the vortex into useful backward movement. At the peak of the exopedes' thrust (X2'–X4'), the endopedes would have formed a continuous floor, virtually preventing the formation of the lower part of the vortex, and the pleura may have served a similar role dorsally. The backward channeling of the exopede power stroke would have peaked in the latter part of the sweep (X3'–X4'), with the posterior position of the exopede ramus diminishing flow around the distal tip of the oar.

The water currents generated by the endopedes and exopedes might have interacted without creating unnecessary turbulence if *Tesnusocaris* moved efficiently. In the model described above, the passage of a cell of water backward along the body would have followed a smoothly undulating course. As the posteriorly directed endopedes stroked upward (N6'–N1"), they pushed water up and back into the path of the exopedes, which were in their power stroke (X1'–X4'). After being forced back along the body by the exopedes, the cell of water was fed back and down into the expanding low-pressure area over the downstroking endopedes (N1'–N6"). As the endopedes again stroked upward, part of the cell was forced back and down between the separated endopedes, and part is fed back up into the next exopede power stroke. The manipulation of water flow in this system could have provided additional enhancement of lift and thrust beyond what would have been possible for the paired limbs acting separately.

Consideration of the more passive alternative for endopede function raises a separate series of interesting issues. There is a possibility that the interaction of the endopedes' and the exopedes' power stroke could have created a functional unit based on slotted wing design. The biomechanical aspects of slotted wings have been investigated in birds (Saveile 1957), and the principles involved are also well known in aircraft design (Clancy 1975). Bird wings are

slotted both in the middle, by the alula, and at the tip, by the digital arrangement of the primaries. The several forms of slotted wing design in aircraft all depend on the placement of a small secondary wing near the leading or trailing edge of the large primary wing. The configurations most closely resembling the arrangement of the endopedes are the avian primary feathers and the Fowler flap, in which the secondary wing lies just behind and above the trailing edge of the primary wing. All slotted designs increase the efficiency of the primary wing and enhance lift by increasing the aspect ratio so that the effective proportion of the wing is enlarged, and by delaying turbulent breakup so that the stalling speed is lowered.

We have already pointed out that the extensive overlap of the endopedes could have prevented them from achieving the optimum angle of attack in the downstroke, considerably reducing their efficiency as wings. The overlap of several layers of limbs (Fig. 29A) also added substantial bulk, mass, and surface area to the endopedes, all of which would have further reduced their efficiency as individual hydrofoils. Although the distal overlap of the endopedes allowed them to function as a continuous fin during the downstroke, the narrowing of the proximal part of the limbs created gaps through which the leaking of water would have reduced the efficiency of this design. The extreme overlap, however, of the endopedes and the proximal gaps between the limbs may have been adaptations to take advantage of slotted wing design. If this was the case, the exopedes could have functioned as a turbine, forcing water over the endopedes and between them. This interaction may have created a cascade effect.

Cascade effects can occur when the fluid medium is forced through a series of slotted wings, each of which boosts the efficiency of the next wing, greatly enhancing the lift and propulsion of the system. The increased velocity of flow over the endopedes caused by the exopedes' power stroke would have created a low-pressure area that could have helped raise the endopedes and enhance their upward lift. The acceleration of fluid velocity between the rising endopedes as the gaps between them narrowed and the exopedes' power stroke peaked may have amplified this effect. Cascade effects are important in the operation of rotary turbine guide blades. Attempts to create a cascade wing for aircraft that would realize the theoretical potentials of the design have been notably unsuccessful (e.g., triplanes). This type of locomotion has never been proposed for any animal. Contemplation of the specific characteristics of *Tesnusocaris* locomotion may provide an interesting study in slotted wing design that could result in the development of novel mechanical designs.

Whether the endopedes functioned as typical hydrofoils or as a cascade wing configuration, the exopedes would have been essential in providing the initial forward momentum needed to allow the endopedes to function if the creature ever stopped swimming. The inability of the endopedes to achieve a favorable angle of attack on the downstroke, due to overlap, probably would have prevented them from providing sufficient initial acceleration to overcome inertia.

The relative importance of the endopedes and exopedes in *Tesnusocaris* locomotion may have varied at different times to the advantage of the enantiopodans. If the predators found it necessary to stalk their prey, they could have approached most inconspicuously by using the low-profile rippling of the endopedes, followed by a sudden lunge provided by the exopedes executing a simultaneous power stroke. The latter technique has been noted as an escape response in the Nectiopoda and Copepoda (e.g., see Schram 1986), but its use by the former in feeding is unlikely since visual stalking is impossible for these blind cave dwellers. It may have been that the locomotory emphasis on the endopedes and exopedes changed as *Tesnusocaris* grew larger into adulthood. The fairly small size of the juveniles and the relatively slight degree of overlap of their endopedes suggest that the exopedes provided the main thrust. This is consistent with the fact that for smaller animals in a realm of low Reynolds numbers, drag-based mechanisms are most efficient. As the animals grew larger, however, the relatively lower viscosity of the medium and the virtual closure of the proximal gaps between the endopedes would have made sculling increasingly more efficient. The greater overlap of the endopedes also may have increased their function as slotted wings in the manner discussed above. The relatively slight increase in the length of the trunk segment in the adult would have maintained a nearly constant spacing between limbs that may have been essential to the function of the endopedes as cascade wings. As more trunk segments were added during growth, the increased number of endopedes would have allowed the formation of a series of propulsive waves along the body. The gradual posterior diminution of the trunk limbs in the adult would have concentrated mass and propulsive capability anteriorly. As a result, the adult would have tended to pitch downward when not actively swimming. This is a further indication that the Enantiopoda probably were constant, rapid swimmers, but also suggests that the adults were especially maneuverable.

Up to this point, we have discussed only steady forward locomotion without considering the need for maneuverability. Unlike a short-bodied one, an elongated animal cannot change its direction in water by simply pivoting on the vertical axis through the center of gravity, because drag against the sides of the body would be too great. The Nectiopoda change course while swimming by simply turning the head in a new direction, and the body follows like cars in a train. This probably is the same way *Tesnusocaris* maneuvered, though the relatively short somites of the adult would have decreased lateral flexibility. The anterior position of the centers of lift and gravity in the adult would have made the change of direction by this method more effective. The Nectiopoda decrease the oscillation of the limbs on the side of the body nearest the intended direction of travel, which accelerates the turn (e.g., see Schram et al. 1986: frontispiece). The exopedes would have been most effective in executing this maneuver in *Tesnusocaris*, though the ability of the endopedes to overlap extensively on the inside turn would have been essential to allow the necessary flexibility. Although the endopedes of the convex side would have spread like a fan, they may have overlapped sufficiently to maintain a normal stroke. Maneuverability in the vertical plane probably involved directing the cephalon up or down and the progressive flexion of the body segments. Adjustments in the angle of attack of the exopedal blades would have directed the exopedal thrust anterodorsally or anteroventrally, as required. Although backward propulsion may have been provided by the exopedes, the asymmetrical morphology of the endopedes would have made reverse propulsion virtually impossible for them. The fusiform shape of the body also would have made reverse thrust extremely inefficient.

The trunk limbs may have served additional functions. *Tesnusocaris* apparently lacked specialized respiratory structures, despite its large size and presumably active locomotion. Gills are universally present in the larger malacostracans, which also have large mineralized carapaces. The few soft-bodied living crustaceans that approach *Tesnusocaris* in size, such as the predatory anostracan *Branchinecta gigas* (Fryer 1966), have large respiratory epipods. Respiration in smaller crustaceans usually occurs through the thin cuticle of the ventral body wall and limbs. The apparently thin cuticle and large surface area of the enantiopodan trunk limbs may have been important in respiration as well as locomotion. The known Nectiopoda also lack gills, but they are relatively small and seem to have very low respiratory needs. The waters of the anchialine caves in which nectiopodans occur are nearly anoxic (Schram 1986: p. 40), and they probably have an anaerobic metabolism based on glycolysis.

Although locomotion may have been linked to respiration in the Enantiopoda, there is absolutely no indication that swimming was linked to thoracic feeding. The structure of the cephalic appendages and their close similarity with those of the Nectiopoda (Schram et al. 1986) strongly suggest that cephalic feeding was used by the fossil species. The basal segments of the endopedes lack mesially directed endites adapted to move food anteriorly along a midventral groove.

The large, distinctive caudal rami of the enantiopodans appear to have been adapted for some definite purpose. They are much larger than would have been required to give the body a hydrodynamically advantageous fusiform shape, and their excess length would have increased friction drag. The caudal rami may have functioned as stabilizers like the tail on a kite. The rami may have increased maneuverability by acting as a counterbalance like a tail on a cat, though they would have made poor rudders because of their round cross section. They may have served a sensory function, detecting the approach of predators from the rear. In addition, they could have functioned defensively to attract predators to the less vulnerable posterior end of the body. A similar adaptation occurs among certain large scolopendromorph centipedes, in which the last pair of legs is elongated and possesses mesially directed spines. When the centipede is disturbed, the rear of the body is lifted to expose two eyelike spots on the venter of the body terminus, and the last legs are splayed like antennae. If the false centipede head is touched, the offending object is quickly grasped with surprising force by the spiny most posterior appendages. The close resemblance between the antennules and spiny caudal rami of *Tesnusocaris* makes this form of defense a distinct possibility.

Phylogeny

The importance of the Remipedia in general and of *Tesnusocaris goldichi* in particular has become increasingly evident in the last few years. Schram (1983) reviewed two conflicting theories of crustacean phylogeny. One is the mixopodial or cephalocarid theory, which derives crustaceans from an ancestor with multiramous foliaceous trunk limbs (Sanders 1957, 1963); the other is the biramous theory, which postulates an ancestral form with trunk limbs consisting of biramous paddles (Cannon and Manton 1927). The discovery of the Nectiopoda appeared to support the biramous theory, since they exhibit primitive features such as biramous antennules and antennae, lack of a carapace, absence of trunk tagmosis, a homonomous series of biramous limbs on all trunk segments, and serial homonomy of internal organs such as the gut. Schram (1986: Chap. 44) examined the feeding habits of crustaceans and all potential outgroups, concluding that cephalic feeding probably was the most primitive mode and that some sort of grappling action, rather than a filtratory one, probably was ancestral within the crustaceans. This suggested that the apparently unique mouthparts of remipedes are only a structural specialization of a basically primitive design.

Several characters unite the fossil Enantiopoda with the living order Nectiopoda in the class Remipedia. Chief among the shared plesiomorphies are the biramous antennules and antennae, lack of a true carapace, absence of trunk tagmosis, and a homonomous series of limbs on all trunk segments. Some synapomorphies also unite the class, such as the highly specialized mouthparts that include entognathous mandibles lacking palps, hypodermic maxillules, subchelate or prehensile postmandibular mouthparts, and maxillipedes. The mouthparts are unique among crustaceans in possessing large uniramous postmandibular limbs modified for grappling and a mode of feeding convergently somewhat resembling that of arachnids (Schram and Lewis 1989).

The Nectiopoda possess some autapomorphic characters, such as the absence of eyes and the variable fusion of podomeres in most of the limbs. The reduction in the number of podomeres is most evident in *Godzillius robustus* (Schram et al. 1986). The possession of a pair of frontal processes may also be an autapomorphy, though it is quite possible that these minute, delicate structures were present in the Enantiopoda but not preserved in the fossils at hand. In overall body size and shape of the headshield and trunk tergites the adult Nectiopoda more closely resemble the juveniles of *Tesnusocaris* than they do the adult (cf. Figs. 23, 25A, 26A, 27, and 28), suggesting a possible trend toward paedomorphosis in the modern remipedes paralleling similar trends in other crustaceans (Schram 1986: Chap. 44).

Despite their great age and presumably primitive nature, the Enantiopoda also have some characteristics that seem to be autapomorphic. The most striking of these is the apparent development of the endopedes as hydrofoils in sculling, an adaptation that is shared with few other articulates. The possible function of these limbs as "slotted wings" may be a unique adaptation. It is unfortunate that *Cryptocaris hootchi* is not preserved well enough that details of the trunk anatomy of this smaller and younger species of enantiopodan can be reconstructed.

The most remarkable feature of the Enantiopoda to emerge from this study is the new reconstruction of the trunk limbs. A phylogenetic interpretation of these limbs is difficult because of their distinctiveness. The cephalic synapomorphies of the Enantiopoda and Nectiopoda seem to cast doubt on the possibility that the two groups evolved separately. The main problem lies in the distinct rami of the endopede and exopede on one segment, a condition we refer to as duplopody. However, as mentioned above, other duplopodous animals are known in the fossil record, even though they have not heretofore been recognized as such. *Branchiocaris* (Briggs 1976) is a Cambrian arthropod that we believe (Emerson and Schram 1990a), from the information available, to have had two sets of limbs on each trunk segment, a lateral set of flap-like limbs, and a medial series of long and narrow flippers. In addition, the enigmatic creatures *Anomalocaris* (Whittington and Briggs 1985) and *Opabinia* (Whittington 1975), with distinct sets of ventral and lateral fins and folds, also present certain features evoking duplopody. Just how the possible duplopody of some or all of these animals will affect analyses of arthropod relationships is not clear at this time.

However, two basic evolutionary sequences may be postulated to account for the unique *Tesnusocaris* trunk limbs. First, a more conventional view would hold that the ancestral biramous enantiopodan limb base was fused secondarily with the body wall. An analogous process occurred in the evolution of isopod and amphipod limbs, in which the coxa has become closely associated or fused with the body wall, leaving the ramus with an abbreviated limb base (Schram 1986: Chap. 12 and 13). Although it is impossible to discount this interpretation of the enantiopodan limbs completely, given the limitations of the fossil record, there are several indications that this is an unsatisfactory explanation.

First, the *Tesnusocaris* exopede has five segments, in contrast to the three segments of the exopod in nectiopodans. If the enantiopodan exopede had evolved from a biramous exopod through the extensive fusion of basal segments with the body wall, the exopede presumably would have fewer podomeres than the exopod, rather than more of them. This is true as well of the endopedes of *Tesnusocaris* that have nine podomeres, an unusually large number for any arthropod (Snodgrass 1952). The loss of the protopod, perhaps consisting of a separate coxa and basis, by fusion with the body wall suggests that the ancestral enantiopodan limb would have had ten or eleven podomeres, an unlikely figure.

Second, in many arthropods, the coxa serves as the relatively immobile foundation of the limb distinct from the mobile ramus

and as such has a rather distinct form. The first segments of the endopede and exopede have the functional morphology of typical coxae rather than that of the more distal podomeres of the ramus.

Third, the wide structural and functional separation of the rami suggests distinct musculatures and evolutionary histories. The initial separation of endopede and exopede would seem to be a preadaptation for the evolution of their distinctive functional morphology. It may be significant that the only articulate genera believed to have used hydrofoils in swimming, *Tesnusocaris*, *Cryptocaris*, *Branchiocaris*, *Anomalocaris*, and *Opabinia*, are also the only ones with apparently separated lateral and ventrolateral series of what appear to be duplopodous limbs and fins.

The other possible sequence in the evolution of the enantiopodan and nectiopodan trunk limbs is the derivation of the biramous limb from a duplopodous condition (Emerson and Schram 1990a, b). This would require the formation of a common protopod for the typical biramous crustacean endopod and exopod by fusion of some proximal podomeres of the duplopodous trunk segments. Just how this could have been achieved is an open question. The coxae of the duplopodous limbs could have been either lost or fused with the fused second podomeres to form the protopod. Alternatively, the protopod may have been derived from one or both duplopodous coxae, or from sclerites of the body wall. We can find no evidence in our studies of the living and fossil remipedes that argues against the derivation of the biramous trunk limb of the Nectiopoda from the duplopodous trunk limbs of the Enantiopoda.

Although various evolutionary schemes have been devised, the consensus of opinion among arthropod phylogeneticists seems to be that there is a clear distinction between two major groups of arthropods, the uniramians (e.g., Manton 1977) and the primitively biramous schizoramians (Hessler and Newman 1975). These groups may be either phylogenetic clades or morphological grades. Uniramians are characterized by uniramous limbs that may occur in one, two, or three pairs on each trunk segment. Modern uniramians are primarily terrestrial, including insects, myriapods (centipedes, millipedes, etc.), and possibly onychophorans. A few fossil uniramians apparently were marine (e.g., *Aysheaia*, Whittington 1978) or limnitic (e.g., Euthycarcinoidea, Schram and Rolfe 1982). There is general agreement that at least the insects and myriapods among the Uniramia constitute a monophyletic clade, although some workers consider the major subdivisions derived independently from early ancestors.

Schizoramians are characterized by primitively biramous limbs that occur one per segment. Despite the shared character of biramy, there is little evidence, heretofore, that the Schizoramia are monophyletic, and they may constitute a morphological grade (Bergström 1979). Schizoramians are believed to have evolved in marine habitats, and many groups remained there, including trilobites and their relatives, pycnogonids, and most crustaceans. Other biramous groups radiated into freshwater and terrestrial habitats, as did crustaceans and arachnid chelicerates. Schizoramian limbs adapted to walking on land or benthos typically are secondarily uniramous, with the exopod reduced or lost altogether. Although secondarily uniramous limbs may resemble primary uniramous limbs superficially, evidence of their biramous ancestry can always be found in the details of their musculature, development, serial homology, or comparative anatomy (Snodgrass 1935, 1952; Manton 1977). A number of other characters distinguish uniramians and schizoramians, especially differences in the functional morphology of the jaws (Manton 1964). Uniramians bite with the tips of whole-limb, uniramous jaws, but schizoramians bite with the gnathobases of primitively biramous jaws.

In all previous discussion of arthropod phylogeny, it has been assumed that individual limbs were homologous on a unit basis, whether uniramous or biramous. This system of homology also is applied to the serial homology of body somites, so that a diplosegment of a diplopodous uniramian is considered homologous to two adjacent somites of a schizoramian with each bearing a single pair of biramous appendages. This system of homology, however, has not produced a coherent assessment of the phylogenetic relationships between the major arthropod groups. Although it has been long assumed that the arthropods are a monophyletic phylum, recent studies have shown that it is difficult to impossible to derive any major group from another by means of the existing system of homology (e.g., see Manton 1977). Although phylogeneticists have disagreed as to whether the arthropods are monophyletic or polyphyletic (e.g., Gupta 1979, Schram 1979), there has never been, until now, any physical evidence from living or fossil animals that a clear link between the uniramous and schizoramous forms could be demonstrated.

Tesnusocaris goldichi appears to be a chimera with the head of a crustacean (evidenced by the possession of two biramous preoral sensory limbs as well as at least two sets of postmandibular mouthparts) and the body of a uniramian (evidenced by the presence of uniramous trunk limbs). The Nectiopoda have typical crustacean trunk limbs. The hypothesis that the duplopodous *T. goldichi* constitutes a link between a diplopodous uniramian ancestor and typical biramous crustaceans is too radical a departure from existing theories to be sustained merely on the basis of the evidence presented here, and the question is beyond the scope of this monograph. The phylogenetic implications of this possibility are profound and upset fundamental assumptions of limb homology, genetics, and development that are the foundation for the current understanding of the evolution of arthropods. We explore these questions further elsewhere (e.g., see Emerson and Schram 1990a, b, Schram and Emerson in press).

CONCLUSIONS

On the basis of morphological similarities between the new specimens and the holotype, it can be concluded with reasonable certainty that the new specimens are juveniles of *Tesnusocaris goldichi*. It is equally clear, from detailed similarities of the specialized cephalic appendages, that the Enantiopoda and Nectiopoda are sister orders of the class Remipedia. It is noteworthy that there apparently are few significant differences in the degree of specialization between the cephalic appendages of the fossils and those of the living nectiopodans. So these characters reveal little of the evolution within the Remipedia. The loss of eyes in the Nectiopoda is a secondary adaptation to cavernicolous life. Though clearly autapomorphic, the phylogenetic significance of this character is slight.

An analysis of the parts shared by the enantiopodan adult and juveniles allows an assessment of the growth factors involved in the development of the species (Table 1). One of the more interesting correlates of growth is that the length of the trunk segments did not increase as rapidly as did their width, or as did the length of the limbs, resulting in the adult in lengthwise crowding and overlap of the trunk limbs. The pronounced overlap of the endopedes may have allowed the animals to employ a unique form of sculling with the endopedes functioning alternately as hydrofoils, continuous fins, and possibly as slotted wings. The exopedes apparently functioned as oars in rowing, much as do the biramous trunk limbs of the Nectiopoda, though their synchronization with the endopedes may have allowed hydrodynamic interactions that enhanced locomotory efficiency. The potential interaction of the exopedes and endopedes as a turbine over a cascade wing is unique and may have greatly increased the efficiency of *Tesnusocaris* swimming.

The phylogenetic significance of the quite unexpected finding that the trunk segments of *Tesnusocaris* bore two sets of uniramous limbs is potentially controversial but must be dealt with if evolution within the Remipedia and the relationship of this group to other crustaceans and arthropods as a whole is to be understood. The synapomorphies of the remipede cephalon indicate that the remipede trunk limbs might have been derived from a shared ancestral pattern and did not evolve independently. The biramous limb is widespread among the Crustacea and some other fossil groups (Schram 1983). Although the duplopodous condition is unique to the Enantiopoda among crustaceans, it is apparently found in several other arthropod groups. The isolated phylogenetic position of the duplopodous enantiopodan trunk limbs makes it tempting to interpret them as autapomorphic adaptations connected with the development of hydrofoils. A detailed comparison, however, of the fossils with nectiopodans suggests that the *Tesnusocaris* trunk limbs are not secondary modifications of a primarily biramous condition. The biramous trunk limb of the Nectiopoda may have evolved from the duplopodous trunk limbs of an enantiopodan ancestor through fusion of two primitively uniramous limbs at their bases to form a protopod bearing two distal rami. Detailed comparisons of the fossil and living remipedes, although not conclusive in themselves, reveal no evidence that argues against this possibility, and certain facts seem to reinforce this hypothesis. To consider further the implications of this novel suggestion seems worthwhile.

ACKNOWLEDGMENTS

We wish to thank Mrs. Nina Evans and her family for permission to collect on the Rough Creek Ranch, Brewster Co., Texas, her son Robert for his valuable assistance in the field, and Mr. Eb Chrowder for his hospitality while we camped along Rough Creek. This research was supported in part by NSF grant BSR 82-12335. Mr. Brad Riney did extensive preparation on two of the specimens, Mr. John M. Simpson helped with art work, and Mr. William Estevillo assisted with mineral identification. Dr. Derek Briggs and Michel Boudrias offered valuable critiques of the manuscript and our ideas. Manuscript preparation and publication were facilitated by donations from Dominique Emerson and the Burkenroad Fund.

REFERENCES

Alexander, R. M. 1982. Locomotion of Animals. Blackie, London.

Baker, C. L., and W. F. Bowman. 1916. Geologic exploration of the southeastern Front Range of Trans-Pecos Texas. University of Texas Bulletin 1753:61–177.

Barlow, D. I., and M. A. Sleigh. 1980. The propulsion and use of water currents for swimming and feeding in larval and adult *Artemia*. Pp. 61–78 *in* G. Personne, P. Sorgeloos, O. Roels, and E. Jaspers (eds.). The Brine Shrimp *Artemia*, Vol. 1. Morphology, Genetics, Radiobiology, Toxicology. University of Wetteren, Belgium.

Bergström, J. 1979. Morphology of fossil arthropods as a guide to phylogenetic relationships. Pp. 3–56 *in* A. P. Gupta (ed.). Arthropod Phylogeny. Van Nostrand Reinhold, New York.

Birshtein, Ya. A.. 1960. Podklass Cephalocarida. Pp. 421–422 in Ya. A. Orlov (ed.). Osnovy Paleontologii: Chlenistongie, Trilobitobraznie, Rakoobraznie. Akademii Nauk, Moskva.

Briggs, D. E. G. 1976. The arthropod *Branchiocaris* n. gen., Middle Cambrain, Burgess Shale, British Columbia. Bulletin of the Geological Survey of Canada 264:1–29.

Brooks, H. K.. 1955. A crustacean from the Tesnus formation of Texas. Journal of Paleontology 29:852–856.

Cannon, H. G., and S. M. Manton. 1927. On the feeding mechanism of a mysid crustacean, *Heteromysis lamornae*. Transactions of the Royal Society of Edinburgh 55:219–252.

Carman, M. R. 1990. Catalog of type, figured, and referred Mazon Creek fossils in private collections. Fieldiana: Geology 19:1–29.

Clancy, L. T. 1975. Aerodynamics. Wiley, New York.

Crosby, E. J., and W. J. Mapel. 1975. Central and west Texas. United States Geological Survey Professional Paper 853:197–232.

Dutro, J. T., M. Gordon, Jr., and J. W. Huddle. 1979. Paleontological zonation of the Mississippian system. United States Geological Survey Professional Paper 1010:407–429.

Elias, M. K. 1959. Some Mississippian conodonts from the Ouachita Mountains. Pp. 141–159 *in* L. M. Cline, W. J. Hilseweck, and D. E. Feray (eds.). The Geology of the Ouachita Mountains, A Symposium. Dallas Geological Society and the Ardmore Geological Society, Dallas.

Ellison, S. P. 1962. Conodonts from the Trans-Pecos Paleozoic of Texas. American Association of Petroleum Geologists Bulletin 46:266.

Emerson, M. J., and F. R. Schram. 1990a. A novel hypothesis for the origin of biramous appendages in crustaceans. Short Courses in Paleontology 3:157–176.

Emerson, M. J., and F. R. Schram. 1990b. The origin of crustacean biramous appendages and the evolution of Arthropoda. Science 250:667–669.

Flawn, P. T., A. Goldstein, Jr., P. B. King, and C. E. Weaver. 1961. The Ouachita system. University of Texas Publication 6120:1–401.

Fryer, G. 1966. *Branchinecta gigas*, a nonfilter-feeding raptatory anostracan, with notes on the feeding habits of certain other anostracans. Proceedings of the Linnean Society, London 177:19–34.

Gupta, A. P. (ed.). 1979. Arthropod Phylogeny. Van Nostrand Reinhold, New York.

Hargreaves, B. R. 1981. Energetics of crustacean swimming. Pp. 453–490 *in* C. F. Herreid II and C. R. Fourtner (eds.). Locomotion and Energetics in Arthropods. Plenum, New York.

Hass, W. H. 1956. Conodonts from the Arkansas novaculite, Stanley Shale and Jackfork Sandstone. Pp. 25–33 *in* Guidebook Ouchita Mountains Field Conference, 1956. Ardmore Geological Society, Ardmore, Oklahoma.

Hessler, R. R. 1969. Cephalocarida. Pp. R120–R128 *in* R. C. Moore (ed.). Treatise on Invertebrate Paleontology, Part R, Arthropoda 4(1). Geological Society of America and University of Kansas Press, Lawrence.

Hessler, R. R. 1981. Evolution of arthropod locomotion: A crustacean model. Pp. 9–30 *in* C. F. Herreid II and C. R. Fourtner (eds.). Locomotion and Energetics in Arthropods. Plenum, New York.

Hessler, R. R., and W. A. Neuman. 1975. A trilobitomorph origin for the Crustacea. Fossils and Strata 4:437–459.

Ito, T., and F. R. Schram. 1988. Gonopores and the reproductive system of nectiopodan Remipedia. Journal of Crustacean Biology 8:250–253.

Jones, T. S. 1953. Stratigraphy of the Permian Basin of west Texas. West Texas Geological Society and Wiley, New York.

King, P. B. 1930. The geology of the Glass Mountains, Texas, Part 1, Descriptive geology. University of Texas Bulletin 3038:1–245.

King, P. B. 1937. Geology of the Marathon region, Texas. United States Geological Survey Professional Paper 187:1–148.

Lochhead, J. H. 1977. Unsolved problems of interest in the locomotion of Crustacea. Pp. 257–268 *in* T. J. Podley (ed.). Scale Effects in Animal Locomotion. Academic Press, New York.

Manton, S. M. 1964. Mandibular mechanisms and evolution of Arthropoda. Philosophical Transactions of the Royal Society London (B)247:1–183.

Manton, S. M. 1977. The Arthropoda. Clarendon, Oxford.

Mapel, W. J., R. B. Johnson, G. O. Bachman, and K. L. Varnes. 1979. Southern midcontinent and southern Rocky Mountains region. United States Geological Survey Professional Paper 1010:161–187.

Maxwell, R. A., J. T. Lonsdale, R. T. Hazzard, and J. A. Wilson. 1967. Geology of Big Bend National Park, Brewster County, Texas. University of Texas Publication 6711:1–320.

Moore, R. C. 1969. *Tesnusocaris*. P. R552 *in* R. C. Moore (ed.). Treatise on Invertebrate Paleontology, Part R, Arthropoda 4(21). Geological Society of America and University of Kansas Press, Lawrence.

Plotnick, R. E. 1985. Lift-based mechanisms for swimming in eurypterids and portunid crabs. Transactions of the Royal Society of Edinburgh: Earth Science 76:325–337.

Robinson, J. A. 1975. The locomotion of plesiosaurs. Neues Jahrbuch Geologie und Paläontologie Abhandlung 149:286–322.

Sanders, H. L. 1957. The Cehalocarida and crustacean phylogeny. Systematic Zoology 6:112–129.

Sanders, H. L. 1963. Significance of the Cephalocarida. Pp. 163–175 *in* H. B. Whittington and W. D. I. Rolfe (eds.). Phylogeny and Evolution of Crustacea. Museum of Comparative Zoology, Cambridge, Massachusetts.

Saveile, D. B. O. 1957. Adaptive evolution in the avian wing. Evolution 11:212–224.

Schram, F. R. 1974. Late Paleozoic Peracarida of North America. Fieldiana: Geology 33:95–124.

Schram, F. R. 1982. The fossil record and evolution of Crustacea. Pp. 91–147 *in* L. G. Abele (ed.). The Biology of Crustacea, Vol. 1. Academic Press, New York.

Schram, F. R. 1983. Remipedia and crustacean phylogeny. Crustacean Issues 1:23–28.

Schram, F. R. 1986. Crustacea. Oxford University Press, New York.

Schram, F. R. 1989. Designation of a new name and type for the Mazon Creek (Pennsylvania, Francis Creek Shale) Tanaidacean. Journal of Paleontology 63:536.

Schram, F. R., and M. J. Emerson. 1986. The Great Tesnus Fossil Expedition of 1985. Environment Southwest 515:16–21.

Schram, F. R., and M. J. Emerson. In press. Arthropod pattern theory: A new approach to arthropod phylogeny. Memoirs of the Queensland Museum.

Schram, F. R., and C. Lewis. 1989. Functional morphology of feeding in the Nectiopoda. Crustacean Issues 6:115–122.

Schram, F. R., J. Sieg, and E. Malzahn. 1986. Fossil Tanaidacea. Transactions of the San Diego Society of Natural History 21:127–144.

Schram, F. R., J. Yager, and M. J. Emerson. 1986. Remipedia, Part 1. Systematics. San Diego Society of Natural History Memoir 15:1–60.

Selden, P. A. 1981. Functional morphology of the prosoma of *Baltoeurypterus tetragonophthalmus* (Fischer) (Chelicerata: Eurypterida). Transactions of the Royal Society of Edinburgh: Earth Science 72:9–48.

Snodgrass, R. E. 1935. Principles of Insect Morphology. McGraw-Hill, New York.

Snodgrass, R. E. 1952. A Textbook of Arthropod Anatomy. Comstock, Ithaca, New York.

Tricker, R. A. R., and B. J. K. Tricker. 1966. The Science of Movement. Mills & Boon, London.

Whittington, H. B. 1971. Redescription of *Marrella splendens* (Trilobitoidea) from the Burgess Shale, Middle Cambrian, British Columbia. Bulletin of the Geological Survey of Canada 209:1–24.

Whittington, H. B. 1975. The enigmatic animal *Opabinia regalis*, Middle Cambrian, Burgess Shale, British Columbia. Philosophical Transactions of the Royal Society London (B)271:1–43.

Whittington, H. B., and D. E. G. Briggs. 1985. The largest Cambrian animal, *Anomalocaris*, Burgess Shale, British Columbia. Philosophical Transactions of the Royal Society London (B)309:569–609.

Yager, J. 1981. Remipedia, a new class of Crustacea from a marine cave in the Bahamas. Journal of Crustacean Biology 1:328–333.

Yager, J. 1987a. *Cryptocorynetes haptodiscus*, new genus, new species, and *Speleonectes benjamini*, new species, of remipede crustaceans from anchialine caves in the Bahamas, with remarks on the distribution and ecology. Proceedings of the Biological Society of Washington 100:302–320.

Yager, J. 1987b. *Speleonectes tulumensis* n. sp. (Crustacea: Remipedia) from two anchialine cenotes of the Yucatan Peninsula, Mexico. Stygologia 3:160–166.

Yager, J. 1989. *Pleomothra apletocheles* and *Godzilliognomus frondosus*, two new genera and species of remipede crustaceans (Godzilliidae) from anchialine caves of the Bahamas. Bulletin of Marine Science 44:1195–1206.